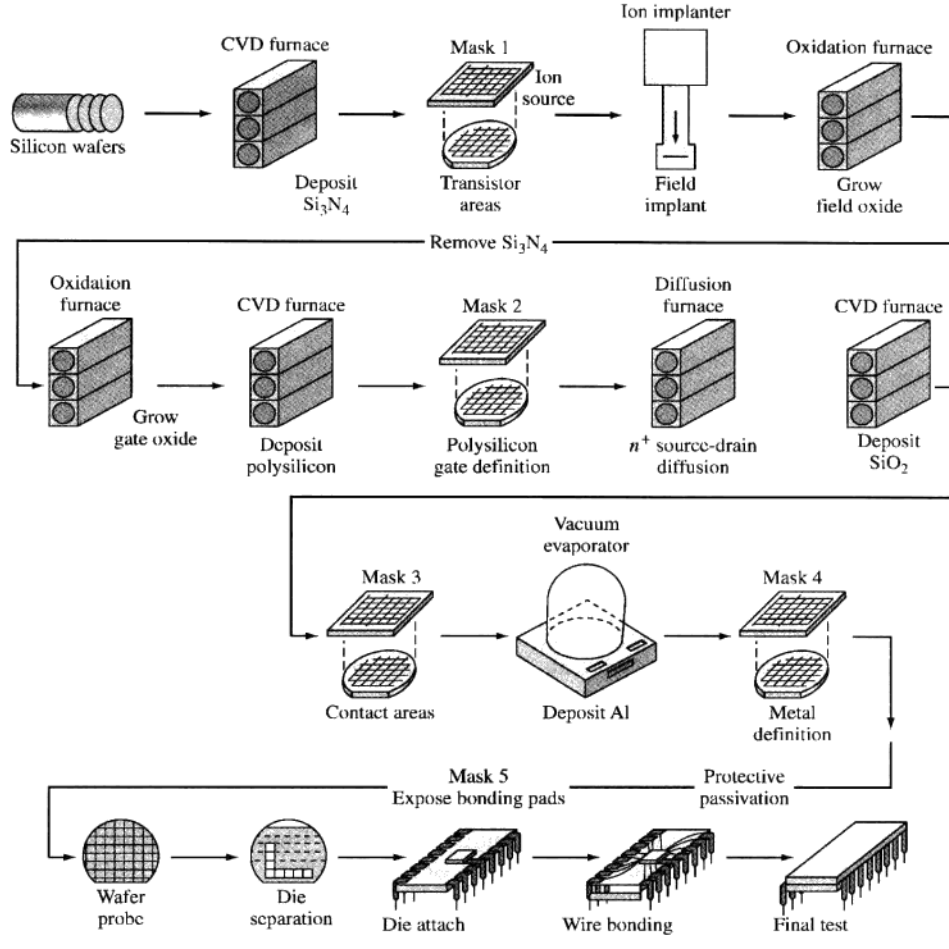

Figure 13.47
A manufacturing process for NMOS silicon-gate integrated circuits. (The processes used to make NMOS integrated circuits vary considerably from company to company. This sequence is given as an outline.) (*Reprinted by permission of Chipworks.*)

1. (See Fig. 13.46*a*.) A *chemical vapor deposition* (CVD) process deposits a thin layer of silicon nitride (Si_3N_4) on the entire wafer surface. The first photolithographic step defines areas where transistors are to be formed. The silicon nitride is removed outside the transistor areas by chemical etching. Boron (p-type) ions are implanted in the exposed regions to suppress unwanted conduction between the transistor sites. Next, a layer of silicon dioxide (SiO_2) about 1 μm thick is grown thermally in these inactive, or field, regions by exposing the wafer to oxygen in an electric furnace. This is known as a *selective,* or *local,* oxidation process. The Si_3N_4 is impervious to oxygen and thus inhibits growth of the thick oxide in the transistor regions.

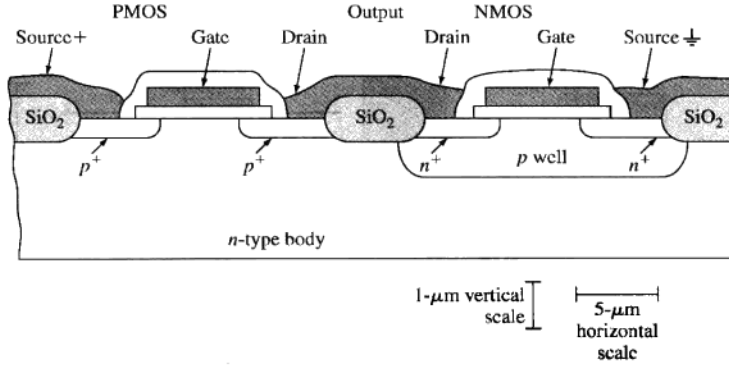

Figure 13.48
Complementary MOS field-effect transistors (CMOS). Both n- and p-type transistors are fabricated on the same silicon substrate.
(From D.A. Hodges and H.G. Jackson, "Analysis and Design of Digital Integrated Circuits," McGraw-Hill, 1983, p. 42. Reproduced with permission of The McGraw-Hill Companies.)

2. (See Fig. 13.46*b*.) The Si_3N_4 is next removed by an etchant that does not attack SiO_2. A clean thermal oxide about 0.1 μm thick is grown in the transistor areas, again by exposure to oxygen in a furnace. Another CVD process deposits a layer of polycrystalline silicon (poly) over the entire wafer. The second photolithographic step defines the desired patterns for the gate electrodes. The undesired poly is removed by chemical or plasma (reactive-gas) etching. An n-type dopant (phosphorus or arsenic) is introduced into the regions that will become the transistor source and drain. Either thermal diffusion or ion implantation may be used for this doping process. The thick field oxide and the poly gate are barriers to the dopant, but in the process, the poly becomes heavily doped n-type.

3. (See Fig. 13.46*c*.) Another CVD process deposits an insulating layer, often SiO_2, over the entire wafer. The third masking step defines the areas in which contacts to the transistors are to be made, as shown in Fig. 13.46*c*. Chemical or plasma etching selectively exposes bare silicon or poly in the contact areas.

4. Aluminum (Al) is deposited over the entire wafer by evaporation from a hot crucible in a vacuum evaporator. The fourth masking step patterns the Al as desired for circuit connections, as shown in Fig. 13.46*d*.

5. A protective passivating layer is deposited over the entire surface. A final masking step removes this insulating layer over the pads where contacts will be made. Circuits are tested by using needlelike probes on the contact pads. Defective units are marked, and the wafer is then sawed into individual chips. Good chips are packaged and given a final test.

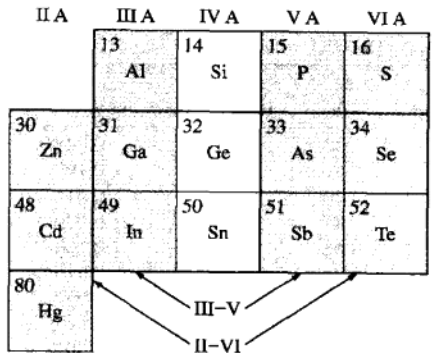

Figure 13.49
Part of the periodic table containing elements used in the formation of MX-type III–V and II–VI semiconductor compounds.

This is the simplest process for forming NMOS circuits, and it is summarized schematically in Fig. 13.47. More-advanced NMOS circuit processes require more masking steps.

Complementary Metal Oxide Semiconductor (CMOS) Devices It is possible to manufacture a chip containing both types of MOSFETs (NMOS and PMOS) but only by increasing the complexity of the circuitry and lowering the density of the transistors. Circuits containing both NMOS and PMOS devices are called *complementary,* or *CMOS, circuits* and can be made, for example, by isolating all NMOS devices with islands of p-type material (Fig. 13.48). An advantage of CMOS circuits is that the MOS devices can be arranged to achieve lower power consumption. CMOS devices are used in a variety of applications. For example, large-scale integrated CMOS circuits are used in almost all the modern electronic watches and calculators. Also, CMOS technology is becoming of increasing importance for use in microprocessors and computer memories.

13.7 COMPOUND SEMICONDUCTORS

There are many compounds of different elements that are semiconductors. Among the major types of semiconducting compounds are the MX ones, where M is a more electropositive element and X a more electronegative element. Of the MX semiconductor compounds, two important groups are the III-V and II-VI compounds formed by elements adjacent to the group IVA of the periodic table (Fig. 13.49). The III-V semiconductor compounds consist of M group III elements such as Al, Ga, and In combined with X group V elements such as P, As, and Sb. The II-VI compounds consist of M group II elements such as Zn, Cd, and Hg combined with X group VI elements such as S, Se, and Te.

Table 13.6 Electrical properties of intrinsic semiconducting compounds at room temperature (300 K)

Group	Material	E_g eV	μ_n $m^2/(V \cdot s)$	μ_p $m^2/(V \cdot s)$	Lattice constant	n_i carriers/m^3
IVA	Si	1.10	0.135	0.048	5.4307	1.50×10^{16}
	Ge	0.67	0.390	0.190	5.257	2.4×10^{19}
IIIA–VA	GaP	2.25	0.030	0.015	5.450	
	GaAs	1.47	0.720	0.020	5.653	1.4×10^{12}
	GaSb	0.68	0.500	0.100	6.096	
	InP	1.27	0.460	0.010	5.869	
	InAs	0.36	3.300	0.045	6.058	
	InSb	0.17	8.000	0.045	6.479	1.35×10^{22}
IIA–VIA	ZnSe	2.67	0.053	0.002	5.669	
	ZnTe	2.26	0.053	0.090	6.104	
	CdSe	2.59	0.034	0.002	5.820	
	CdTe	1.50	0.070	0.007	6.481	

Source: W.R. Runyun and S.B. Watelski, in C. A. Harper (ed.), *Handbook of Materials and Processes for Electronics*, McGraw-Hill, New York, 1970.

Table 13.6 lists some electrical properties of selected compound semiconductors. From this table the following trends can be observed.

1. When the molecular mass of a compound within a family increases by moving down in the columns of the periodic table, the energy band gap decreases, electron mobility increases (exceptions are GaAs and GaSb), and the lattice constant increases. The electrons of the larger and heavier atoms have, in general, more freedom to move and are less tightly bound to their nuclei and thus tend to have smaller band gaps and higher electron mobilities.

2. By moving across the periodic table from the group IVA elements to the III–V and II–VI materials, the increased ionic bonding character causes the energy band gaps to increase and the electron mobilities to decrease. The increased ionic bonding causes a tighter binding of the electrons to their positive-ion cores, and thus II–VI compounds have larger band gaps than comparable III–V compounds.

Gallium arsenide is the most important of all the compound semiconductors and is used in many electronic devices. GaAs has been used for a long time for discrete components in microwave circuits. Today, many digital integrated circuits are made with GaAs. The GaAs *metal-semiconductor field-effect transistors* (MESFETs) are the most widely used GaAs transistors (Fig. 13.50).

GaAs MESFETs offer some advantages over silicon as devices for use in high-speed digital integrated circuits. Some of these are:

1. Electrons travel faster in n-GaAs as is indicated by their higher mobility in GaAs than in Si [$\mu_n = 0.720\ m^2/(V \cdot s)$ for GaAs versus $0.135\ m^2/(V \cdot s)$ for Si].

2. Because of its larger band gap of 1.47 eV and the absence of a critical-gate oxide, GaAs devices are said to have better radiation resistance. This consideration is important for space and military applications.

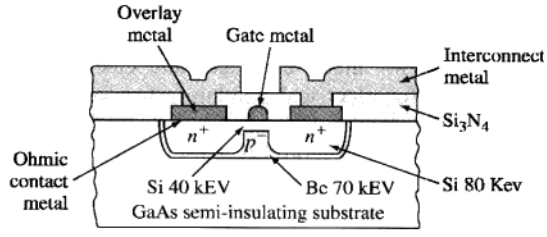

Figure 13.50
Cross-sectional view of a GaAs MESFET.
[From A.N. Sato et al., IEEE Electron. Devices Lett., 9(5):238 (1988). Copyright 1988. Used by permission of IEEE.]

Unfortunately, the major limitation of GaAs technology is that the yield for complex IC circuitry is much lower than for silicon due mainly to the fact that GaAs contains more defects in the base material than silicon. The cost of producing the base material is also higher for GaAs than silicon. However, the use of GaAs is expanding, and much research is being done in this area.

EXAMPLE PROBLEM 13.10

a. Calculate the intrinsic electrical conductivity of GaAs at (1) room temperature (27°C) and (2) 70°C.
b. What fraction of the current is carried by the electrons in the intrinsic GaAs at 27°C?

■ **Solution**

a. (1) σ at 27°C:

$$\begin{aligned}\sigma &= n_i q(\mu_n + \mu_p)\\ &= (1.4 \times 10^{12}\ \text{m}^{-3})(1.60 \times 10^{-19}\ \text{C})[0.720\ \text{m}^2/(\text{V}\cdot\text{s}) + 0.020\ \text{m}^2/(\text{V}\cdot\text{s})]\\ &= 1.66 \times 10^{-7}\ (\Omega\cdot\text{m})^{-1}\ \blacktriangleleft\end{aligned}$$

(2) σ at 70°C:

$$\sigma = \sigma_0 e^{-E_g/2kT} \qquad (13.16a)$$

$$\frac{\sigma_{343}}{\sigma_{300}} = \frac{\exp\{-1.47\ \text{eV}/[(2)(8.62 \times 10^{-5}\ \text{eV/K})(343\ \text{K})]\}}{\exp\{-1.47\ \text{eV}/[(2)(8.62 \times 10^{-5}\ \text{eV/K})(300\ \text{K})]\}}$$

$$\begin{aligned}\sigma_{343} &= \sigma_{300} e^{3.56} = 1.66 \times 10^{-7}\ (\Omega\cdot\text{m})^{-1}\ (35.2)\\ &= 5.84 \times 10^{-6}\ (\Omega\cdot\text{m})^{-1}\ \blacktriangleleft\end{aligned}$$

b. $$\frac{\sigma_n}{\sigma_n + \sigma_p} = \frac{n_i q \mu_n}{n_i q(\mu_n + \mu_p)} = \frac{0.720\ \text{m}^2/(\text{V}\cdot\text{s})}{0.720\ \text{m}^2/(\text{V}\cdot\text{s}) + 0.020\ \text{m}^2(\text{V}\cdot\text{s})} = 0.973\ \blacktriangleleft$$

13.8 ELECTRICAL PROPERTIES OF CERAMICS

Ceramic materials are used for many electrical and electronic applications. Many types of ceramics are used for electrical insulators for low- and high-voltage electric currents. Ceramic materials also find application in various types of capacitors, especially where miniaturization is required. Other types of ceramics called *piezoelectrics* can convert weak pressure signals into electrical signals, and vice versa.

Before discussing the electrical properties of the various types of ceramic materials, let us first briefly look at some of the basic properties of insulators, or **dielectrics** as they are sometimes called.

13.8.1 Basic Properties of Dielectrics

There are three important properties common to all insulators or dielectrics: (1) the *dielectric constant,* (2) the *dielectric breakdown* strength, and (3) the loss factor.

Dielectric Constant Consider a simple parallel-plate **capacitor**[4] with metal plates of area A separated by distance d, as shown in Fig. 13.51. Consider first the case in which the space between the plates is a vacuum. If a voltage V is applied across the plates, one plate will acquire a net charge of $+q$ and the other a net charge of $-q$. The charge q is found to be directly proportional to the applied voltage V as

$$q = CV \qquad \text{or} \qquad C = \frac{q}{V} \tag{13.23}$$

where C is a proportionality constant called the **capacitance** of the capacitor. The SI unit of capacitance is coulombs per volt (C/V), or the *farad* (F). Thus,

$$1 \text{ farad} = \frac{1 \text{ coulomb}}{\text{volt}}$$

Since the farad is a much larger unit of capacitance than is normally encountered in electrical circuitry, the commonly used units are the *picofarad* ($1 \text{ pF} = 10^{-12}$ F) and the *microfarad* ($1\ \mu\text{F} = 10^{-6}$ F).

The capacitance of a capacitor is a measure of its ability to store electric charge. The more charge stored at the upper and lower plates of a capacitor, the higher is its capacitance.

The capacitance C for a parallel-plate capacitor whose area dimensions are much greater than the separation distance of the plates is given by

$$C = \epsilon_0 \frac{A}{d} \tag{13.24}$$

where ϵ_0 = permittivity of free space $= 8.854 \times 10^{-12}$ F/m.

When a dielectric (electrical insulator) fills the space between the plates (Fig. 13.52), the capacitance of the capacitor is increased by a factor κ, which is called the **dielectric constant** of the dielectric material. For a parallel-plate capacitor

[4]A **capacitor** is a device that stores electric energy.

with a dielectric between the capacitor plates,

$$C = \frac{\kappa \epsilon_0 A}{d} \tag{13.25}$$

Table 13.7 lists the dielectric constants for some ceramic insulator materials.

The energy stored in a capacitor of a given volume at a given voltage is increased by the factor of the dielectric constant when the dielectric material is present. By using a material with a very high dielectric constant, very small capacitors with high capacitances can be produced.

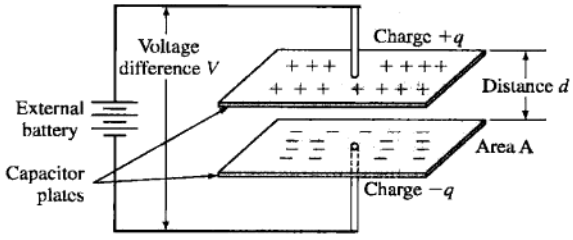

Figure 13.51
Simple parallel-plate capacitor.

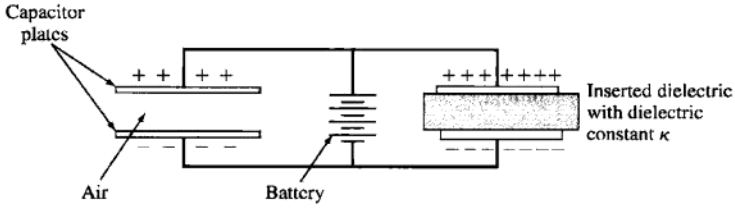

Figure 13.52
Two parallel-plate capacitors under the same applied voltage. The capacitor on the right has a dielectric (insulator inserted between the plates), and as a result the charge on the plates is increased by a factor of κ above that on the plates of the capacitor without the dielectric.

Table 13.7 Electrical properties of some ceramic insulator materials

Material	Volume resistivity ($\Omega \cdot$ m)	Dielectric strength		Dielectric constant κ		Loss factor	
		V/mil	kV/mm	60 Hz	10^6 Hz	60 Hz	10^6 Hz
Electrical porcelain insulators	10^{11}–10^{13}	55–300	2–12	6	···	0.06	
Steatite insulators	$>10^{12}$	145–280	6–11	6	6	0.008–0.090	0.007–0.025
Fosterite insulators	$>10^{12}$	250	9.8	···	6	···	0.001–0.002
Alumina insulators	$>10^{12}$	250	9.8	···	9	···	0.0008–0.009
Soda-lime glass	···	···	···	···	7.2	···	0.009
Fused silica	···	8	···	···	3.8	···	0.00004

Source: Materials Selector, *Mater. Eng.*, December 1982.

Dielectric Strength Another property besides the dielectric constant that is important in evaluating dielectrics is the **dielectric strength.** This quantity is a measure of the ability of the material to hold energy at high voltages. Dielectric strength is defined as the voltage per unit length (electric field or voltage gradient) at which failure occurs and thus is the maximum electric field that the dielectric can maintain without electrical breakdown.

Dielectric strength is most commonly measured in volts per mil (1 mil = 0.001 in.) or kilovolts per millimeter. If the dielectric is subjected to a voltage gradient that is too intense, the strain of the electrons or ions in trying to pass through the dielectric may exceed its dielectric strength. If the dielectric strength is exceeded, the dielectric material begins to break down and the passage of current (electrons) occurs. Table 13.7 lists the dielectric strengths for some ceramic insulator materials.

Dielectric Loss Factor If the voltage used to maintain the charge on a capacitor is sinusoidal, as is generated by an alternating current, the current leads the voltage by 90 degrees when a loss-free dielectric is between the plates of a capacitor. However, when a real dielectric is used in the capacitor, the current leads the voltage by $90° - \delta$, where the angle δ is called the *dielectric loss angle.* The product of $\kappa \tan \delta$ is designated the *loss factor* and is a measure of the electric energy lost (as heat energy) by a capacitor in an ac circuit. Table 13.7 lists the loss factors for some ceramic insulator materials.

EXAMPLE PROBLEM 13.11

A simple parallel-plate capacitor is to be made to store 5.0×10^{-6} C at a potential of 8000 V. The separation distance between the plates is to be 0.30 mm. Calculate the area (in square meters) that the plates must have if the dielectric between the plates is (*a*) a vacuum ($\kappa = 1$) and (*b*) alumina ($\kappa = 9$). ($\epsilon_0 = 8.85 \times 10^{-12}$ F/m.)

■ **Solution**

$$C = \frac{q}{V} = \frac{5.0 \times 10^{-6}\,\text{C}}{8000\,\text{V}} = 6.25 \times 10^{-10}\,\text{F}$$

$$A = \frac{Cd}{\epsilon_0 \kappa} = \frac{(6.25 \times 10^{-10}\,\text{F})(0.30 \times 10^{-3}\,\text{m})}{(8.85 \times 10^{-12}\,\text{F/m})(\kappa)}$$

a. For vacuum, $\kappa = 1$: $A = 0.021\,\text{m}^2$
b. For alumina, $\kappa = 9$: $A = 2.35 \times 10^{-3}\,\text{m}^2$

As can be seen by these calculations, the insertion of a material with a high dielectric constant can appreciably reduce the area of the plates required.

13.8.2 Ceramic Insulator Materials

Ceramic materials have electrical and mechanical properties that make them especially suitable for many insulator applications in the electrical and electronic industries. The ionic and covalent bonding in ceramic materials restricts electron and ion mobility and thus makes these materials good electrical insulators. These bondings make most ceramic materials strong but relatively brittle. The chemical compositions and microstructure of electrical- and electronic-grade ceramics must be more closely

controlled than for structural ceramics such as bricks or tiles. Some aspects of the structure and properties of several insulator ceramic materials will now be discussed.

Electrical Porcelain Typical electrical porcelain consists of approximately 50 percent clay ($Al_2O_3 \cdot 2SiO_2 \cdot 2H_2O$), 25 percent silica ($SiO_2$), and 25 percent feldspar ($K_2O \cdot Al_2O_3 \cdot 6SiO_2$). This composition makes a material that has good green-body plasticity and a wide firing temperature range at a relatively low cost. The major disadvantage of electrical insulator material is that it has a high power-loss factor compared to other electrical insulator materials (Table 13.7), which is due to highly mobile alkali ions. Figure 11.33 shows the microstructure of an electrical porcelain material.

Steatite Steatite porcelains are good electrical insulators because they have low power-loss factors, low moisture absorption, and good impact strength and are used extensively by the electronic and electrical appliance industries. Industrial steatite compositions are based on about 90 percent talc ($3MgO \cdot 4SiO_2 \cdot H_2O$) and 10 percent clay. The microstructure of fired steatite consists of enstatite ($MgSiO_3$) crystals bonded together by a glassy matrix.

Fosterite Fosterite has the chemical formula Mg_2SiO_4 and thus has no alkali ions in a vitreous phase so that it has a higher resistivity and lower electrical loss with increasing temperature than the steatite insulators. Fosterite also has lower-loss dielectric properties at high frequencies (Table 13.7).

Alumina Alumina ceramics have aluminum oxide (Al_2O_3) as the crystalline phase bonded with a glassy matrix. The glass phase, which is normally alkali-free, is compounded from mixtures of clay, talc, and alkaline earth fluxes and is usually alkali-free. Alumina ceramics have relatively high dielectric strengths and low dielectric losses along with relatively high strengths. Sintered alumina (99 percent Al_2O_3) is widely used as a substrate for electronic-device applications because of its low dielectric losses and smooth surface. Alumina is also used for ultralow-loss applications where a large energy transfer through a ceramic window is necessary as, for example, for radomes.

13.8.3 Ceramic Materials for Capacitors

Ceramic materials are commonly used as dielectric materials for capacitors, with disk ceramic capacitors being by far the most common type of ceramic capacitor (Fig. 13.53). These very small flat-disk ceramic capacitors consist mainly of barium titanate ($BaTiO_3$) along with other additives (Table 13.8). $BaTiO_3$ is used because of its very high dielectric constant of 1200 to 1500. With additives its dielectric constant can be raised to values of many thousands. Figure 13.53b shows the stages in the manufacture of one type of disk ceramic capacitor. In this type of capacitor, a silver layer on the top and bottom of the disk provides the metal "plates" of the capacitor. For very high capacitances with a minimum-size device, small, multilayered ceramic capacitors have been developed.

Ceramic chip capacitors are used in some ceramic-based thick-film hybrid electronic circuits. Chip capacitors can provide appreciably higher capacitance per unit area values and can be added to the thick-film circuit by a simple soldering or bonding operation.

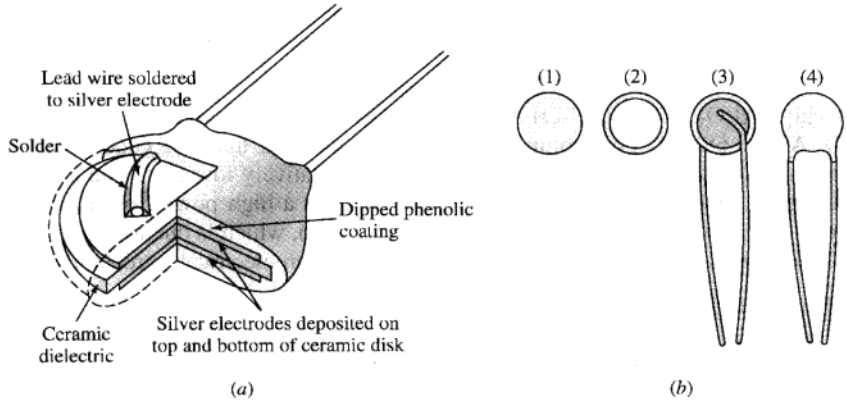

Figure 13.53
Ceramic capacitors. (*a*) Section showing construction.
(*Courtesy of Sprague Products Co.*)
(*b*) Steps in manufacture: (1) after firing ceramic disk; (2) after applying silver electrodes; (3) after soldering leads; (4) after applying dipped phenolic coating.
(*Used by permission of Radio Materials Corporation.*)

Table 13.8 Representative formulations for some ceramic dielectric materials for capacitors

Dielectric constant κ	Formulation
325	$BaTiO_3 + CaTiO_3$ + low % $Bi_2Sn_3O_9$
2100	$BaTiO_3$ + low % $CaZrO_3$ and Nb_2O_5
6500	$BaTiO_3$ + low % $CaZrO_3$ or $CaTiO_3 + BaZrO_3$

Source: C.A. Harper (ed.), *Handbook of Materials and Processes for Electronics*, McGraw-Hill, 1970, pp. 6–61.

13.8.4 Ceramic Semiconductors

Some ceramic compounds have semiconducting properties that are important for the operation of some electrical devices. One of these devices is the **thermistor,** or thermally sensitive resistor, which is used for temperature measurement and control. For our discussion we shall be concerned with the *negative temperature coefficient* (NTC) type of thermistor whose resistance decreases with increasing temperature. That is, as the temperature increases, the thermistor becomes more conductive, as in the case of a silicon semiconductor.

The ceramic semiconducting materials most commonly used for NTC thermistors are sintered oxides of the elements Mn, Ni, Fe, Co, and Cu. Solid-solution combinations of the oxides of these elements are used to obtain the necessary range of electrical conductivities with temperature changes.

Let us first consider the ceramic compound magnetite, Fe_3O_4, which has a relatively low resistivity of about $10^{-5}\ \Omega \cdot m$ as compared to a value of about $10^{8}\ \Omega \cdot m$ for most regular transition metal oxides. Fe_3O_4 has the inverse spinel structure with

the composition $FeO \cdot Fe_2O_3$ that can be written as

$$Fe^{2+}(Fe^{3+}, Fe^{3+})O_4$$

In this structure the oxygen ions occupy FCC lattice sites, with the Fe^{2+} ions in octahedral sites and the Fe^{3+} ions half in octahedral sites and half in tetrahedral sites. The good electrical conductivity of Fe_3O_4 is attributed to the random location of the Fe^{2+} and Fe^{3+} ions in the octahedral sites so that electron "hopping" (transfer) can take place between the Fe^{2+} ions and Fe^{3+} ions while maintaining charge neutrality. The structure of Fe_3O_4 is discussed further in Sec. 15.10.

The electrical conductivities of metal oxide semiconducting compounds for thermistors can be controlled by forming solid solutions of different metal oxide compounds. By combining a low-conducting metal oxide with a high-conducting one with a similar structure, a semiconducting compound with an intermediate conductivity can be produced. This effect is illustrated in Fig. 13.54, which shows how the conductivity of Fe_3O_4 is reduced gradually by adding increasing amounts in solid

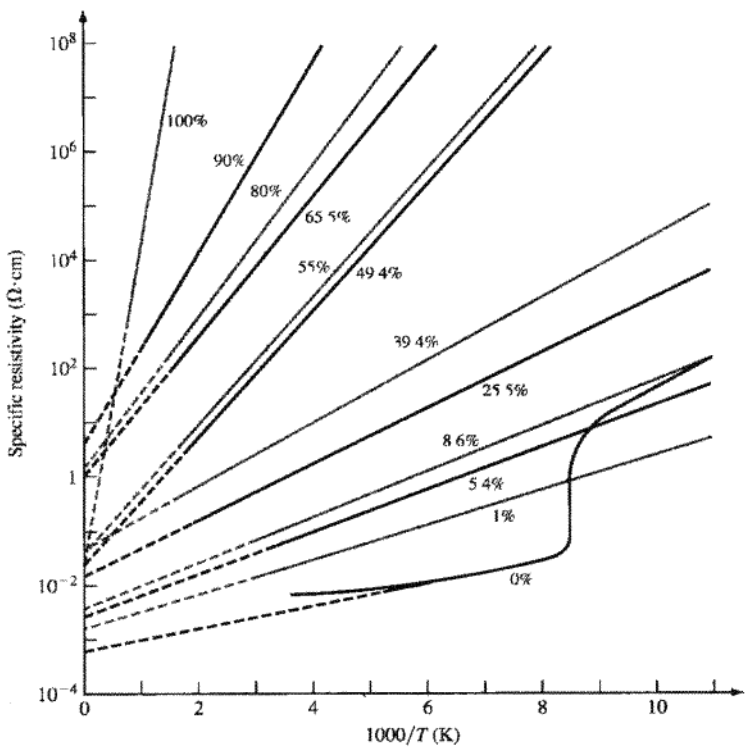

Figure 13.54
Specific resistivity of solid solution of Fe_3O_4 and $MgCr_2O_4$. Mole percent $MgCr_2O_4$ is indicated on the curves
(from E.J. Verwey, P.W. Haagman, and F.C. Romeijn, J. Chem. Phys., 15:181(1947))

solution of $MgCr_2O_4$. Most NTC thermistors with controlled temperature coefficients of resistivity are made of solid solutions of Mn, Ni, Fe, and Co oxides.

13.8.5 Ferroelectric Ceramics

Ferroelectric Domains Some ceramic ionic crystalline materials have unit cells that do not have a center of symmetry, and as a result their unit cells contain a small electric dipole and are called ferroelectric. An industrially important ceramic material in this class is barium titanate, $BaTiO_3$. Above 120°C, $BaTiO_3$ has the regular cubic symmetrical perovskite crystal structure (Fig. 13.55*a*). Below 120°C, the central Ti^{4+} ion and the surrounding O^{2-} ions of the $BaTiO_3$ unit cell shift slightly in opposite directions to create a small electric dipole moment (Fig. 13.55*b*). This shifting of the ion positions at the critical temperature of 120°C, called the **Curie temperature,** changes the crystal structure of $BaTiO_3$ from cubic to slightly tetragonal.

On a larger scale, solid barium titanate ceramic material has a domain structure (Fig. 13.56) in which the small electric dipoles of the unit cells line up in one direction. The resultant dipole moment of a unit volume of this material is the sum of the small dipole moments of the unit cells. If polycrystalline barium titanate is slowly cooled through its Curie temperature in the presence of a strong electric field, the dipoles of all the domains tend to line up in the direction of the electric field to produce a strong dipole moment per unit volume of the material.

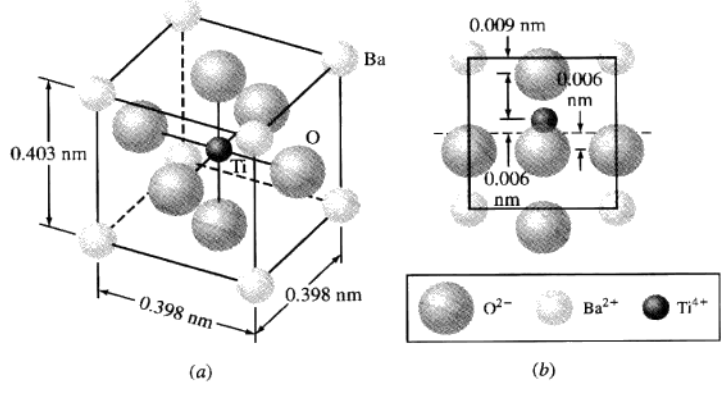

MatVis

Figure 13.55
(*a*) The structure of $BaTiO_3$ above 120°C is cubic. (*b*) The structure of $BaTiO_3$ below 120°C (its Curie temperature) is slightly tetragonal due to a slight shift of the Ti^{4+} central ion with respect to the surrounding O^{2-} ions of the unit cell. A small electric dipole moment is present in this asymmetrical unit cell.
(From K.M. Ralls, T.H. Courtney and J. Wulff, "An Introduction to Materials Science and Engineering," Wiley, 1976, p. 610. Reprinted with permission of John Wiley & Sons, Inc.)

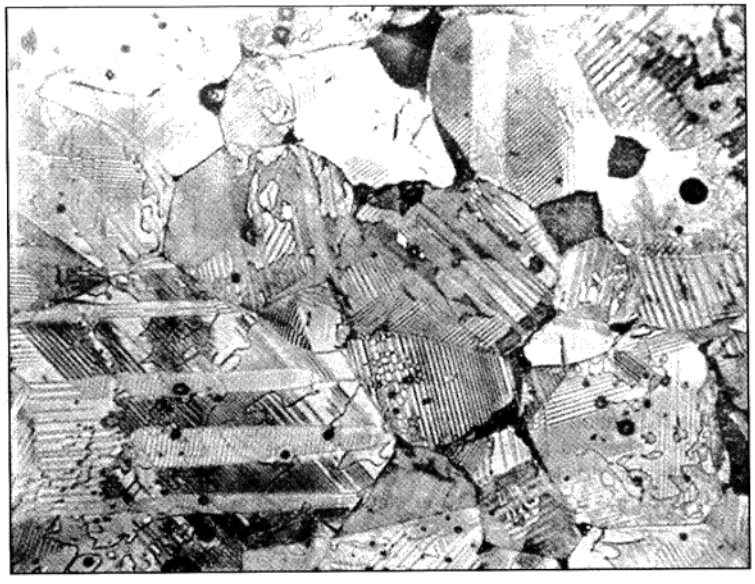

Figure 13.56
Microstructure of barium titanate ceramic showing different ferroelectric domain orientations as revealed by etching. (Magnification 500×.)
(After R.D. DeVries and J.E. Burke, J. Am. Ceram. Soc., **40:***200 (1957).)*

The Piezoelectric Effect[5] Barium titanate and many other ceramic materials exhibit what is called the **piezoelectric (PZT) effect,** illustrated schematically in Fig. 13.57. Let us consider a sample of a ferroelectric ceramic material that has a resultant dipole moment due to the alignment of many small unit dipoles, as indicated in Fig. 13.57*a*. In this material, there will be an excess of positive charge at one end and negative charge at the other end in the direction of the polarization. Now let us consider the sample when compressive stresses are applied, as shown in Fig. 13.57*b*. The compressive stresses reduce the length of the sample between the applied stresses and thus reduce the distance between the unit dipoles, which in turn reduces the overall dipole moment per unit volume of the material. The change in dipole moment of the material changes the charge density at the ends of the sample and thus changes the voltage difference between the ends of the sample if they are insulated from each other.

[5]The prefix *piezo-* means "pressure" and comes from the Greek word *piezein*, which means "to press."

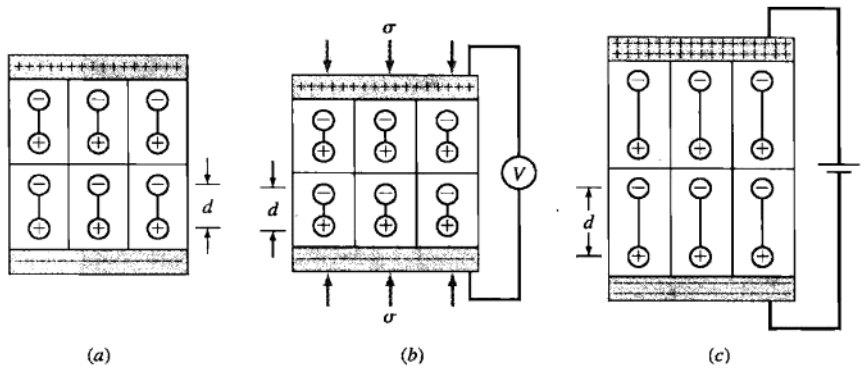

Figure 13.57
(*a*) Schematic illustration of electric dipoles within a piezoelectric material. (*b*) Compressive stresses on material cause a voltage difference to develop due to change in electric dipoles. (*c*) Applied voltage across ends of a sample causes a dimensional change and changes the electric dipole moment.
(After L.H. Van Vlack, "Elements of Materials Science and Engineering," 4th ed., Addison-Wesley, 1980, Fig. 8-6.3, p. 305.)

On the other hand, if an electric field is applied across the ends of the sample, the charge density at each end of the sample will be changed (Fig. 13.57*c*). This change in charge density will cause the sample to change dimensions in the direction of the applied field. In the case of Fig. 13.57*c*, the sample is slightly elongated due to an increased amount of positive charge attracting the negative poles of the dipoles, and the reverse at the other end of the sample. Thus, the piezoelectric effect is an electromechanical effect by which mechanical forces on a ferroelectric material can produce an electrical response, or electrical forces a mechanical response.

Piezoelectric ceramics have many industrial applications. Examples for the case of converting mechanical forces into electrical responses are the piezoelectric compression accelerometer (Fig. 13.58*a*), which can measure vibratory accelerations occurring over a wide range of frequencies, and the phonograph cartridge in which electrical responses are "picked up" from a stylus vibrating in record grooves. An example for the case of converting electrical forces into mechanical responses is the ultrasonic cleaning **transducer** that is caused to vibrate by ac power input so that it can induce violent agitation of the liquid in a tank (Fig. 13.58*b*). Another example of this type is the underwater sound transducer in which electric power input causes the transducer to vibrate to transmit sound waves.

Piezoelectric Materials Although $BaTiO_3$ is commonly used as a piezoelectric material, it has largely been replaced by other piezoelectric ceramic materials. Of particular importance are the ceramic materials made from solid solutions of lead

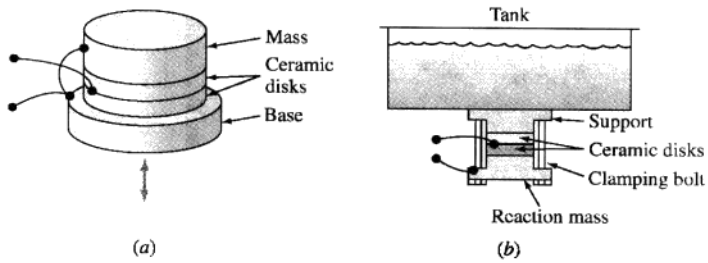

Figure 13.58
(*a*) Piezoelectric compression accelerometer. (*b*) Piezoelectric ceramic elements in an ultrasonic cleaning apparatus.
(*Courtesy of Morgan Electric Ceramics (formerly Vernitron), Bedford, Ohio, USA.*)

zirconate ($PbZrO_3$) and lead titanate ($PbTiO_3$) to make what are called *PZT ceramics.* The PZT materials have a broader range of piezoelectric properties, including a higher Curie temperature, than $BaTiO_3$.

13.9 NANOELECTRONICS

The ability to characterize and study nanomaterials and nanodevices has improved significantly with the advent of *scanning probe microscope* (SPM) techniques (Chap. 4). Researchers have shown that by varying the imposed voltage between the STM tip and the surface, it is possible to pick up an atom (or a cluster of atoms) and manipulate its position on the surface. For instance, scientists have used the STM to create dangling (incomplete) bonds on the surface of silicon at specific positions. Then, by exposing the sample's surface to gases containing molecules of interest, these dangling bonds can become the sites of molecular adsorption. By positioning the dangling bonds and therefore the adsorbed molecules at specific points on the surface, nanoscale molecular electronics can be designed. Another example of the use of STM in nanotechnology is the formation of *quantum corrals.* STM is used to position metal atoms on the surface in a circular or elliptical form. Since electrons are confined to the path of the metal atoms, a quantum corral is formed that represents a "hot zone" of electron waves. This is similar to a hot zone of electromagnetic waves in a dish antenna. The size of the corral is in tens of nanometers. If a magnetic atom such as a cobalt atom is placed at one focus point in an elliptical corral with two focus points, some of its properties (such as a change in the surface electrons due to the cobalt's magnetism) appear at the other focus point (Fig. 13.59). On the other hand, if the single atom is placed at nonfocal positions, its properties will not show up anywhere else in the corral. The spot at which the quantum corral is formed is called *a quantum mirage.* A quantum mirage is envisioned as a vehicle for transfering data at the

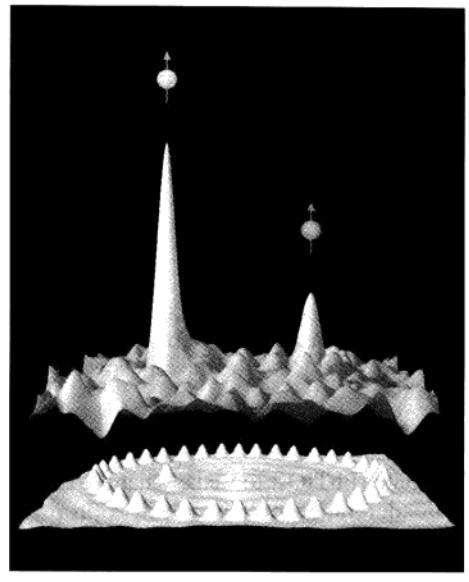

Figure 13.59
In this figure a single atom of cobalt is placed at one of the focus points of the elliptical corral of 36 cobalt atoms (left peak). Some of its properties then appear at the other focus point (right peak) where no atoms exist.
(*IBM Research.*)

nanorange scale. Although this may be many years in the future, the overall goal is to develop techniques that allow delivery of current in nanodevices where conventional electrical wiring is impossible because of the small dimensions.

13.10 SUMMARY

In the classic model for electrical conduction in metals, the outer valence electrons of the atoms of the metal are assumed to be free to move between the positive-ion cores (atoms without their valence electrons) of the metal lattice. In the presence of an applied electric potential, the free electrons attain a directed drift velocity. The movement of electrons and their associated electric charge in a metal constitute an electric current. By convention, electric current is considered to be positive charge flow, which is in the opposite direction to electron flow.

In the energy-band model for electrical conduction in metals, the valence electrons of the metal atoms interact and interpenetrate each other to form energy bands. Since the energy bands of the valence electrons of metal atoms overlap, producing partially filled composite energy bands, very little energy is required to excite the highest-energy electrons so that they become free to be conductive. In insulators, the valence electrons are tightly bound to their atoms by ionic and covalent bonding and are not free to conduct electricity unless highly energized. The energy-band model for an insulator consists of a lower filled valence band and a higher empty conduction band. The valence band is separated from the conduction band by a large energy gap (about 6 to 7 eV, for example). Thus, for insulators to be conductive, a large amount of energy must be applied to cause the valence electrons to "jump" the gap. Intrinsic semiconductors have a relatively small energy gap (i.e., about 0.7 to 1.1 eV) between their valence and conduction bands. By doping the intrinsic semiconductors with impurity atoms to make them extrinsic, the amount of energy required to cause semiconductors to be conductive is greatly reduced.

Extrinsic semiconductors can be n-type or p-type. The n-type (negative) semiconductors have electrons for their majority carriers. The p-type (positive) semiconductors have holes (missing electrons) for their majority charge carriers. By fabricating pn junctions in a single crystal of a semiconductor such as silicon, various types of semiconducting devices can be made. For example, pn junction diodes and npn transistors can be produced by using these junctions. Modern microelectronic technology has developed to such an extent that thousands of transistors can be placed on a "chip" of semiconducting silicon less than about 0.5 cm square and about 0.2 mm thick. Complex microelectronic technology has made possible highly sophisticated microprocessors and computer memories.

Ceramic materials are usually good electrical and thermal insulators due to the absence of conduction electrons, and thus many ceramics are used for electrical insulation and refractories. Some ceramic materials can be highly polarized with electric charge and are used for dielectric materials for capacitors. Permanent polarization of some ceramic materials produces piezoelectric properties that permit these materials to be used as electromechanical transducers. Other ceramic materials, for example, Fe_3O_4, are semiconductors and find application for thermistors for temperature measurement.

Nanotechnology research is making progress toward manufacturing electronic devices with nanometer dimensions. Quantum corrals are envisioned to deliver currents in nanodevices where electrical wiring is impossible.

13.11 DEFINITIONS

Sec. 13.1

Electric current: the time rate passage of charge through material; electric current i is the number of coulombs per second that passes a point in a material. The SI unit for electric current is the ampere (1 A = 1 C/s).

Electrical resistance R: the measure of the difficulty of electric current's passage through a volume of material. Resistance increases with the length and increases with decreasing cross-sectional area of the material through which the current passes. SI unit: ohm (Ω).

Electrical resistivity ρ_e: a measure of the difficulty of electric current's passage through a *unit* volume of material. For a volume of material, $\rho_e = RA/l$, where R = resistance of material, Ω; l = its length, m; A = its cross-sectional area, m^2. In SI units, ρ_e = ohm-meters ($\Omega \cdot m$).

Electrical conductivity σ_e: a measure of the ease with which electric current passes through a unit volume of material. Units: $(\Omega \cdot m)^{-1}$. σ_e is the inverse of ρ_e.

Electrical conductor: a material with a high electrical conductivity. Silver is a good conductor and has a $\sigma_e = 6.3 \times 10^7\ (\Omega \cdot m)^{-1}$.

Electrical insulator: a material with a low electrical conductivity. Polyethylene is a poor conductor and has a $\sigma_e = 10^{-15}$ to $10^{-17}\ (\Omega \cdot m)^{-1}$.

Semiconductor: a material whose electrical conductivity is approximately midway between the values for good conductors and insulators. For example, pure silicon is a semiconducting element and has $\sigma_e = 4.3 \times 10^{-4}\ (\Omega \cdot m)^{-1}$ at 300 K.

Electric current density J: the electric current per unit area. SI units: amperes/meter^2 (A/m^2).

Sec. 13.2

Energy-band model: in this model, the energies of the bonding valence electrons of the atoms of a solid form a band of energies. For example, the 3*s* valence electrons in a piece of sodium form a 3*s* energy band. Since there is only one 3*s* electron (the 3*s* orbital can contain two electrons), the 3*s* energy band in sodium metal is half-filled.

Valence band: the energy band containing the valence electrons. In a conductor, the valence band is also the conduction band. The valence band in a conducting metal is not full, and so some electrons can be energized to levels within the valence band and become conductive electrons.

Conduction band: the unfilled energy levels into which electrons can be excited to become conductive electrons. In semiconductors and insulators, there is an energy gap between the filled lower valence band and the upper empty conduction band.

Sec. 13.3

Intrinsic semiconductor: a semiconducting material that is essentially pure and for which the energy gap is small enough (about 1 eV) to be surmounted by thermal excitation; current carriers are electrons in the conduction band and holes in the valence band.

Electron: a negative charge carrier with a charge of 1.60×10^{-19} C.

Hole: a positive charge carrier with a charge of 1.60×10^{-19} C.

Sec. 13.4

n-type extrinsic semiconductor: a semiconducting material that has been doped with an n-type element (e.g., silicon doped with phosphorus). The n-type impurities donate electrons that have energies close to the conduction band.

Donor levels: in the band theory, local energy levels near the conduction band.

Acceptor levels: in the band theory, local energy levels close to the valence band.

p-type extrinsic semiconductor: a semiconducting material that has been doped with a p-type element (e.g., silicon doped with aluminum). The p-type impurities provide electron holes close to the upper energy level of the valence band.

Majority carriers: the type of charge carrier most prevalent in a semiconductor; the majority carriers in an n-type semiconductor are conduction electrons, and in a p-type semiconductor, they are conduction holes.

Minority carriers: the type of charge carrier in the lowest concentration in a semiconductor. The minority carriers in n-type semiconductors are holes, and in p-type semiconductors, they are electrons.

Sec. 13.5

pn junction: an abrupt junction or boundary between p- and n-type regions within a single crystal of a semiconducting material.

Bias: voltage applied to two electrodes of an electronic device.

Forward bias: bias applied to a pn junction in the conducting direction; in a pn junction under forward bias, majority-carrier electrons and holes flow toward the junction so that a large current flows.

Reverse bias: bias applied to a pn junction so that little current flows; in a pn junction under reverse bias, majority-carrier electrons and holes flow away from the junction.

Rectifier diode: a pn junction diode that converts alternating current to direct current (AC to DC).

Bipolar junction transistor: a three-element, two-junction semiconducting device. The three basic elements of the transistor are the emitter, base, and collector. Bipolar junction transistors can be of the npn or pnp types. The emitter-base junction is forward-biased and the collector-base junction is reverse-biased so that the transistor can act as a current amplification device.

Sec. 13.8

Dielectric: an electrical insulator material.

Capacitor: an electric device consisting of conducting plates or foils separated by layers of dielectric material and capable of storing electric charge.

Capacitance: a measure of the ability of a capacitor to store electric charge. Capacitance is measured in farads; the units commonly used in electrical circuitry are the picofarad ($1\ \text{pF} = 10^{-12}\ \text{F}$) and the microfarad ($1\ \mu\text{F} = 10^{-6}\ \text{F}$).

Dielectric constant: the ratio of the capacitance of a capacitor using a material between the plates of a capacitor compared to that of the capacitor when there is a vacuum between the plates.

Dielectric strength: the voltage per unit length (electric field) at which a dielectric material allows conduction, that is, the maximum electric field that a dielectric can withstand without electrical breakdown.

Thermistor: a ceramic semiconductor device that changes in resistivity as the temperature changes and is used to measure and control temperature.

Ferroelectric material: a material that can be polarized by applying an electric field.

Curie temperature (of a ferroelectric material): the temperature at which a ferroelectric material on cooling undergoes a crystal structure change that produces spontaneous polarization in the material. For example, the Curie temperature of $BaTiO_3$ is 120°C.

Piezoelectric effect: an electromechanical effect by which mechanical forces on a ferroelectric material can produce an electrical response and electrical forces produce a mechanical response.

Transducer: a device that is actuated by power from one source and transmits power in another form to a second system. For example, a transducer can convert input sound energy into an output electrical response.

13.12 PROBLEMS

Answers to problems marked with an asterisk are given at the end of the book.

Knowledge and Comprehension Problems

13.1 Describe the classic model for electrical conduction in metals.

13.2 Distinguish between (*a*) positive-ion cores and (*b*) valence electrons in a metallic crystal lattice such as sodium.

13.3 Write equations for the (*a*) macroscopic and (*b*) microscopic forms of Ohm's law. Define the symbols in each of the equations and indicate their SI units.

13.4 How is electrical conductivity related numerically to electrical resistivity?

13.5 Give two kinds of SI units for electrical conductivity.

13.6 Define the following quantities pertaining to the flow of electrons in a metal conductor: (*a*) drift velocity, (*b*) relaxation time, and (*c*) electron mobility.

13.7 What causes the electrical resistivity of a metal to increase as its temperature increases? What is a phonon?

13.8 What structural defects contribute to the residual component of the electrical resistivity of a pure metal?

13.9 What effect do elements that form solid solutions have on the electrical resistivities of pure metals?

13.10 Why are the valence-electron energy levels broadened into bands in a solid block of a good conducting metal such as sodium?

13.11 Why don't the energy levels of the inner-core electrons of a block of sodium metal also form energy bands?

13.12 Why is the 3*s* electron energy band in a block of sodium only half-filled?

13.13 What explanation is given for the good electrical conductivity of magnesium and aluminum even though these metals have filled outer 3*s* energy bands?

13.14 How does the energy-band model explain the poor electrical conductivity of an insulator such as pure diamond?

13.15 Define an intrinsic semiconductor. What are the two most important elemental semiconductors?

13.16 What type of bonding does the diamond cubic structure have? Make a two-dimensional sketch of the bonding in the silicon lattice, and show how electron-hole pairs are produced in the presence of an applied field.

13.17 Why is a hole said to be an imaginary particle? Use a sketch to show how electron holes can move in a silicon crystal lattice.

13.18 Define electron and electron hole mobility as it pertains to charge movement in a silicon lattice. What do these quantities measure, and what are their SI units?

13.19 Explain, using an energy-band diagram, how electrons and electron holes are created in pairs in intrinsic silicon.

13.20 Explain why the electrical conductivity of intrinsic silicon and germanium increases with increasing temperature.

13.21 Define n-type and p-type extrinsic silicon semiconductors.

13.22 Draw energy-band diagrams showing donor or acceptor levels for the following:
(*a*) n-type silicon with phosphorus impurity atoms
(*b*) p-type silicon with boron impurity atoms

13.23 (*a*) When a phosphorus atom is ionized in an n-type silicon lattice, what charge does the ionized atom acquire? (*b*) When a boron atom is ionized in a p-type silicon lattice, what charge does the ionized atom acquire?

13.24 In semiconductors, what are dopants? Explain the process of doping by diffusion.

13.25 What are the majority and minority carriers in an n-type silicon semiconductor? In a p-type one?

13.26 Define the term *microprocessor.*

13.27 Describe the movement of majority carriers in a pn junction diode at equilibrium. What is the depletion region of a pn junction?

13.28 Describe the movement of the majority and minority carriers in a pn junction diode under reverse bias.

13.29 Describe the movement of the majority carriers in a pn junction diode under forward bias.

13.30 Describe how a pn junction diode can function as a current rectifier.

13.31 What is a zener diode? How does this device function? Describe a mechanism to explain its operation.

13.32 What are the three basic elements of a bipolar junction transistor?

13.33 Describe the flow of electrons and holes when an npn bipolar junction transistor functions as a current amplifier.

13.34 Why is a bipolar junction transistor called *bipolar*?

13.35 Describe the structure of a planar npn bipolar transistor.

13.36 Describe how the planar bipolar transistor can function as a current amplifier.

13.37 Describe the structure of an n-type metal oxide semiconductor field-effect transistor (NMOS).

13.38 Describe the photolithographic steps necessary to produce a pattern of an insulating layer of silicon dioxide on a silicon surface.

13.39 Describe the diffusion process for the introduction of dopants into the surface of a silicon wafer.

13.40 Describe the ion implantation process for introducing dopants into the surface of a silicon wafer.

13.41 Describe the general process for fabricating NMOS integrated circuits on a silicon wafer.

13.42 What are complementary metal oxide semiconductor (CMOS) devices? What are the advantages of CMOS devices over NMOS or PMOS devices?

13.43 What are three major applications for ceramic materials in the electrical-electronics industries?

13.44 Define the terms *dielectric, capacitor,* and *capacitance.* What is the SI unit for capacitance? What units are commonly used for capacitance in the electronics industry?

13.45 What is the dielectric constant of a dielectric material? What is the relationship among capacitance, dielectric constant, and the area and distance of separation between the plates of a capacitor?

13.46 What is the dielectric strength of a dielectric material? What units are used for dielectric strength? What is dielectric breakdown?

13.47 What is the dielectric loss angle and dielectric loss factor for a dielectric material? Why is a high dielectric loss factor undesirable?

13.48 What is the approximate composition of electrical porcelain? What is a major disadvantage of electrical porcelain as electrical insulative material?

13.49 What is the approximate composition of steatite? What desirable electrical properties does steatite have as an insulative material?

13.50 What is the composition of fosterite? Why is fosterite an excellent insulator material?

13.51 What is a thermistor? What is an NTC thermistor?

13.52 What materials are used to make NTC thermistors?

13.53 What is believed to be the mechanism for electrical conduction in Fe_3O_4?

13.54 What are ferroelectric domains? How can they be lined toward one direction?

13.55 Describe the piezoelectric effect for producing an electrical response with the application of pressure on a ferroelectric material. Do the same for producing a mechanical response by the application of an electrical force.

13.56 Describe several devices that utilize the piezoelectric effect.

13.57 What are the PZT piezoelectric materials? In what ways are they superior to BaTiO3 piezoelectric materials?

Application and Analysis Problems

***13.58** Calculate the resistance of an iron rod 0.720 cm in diameter and 0.850 m long at 20°C. [ρ_e (20°C) = 10.0 $\times 10^{-6}$ $\Omega \cdot$ cm.]

13.59 A nichrome wire must have a resistance of 120 Ω. How long must it be (in meters) if it has a 0.0015-in. diameter? [σ_c (nichrome) = 9.3×10^5 $(\Omega \cdot m)^{-}1$]

13.60 A wire 0.40 cm in diameter must carry a 25 A current.

(*a*) If the maximum power dissipation along the wire is 0.025 W/cm, what is the minimum allowable electrical conductivity of the wire (give answer in SI units)?

(*b*) What is the current density in the wire?

13.61 Calculate the electrical resistivity (in ohm-meters) of a silver wire 15 m long and 0.030 m in diameter at 160°C. [ρ_e (Fe at 0°C) = 9.0×10^{-6} $\Omega \cdot$ cm.]

***13.62** At what temperature will an iron wire have the same electrical resistivity as an aluminum one at 35°C?

13.63 At what temperature will the electrical resistivity of an iron wire be 25.0×10^{-8} $\Omega \cdot$ m?

13.64 An iron wire is to conduct a 6.5 A current with a maximum voltage drop of 0.005 V/cm. What must be the minimum diameter of the wire in meters at (20°C)?

13.65 What is the ratio of the electron-to-hole mobility in silicon and germanium?

13.66 Calculate the number of germanium atoms per cubic meter.

13.67 Calculate the electrical resistivity of germanium at 300 K.

13.68 The electrical resistivity of pure germanium is 0.46 $\Omega \cdot$ m at 300 K. Calculate its electrical conductivity at 425°C.

13.69 The electrical resistivity of pure silicon is 2.3×10^3 $\Omega \cdot$ m at 300 K. Calculate its electrical conductivity at 325°C.

***13.70** A silicon wafer is doped with 7.0×10^{21} phosphorus atoms/m^3. Calculate (*a*) the electron and hole concentrations after doping and (*b*) the resultant electrical resistivity at 300 K. (Assume $n_i = 1.5 \times 10^{16}/m^3$ and $\mu_n = 0.1350$.)

13.71 Phosphorus is added to make an n-type silicon semiconductor with an electrical con-ductivity of 250 $\Omega \cdot m^{-1}$. Calculate the necessary number of charge carriers required.

13.72 A semiconductor is made by adding boron to silicon to give an electrical resistivity of 1.90 $\Omega \cdot m$. Calculate the concentration of carriers per cubic meter in the material. Assume $\mu_p = 0.048\ m^2/(V \cdot s)$.

13.73 A silicon wafer is doped with 2.50×10^{16} boron atoms/cm^3 plus 1.60×10^{16} phosphorus atoms/cm^3 at 27°C. Calculate (*a*) the electron and hole concentrations (carriers per cubic centimeter), (*b*) the electron and hole mobilities (use Fig. 13.26), and (*c*) the electrical resistivity of the material.

13.74 A silicon wafer is doped with 2.50×10^{15} phosphorus atoms/cm^3, 3.00×10^{17} boron atoms/cm^3, and 3.00×10^{17} arsenic atoms/cm^3. Calculate (*a*) the electron and hole concentrations (carriers per cubic centimeter), (*b*) the electron and hole mobilities (use Fig. 13.26), and (*c*) the electrical resistivity of the material.

***13.75** An arsenic-doped silicon wafer has an electrical resistivity of $7.50 \times 10^{-4}\ \Omega \cdot$ cm at 27°C. Assume intrinsic carrier mobilities and complete ionization.

(*a*) What is the majority-carrier concentration (carriers per cubic centimeter)?

(*b*) What is the ratio of arsenic to silicon atoms in this material?

13.76 A boron-doped silicon wafer has an electrical resistivity of $5.00 \times 10^{-4}\ \Omega \cdot cm$ at 27°C. Assume intrinsic carrier mobilities and complete ionization.

(*a*) What is the majority-carrier concentration (carriers per cubic centimeter)?

(*b*) What is the ratio of boron to silicon atoms in this material?

13.77 Describe the origin of the three stages that appear in the plot of ln α versus $1/T$ for an extrinsic silicon semiconductor (going from low to high temperatures). Why does the conductivity decrease just before the rapid increase due to intrinsic conductivity?

13.78 What fabrication techniques are used to encourage electrons from the emitter of an npn bipolar transistor to go right through to the collector?

13.79 How do NMOSs function as current amplifiers?

13.80 Why is silicon nitride (Si_3N_4) used in producing NMOS integrated circuits on a silicon wafer?

***13.81** Calculate the intrinsic electrical conductivity of GaAs at 125°C.
[$E_g = 1.47$ eV; $\mu_n = 0.720\ m^2/(V \cdot s)$; $\mu_p = 0.020\ m^2/(V \cdot s)$; $n_i = 1.4 \times 10^{12}\ m^{-3}$.]

13.82 Calculate the intrinsic electrical conductivity of InSb at 60°C and at 70°C.
[$E_g = 0.17$ eV; $\mu_n = 8.00\ m^2/(V \cdot s)$; $\mu_p = 0.045\ m^2/(V \cdot s)$; $n_i = 1.35 \times 10^{22}\ m^{-3}$.]

13.83 Calculate the intrinsic electrical conductivity of (*a*) GaAs and (*b*) InSb at 75°C.

13.84 What fraction of the current is carried by (*a*) electrons and (*b*) holes in (*i*) InSb, (*ii*) InB, and (*iii*) InP at 27°C?

13.85 What fraction of the current is carried by (*a*) electrons and (*b*) holes in (*i*) GaSb and (*ii*) GaP at 27°C?

13.86 A simple plate capacitor can store 7.0×10^{-5} C at a potential of 12,000 V. If a barium titanate dielectric material with $\kappa = 2100$ is used between the plates, which have an area of $5.0 \times 10^{-5}\ m^2$, what must be the separation distance between the plates?

13.87 A simple plate capacitor stores 6.5×10^{-5} C at a potential of 12,000 V. If the area of the plates is $3.0 \times 10^{-5}\ m^2$ and the distance between the plates is 0.18 mm, what must be the dielectric constant of the material between the plates?

13.88 Why is sintered alumina widely used as a substance for electronic device applications?

13.89 Why is $BaTiO_3$ used for high-value, small, flat-disk capacitors? How is the capacitance of $BaTiO_3$ capacitors varied? What are the four major stages in the manufacture of a flat-disk ceramic capacitor?

13.90 How is the electrical conductivity of metal oxide semiconductors for thermistors changed?

13.91 What change occurs in the unit cell of $BaTiO_3$ when it is cooled below 120°C? What is this transformation temperature called?

Synthesis and Evaluation Problems

13.92 Select the material for a conducting wire of diameter 20 mm that carries a current of 20 A. The maximum power dissipation is 4 W/m. (Use Table 13.1 and consider cost as a selection criterion.)

13.93 Design a N-type semiconductor based on Si that allows a constant conductivity of 25 $\Omega^{-1}\,m^{-1}$ at room temperature.

13.94 Design a P-type semiconductor based on Si that allows a constant conductivity of 25 $\Omega^{-1}\,m^{-1}$ at room temperature.

13.95 Consider various solid solutions of copper as listed below. Rank the following solid solutions based on the descending order of conductivity. Give reasons for your choices. (*i*) cu–1 wt % Zn, (*ii*) cu–1 wt % Ga and (*iii*) cu–1 wt % Cr.

13.96 Consider the Cu-Ni isomorphous phase system. Draw an approximate diagram showing the conductivity vs. alloy composition.

13.97 Silicon carbide (SiC) is a ceramic with semiconducting characteristics (E_g of 3.02 eV). Investigate the advantages of using SiC over Si as a semiconducting material.

13.98 Gallium nitride (GaN) is a ceramic with semiconducting characteristics (E_g of 3.45 eV). Investigate the advantages of using (GaN) over Si as a semiconducting material.

13.99 Indium nitride (InN) has a band gap, E_g, of of 0.65 eV. Gallium nitride (GaN) has a band gap, E_g, of 3.45 eV. It is possible to produce a mixture of GaN and InN varying the In (x) and Ga (1–x) ratio. What would be the advantage of such flexibility?

13.100 What are photovoltaics (investigte) and what are their applications? What are the best candidate semiconducting materials for photovoltaic applications?

CHAPTER 14

Optical Properties and Superconductive Materials

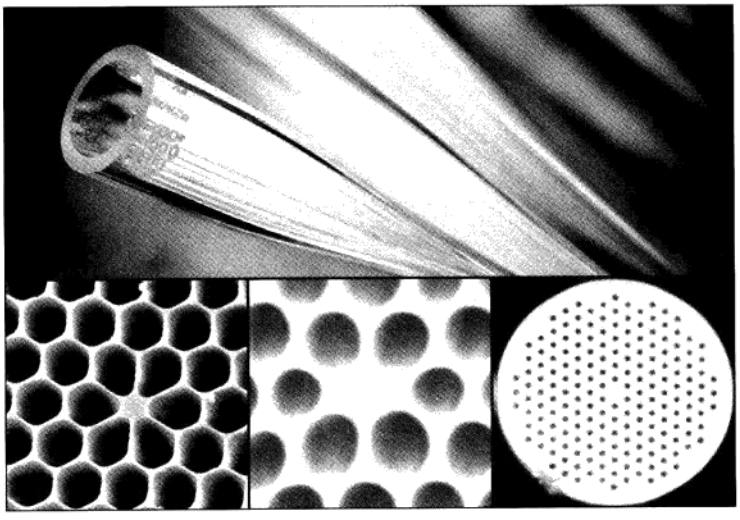

(*Courtesy of Crystal Fibre A/S.*)

A photonic crystal fiber is similar to a normal crystal in structure, with the exception that the repeat pattern exists in a much larger scale (micron range) and only transverse to the length of the fiber. The fiber is manufactured by stacking a number of silica glass tubes to form a cylinder. The cylinder is then drawn at elevated temperatures to a thin fiber with diameters on the order of tens of microns. After the manufacturing process, the fiber will resemble a honeycomb. Because of their structure, light conducted through the fibers can behave in ways that are not completely understood. For example, it is possible to allow light of a certain frequency to propagate along the fiber while other frequencies are blocked. Such characteristics can be used to manufacture devices such as wavelength-tunable light sources and optical switches. The chapter-opening image shows the structure of a photonic crystal fiber. The preforms are shown in the top figure and the cross sections of selected fibers are shown at the bottom.[1] ■

[1]http://www.rikei.co.jp/dbdata/products/producte249.html

LEARNING OBJECTIVES

By the end of this chapter, students will be able to . . .

1. Explain what phenomena can occur with light radiation as it passes from one medium into another.
2. Discuss why metallic materials are opaque to visible light.
3. Explain what determines the color of metallic materials.
4. Briefly describe the phenomenon of superconductivity.
5. Explain why amorphous materials are usually transparent.
6. Briefly describe the construction of a ruby laser.
7. Describe the mechanism of photon absorption for a semiconductor that contains electrically active defects.
8. Explain what laser means.
9. Briefly describe the advantages of high-temperature oxide superconductors.
10. Cite distinctions between opacity, translucency, and transparency.

14.1 INTRODUCTION

Optical properties of materials play an important role in much of today's high technology (Fig. 14.1). In this chapter, we will first examine some of the basics of the refraction, reflection, and absorption of light with some classes of materials. Next we will investigate how some materials interact with light radiation to produce luminescence. Then we will look into the stimulated emission of radiation by lasers. In the optical fibers part of this chapter, we shall see how the development of low light-loss optical fibers has led to the new optical-fiber communications systems.

Finally, we shall look into superconducting materials that have zero electrical resistivity below their critical temperatures, magnetic fields, and current densities. Until around 1987, the highest critical temperature for a superconducting material was about 25 K. In 1987, a spectacular discovery was made that some ceramic materials could be made superconductive up to about 100 K. This discovery set off a tremendous worldwide research effort that has created high expectations for future engineering developments. In this chapter, we will examine some aspects of the structure and properties of types I and II metallic superconductors as well as the new ceramic ones.

14.2 LIGHT AND THE ELECTROMAGNETIC SPECTRUM

Visible light is one form of electromagnetic radiation, with wavelengths extending from about 0.40 to 0.75 μm (Fig. 14.2). Visible light contains color bands ranging from violet through red, as shown in the enlarged scale of Fig. 14.2. The ultraviolet

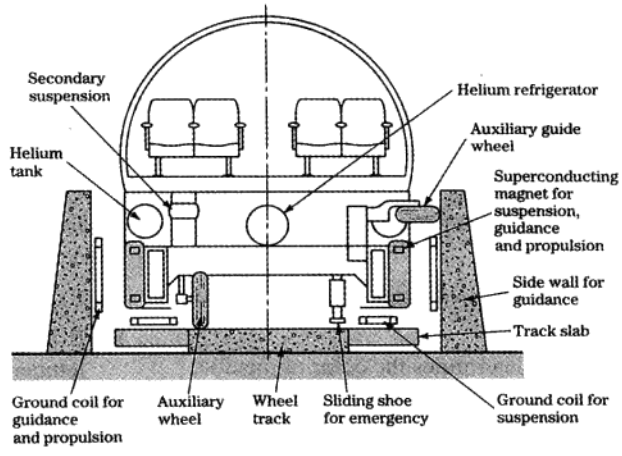

Figure 14.1
New technologies. Cross section of an advanced levitated train design (Japanese National Railway).
(From "Encyclopedia of Materials Science and Technology," MIT Press, 1986, p. 4766.)

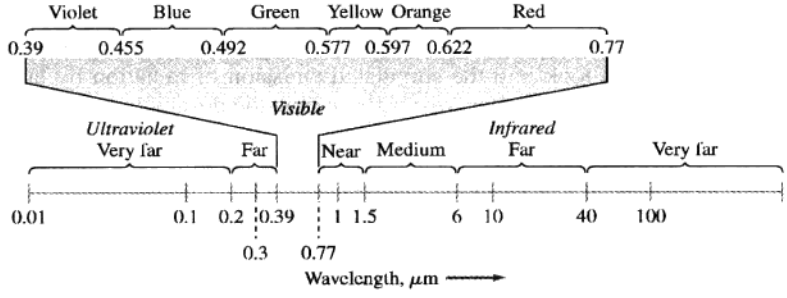

Figure 14.2
The electromagnetic spectrum from the ultraviolet to the infrared regions.

region covers the range from about 0.01 to about 0.40 μm, and the infrared region extends from about 0.75 to 1000 μm.

The true nature of light will probably never be known. However, light is considered to form waves and to consist of particles called *photons*. The energy ΔE,

wavelength λ, and frequency ν of the photons are related by the fundamental equation

$$\Delta E = h\nu = \frac{hc}{\lambda} \tag{14.1}$$

where h is Planck's constant (6.62×10^{-34} J · s) and c is the speed of light in vacuum (3.00×10^{8} m/s). These equations allow us to consider the photon as a particle of energy E or as a wave with a specific wavelength and frequency.

EXAMPLE PROBLEM 14.1

A photon in a ZnS semiconductor drops from an impurity energy level at 1.38 eV below its conduction band to its valence band. What is the wavelength of the radiation given off by the photon in the transition? If visible, what is the color of the radiation? ZnS has an energy band gap of 3.54 eV.

■ Solution

The energy difference for the photon dropping from the 1.38 eV level below the conduction band to the valence band is 3.54 eV − 1.38 eV = 2.16 eV.

$$\lambda = \frac{hc}{\Delta E} \tag{14.1}$$

where $h = 6.62 \times 10^{-34}$ J · s
$c = 3.00 \times 10^{8}$ m/s
1 eV = 1.60×10^{-19} J

Thus,

$$\lambda = \frac{(6.62 \times 10^{-34}\ \text{J} \cdot \text{s})(3.00 \times 10^{8}\ \text{m/s})}{(2.16\ \text{eV})(1.60 \times 10^{-19}\ \text{JeV})(10^{-9}\ \text{m/nm})} = 574.7\ \text{nm} \blacktriangleleft$$

The wavelength of this photon at 574.7 nm is the visible yellow region of the electromagnetic spectrum.

14.3 REFRACTION OF LIGHT

14.3.1 Index of Refraction

When light photons are transmitted through a transparent material, they lose some of their energy, and as a result, the speed of light is reduced and the beam of light changes direction. Figure 14.3 shows schematically how a beam of light entering from the air is slowed when entering a denser medium such as common window glass. Thus, the incident angle for the light beam is greater than the refracted angle for this case.

The relative velocity of light passing through a medium is expressed by the optical property called the **index of refraction** n. The n value of a medium is defined as the ratio of the velocity of light in vacuum, c, to the velocity of light in the medium considered, v:

$$\text{Refractive index } n = \frac{c\ (\text{velocity of light in vacuum})}{v\ (\text{velocity of light in a medium})} \tag{14.2}$$

Typical average refractive indices for some glasses and crystalline solids are listed in Table 14.1. These values range from about 1.4 to 2.6, with most silicate glasses

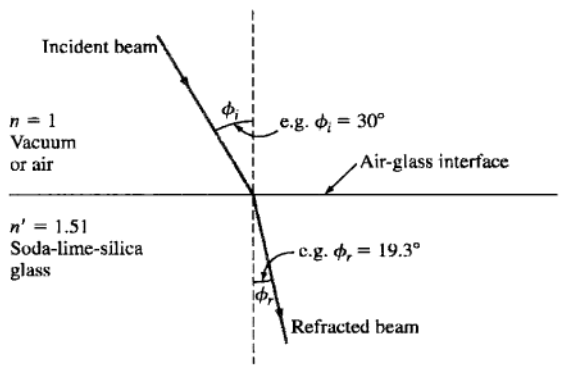

Figure 14.3
Refraction of light beam as it is transmitted from a vacuum (air) through soda-lime-silica glass.

Table 14.1 Refractive indices for selected materials

Material	Average refractive index
Glass compositions:	
Silica glass	1.458
Soda-lime-silica glass	1.51–1.52
Borosilicate (Pyrex) glass	1.47
Dense flint glass	1.6–1.7
Crystalline compositions:	
Corundum, Al_2O_3	1.76
Quartz, SiO_2	1.555
Litharge, PbO	2.61
Diamond, C	2.41
Optical plastics:	
Polyethylene	1.50–1.54
Polystyrene	1.59–1.60
Polymethyl methacrylate	1.48–1.50
Polytetrafluoroethylene	1.30–1.40

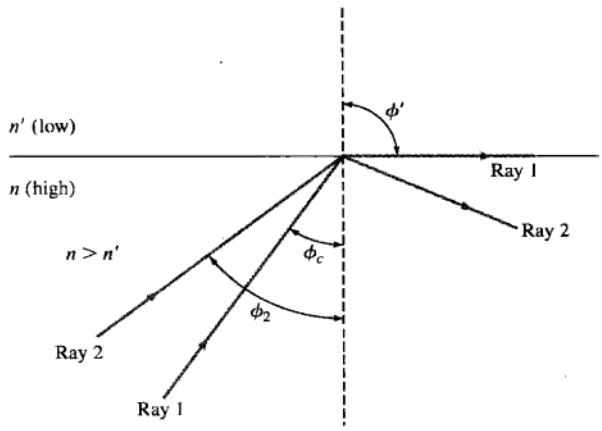

Figure 14.4
Diagram indicating the critical angle ϕ_c for total internal reflection of light passing from a high refractive index medium n to another of low refractive index n'. Note that ray 2, which has an incidence angle ϕ_2 greater than ϕ_c, is totally reflected back into the medium of high refractive index.

having values of about 1.5 to 1.7. The highly refractive diamond ($n = 2.41$) allows multifaceted diamond jewels to "sparkle" because of the multiple internal reflections. Lead oxide (litharge) with a value of $n = 2.61$ is added to some silicate glasses to raise their refractive indices so that they can be used for decorative purposes. It should also be noted that the refractive indices of materials are a function of wavelength and frequency. For example, the refractive index of light flint glass varies from about 1.60 at 0.40 μm to 1.57 at 1.0 μm.

14.3.2 Snell's Law of Light Refraction

The refractive indices for light passing from one medium of refractive index n through another of refractive index n' are related to the incident angle ϕ and the refractive angle ϕ' by the relation

$$\frac{n}{n'} = \frac{\sin \phi'}{\sin \phi} \qquad \text{(Snell's law)} \tag{14.3}$$

When light passes from a medium with a high refractive index to one with a low refractive index, there is a critical angle of incidence ϕ_c, which if increased will result in total internal reflection of the light (Fig. 14.4). This ϕ_c angle is defined at ϕ' (refraction) = 90°.

EXAMPLE PROBLEM 14.2

What is the critical angle ϕ_c for light to be totally reflected when leaving a flat plate of soda-lime-silica glass ($n = 1.51$) and entering the air ($n = 1$)?

■ **Solution**

Using Snell's law (Eq. 14.3),

$$\frac{n}{n'} = \frac{\sin \phi'}{\sin \phi_c}$$

$$\frac{1.51}{1} = \frac{\sin 90°}{\sin \phi_c}$$

where n = refractive index of the glass

n' = refractive index of air

ϕ' = 90° for total reflection

ϕ_c = critical angle for total reflection (unknown)

$$\sin \phi_c = \frac{1}{1.51}(\sin 90°) = 0.662$$

$$\phi_c = 41.5° \blacktriangleleft$$

Note: We shall see in Sec. 14.7 on optical fibers that by using a cladding of a low-refractive-index glass surrounding a core of high refractive index, an optical fiber can transmit light for long distances because the light is continually reflected internally.

14.4 ABSORPTION, TRANSMISSION, AND REFLECTION OF LIGHT

Every material *absorbs* light to some degree because of the interaction of light photons with the electronic and bonding structure of the atoms, ions, or molecules that make up the material (**absorptivity**). The fraction of light transmitted by a particular material thus depends on the amount of light reflected and absorbed by the material. For a particular wavelength λ, the sum of the fractions of the incoming incident light reflected, *absorbed,* and transmitted is equal to 1:

$$(\text{Reflected fraction})_\lambda + (\text{absorbed fraction})_\lambda + (\text{transmitted fraction})_\lambda = 1 \qquad \textbf{(14.4)}$$

Let us now consider how these fractions vary for some selected types of materials.

14.4.1 Metals

Except for very thin sections, metals strongly reflect and/or absorb incident radiation for long wavelengths (radio waves) to the middle of the ultraviolet range. Since the conduction band overlaps the valence band in metals, incident radiation easily

elevates electrons to higher energy levels. Upon dropping to lower energy levels, the photon energies are low and their wavelengths long. This type of action results in strongly reflected beams of light from a smooth surface, as is observed for many metals such as gold and silver. The amount of energy absorbed by metals depends on the electronic structure of each metal. For example, with copper and gold there is a greater absorption of the shorter wavelengths of blue and green and a greater reflection of the yellow, orange, and red wavelengths, and thus smooth surfaces of these metals show the reflected colors. Other metals such as silver and aluminum strongly reflect all parts of the visible spectrum and show a white "silvery" color.

14.4.2 Silicate Glasses

Reflection of Light from a Single Surface of a Glass Plate The proportion of incident light reflected by a single surface of a polished glass plate is very small. This amount depends mainly on the refractive index of the glass n and the angle of incidence of the light striking the glass. For normal light incidence (that is, $\phi_i = 90°$), the fraction of light reflected R (called the *reflectivity*) by a single surface can be determined from the relationship

$$R = \left(\frac{n-1}{n+1}\right)^2 \tag{14.5}$$

where n is the refractive index of the reflecting optical medium. This formula may also be used with good approximation for incident light angles up to about 20 degrees. Using Eq. 14.5, a silicate glass with $n = 1.46$ has a calculated R value of 0.035, or a percent reflectivity of 3.5 percent (see Example Problem 14.3).

EXAMPLE PROBLEM 14.3

Calculate the reflectivity of ordinary incident light from the polished flat surface of a silicate glass with a refractive index of 1.46.

■ **Solution**

Using Eq. 14.5 and $n = 1.46$ for the glass,

$$\text{Reflectivity} = \left(\frac{n-1}{n+1}\right)^2 = \left(\frac{1.46-1.00}{1.46+1.00}\right)^2 = 0.035$$

$$\%\ \text{Reflectivity} = R(100\%) = 0.035 \times 100\% = 3.5\% \blacktriangleleft$$

Absorption of Light by a Glass Plate Glass absorbs energy from the light that it transmits so that the light intensity decreases as the light path increases. The relationship between the fraction of light entering, I_0, and the fraction of light exiting, I, from a glass sheet or plate of thickness t that is free of scattering centers is

$$\frac{I}{I_0} = e^{-\alpha t} \tag{14.6}$$

The constant α in this relation is called the *linear absorption coefficient* and has the units cm^{-1} if the thickness is measured in centimeters. As shown in Example Problem 14.4, there is a relatively small loss of energy by absorption through a clear silicate glass plate.

EXAMPLE PROBLEM 14.4

Ordinary incident light strikes a polished glass plate 0.50 cm thick that has a refractive index of 1.50. What fraction of light is absorbed by the glass as the light passes between the surfaces of the plate? ($\alpha = 0.03\ cm^{-1}$)

■ **Solution**

$$\frac{I}{I_0} = e^{-\alpha t} \qquad I_0 = 1.00 \qquad \alpha = 0.03\ cm^{-1}$$

$$I = ? \qquad t = 0.50\ cm$$

$$\frac{I}{1.00} = e^{-(0.03\ cm^{-1})(0.50\ cm)}$$

$$I = (1.00)e^{-0.015} = 0.985$$

Thus, the fraction of light lost by absorption by the glass is: $1 - 0.985 = 0.015$, or 1.5 percent. ◀

Reflectance, Absorption, and Transmittance of Light by a Glass Plate The amount of incident light transmitted through a glass plate is determined by the amount of light reflected from both upper and lower surfaces as well as the amount absorbed within the plate. Let us consider the transmittance of light through a glass plate, as shown in Fig. 14.5. The fraction of incident light reaching the lower surface of the glass is $(1 - R)(I_0e^{-\alpha t})$. The fraction of incident light reflected from the lower surface will therefore be $(R)(1 - R)(I_0e^{-\alpha t})$. Thus, the difference between the light reaching the lower surface of the glass plate and that which is reflected from the lower surface is the fraction of light transmitted I, which is:

$$I = [(1 - R)(I_0e^{-\alpha t})] - [(R)(1 - R)(I_0e^{-\alpha t})]$$

$$= (1 - R)(I_0e^{-\alpha t})(1 - R) = (1 - R)^2(I_0e^{-\alpha t}) \qquad (14.7)$$

Figure 14.6 shows that about 90 percent of incident light is transmitted by silica glass if the wavelength of the incoming light is greater than about 300 nm. For shorter-wavelength ultraviolet light, much more absorption takes place, and the transmittance is lowered considerably.

14.4.3 Plastics

Many noncrystalline plastics such as polystyrene, polymethyl methacrylate, and polycarbonate have excellent transparency. However, in some plastic materials, there are

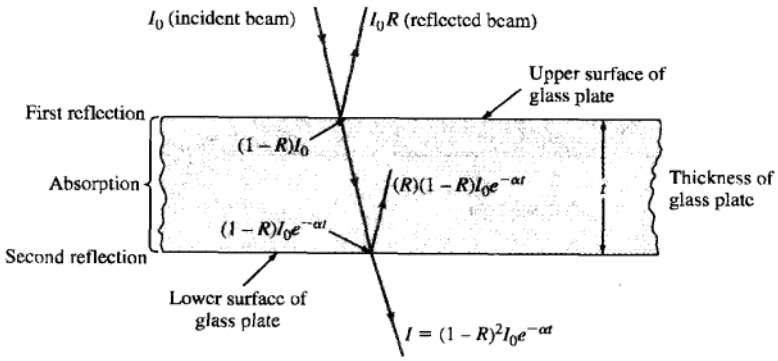

Figure 14.5
Transmittance of light through a glass plate in which reflectance takes place at upper and lower surfaces and absorption within the plate.

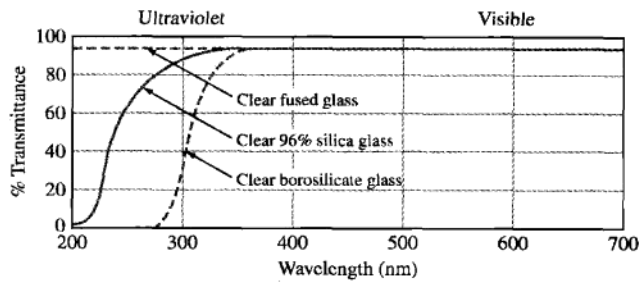

Figure 14.6
Percent transmittance versus wavelength for several types of clear glasses.

crystalline regions having a higher refractive index than their noncrystalline matrix. If these regions are greater in size than the wavelength of the incoming light, the light waves will be scattered by reflection and refraction, and hence the transparency of the material decreases (Fig. 14.7). For example, thin-sheet polyethylene, which has a branched-chain structure and hence a lower degree of crystallinity, has higher transparency than the higher-density, more crystalline linear-chain polyethylene. The transparencies of other partly crystalline plastics can range from cloudy to opaque, depending mainly on their degree of crystallinity, impurity content, and filler content.

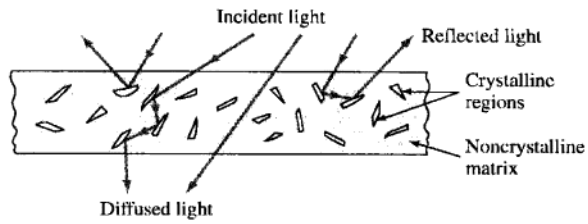

Figure 14.7
Multiple internal reflections at the crystalline-region interfaces reduce the transparency of partly crystalline thermoplastics.

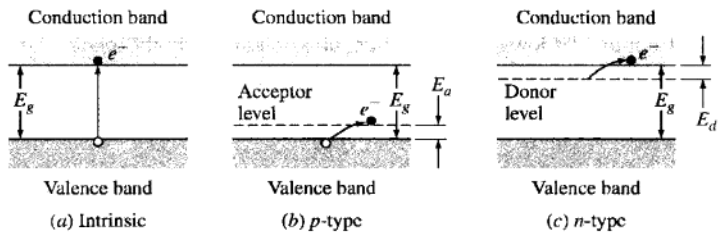

Figure 14.8
Optical absorption of photons in semiconductors. Absorption takes place in (*a*) if $h\nu > E_g$, (*b*) if $h\nu > E_a$, and (*c*) if $h\nu > E_d$.

14.4.4 Semiconductors

In semiconductors, light photons can be absorbed in several ways (Fig. 14.8). In intrinsic (pure) semiconductors such as Si, Ge, and GaAs, photons may be absorbed to create electron-hole pairs by causing electrons to jump across the energy band gap from the valence band to the conduction band (Fig. 14.8*a*). For this to occur, the incoming light photon must have an energy value equal to or greater than the energy gap E_g. If the energy of the photon is greater than E_g, the excess energy is dissipated as heat. For semiconductors containing donor and acceptor impurities, much lower-energy (and hence much longer-wavelength) photons are absorbed in causing electrons to jump from the valence band into acceptor levels (Fig. 14.8*b*) or from donor levels into the conduction band (Fig. 14.8*c*). Semiconductors are therefore opaque to high- and intermediate-energy (short- and intermediate-wavelength) light photons and transparent to low-energy, very long wavelength photons.

EXAMPLE PROBLEM 14.5

Calculate the minimum wavelength for photons to be absorbed by intrinsic silicon at room temperature ($E_g = 1.10$ eV).

■ **Solution**

For absorption in this semiconductor, the minimum wavelength is given by Eq. 14.1:

$$\lambda_c = \frac{hc}{E_g} = \frac{(6.62 \times 10^{-34}\,\text{J} \cdot \text{s})(3.00 \times 10^{8}\,\text{m/s})}{(1.10\,\text{eV})(1.60 \times 10^{-19}\,\text{J/eV})}$$
$$= 1.13 \times 10^{-6}\,\text{m or } 1.13\,\mu\text{m} \blacktriangleleft$$

Thus, for absorption the photons must have a wavelength at least as short as 1.13 μm so that electrons can be excited across the 1.10 eV band gap.

14.5 LUMINESCENCE

Luminescence may be defined as the process by which a substance absorbs energy and then spontaneously emits visible or near-visible radiation. In this process the input energy excites electrons of a luminescent material from the valence band into the conduction band. The source of the input energy may be, for example, high-energy electrons or light photons. The excited electrons during luminescence drop to lower energy levels. In some cases, the electrons may recombine with holes. If the emission takes place within 10^{-8} s after excitation, the luminescence is called **fluorescence,** and if the emission takes longer than 10^{-8} s, it is referred to as **phosphorescence.**

Luminescence is produced by materials called *phosphors* that can absorb high-energy, short-wave radiation and spontaneously emit lower-energy, longer-wavelength light radiation. The emission spectra of luminescent materials are controlled industrially by added impurities called *activators.* The activators provide discrete energy levels in the energy gap between the conduction and valence bands of the host material (Fig. 14.9). One mechanism postulated for the phosphorescent process is that

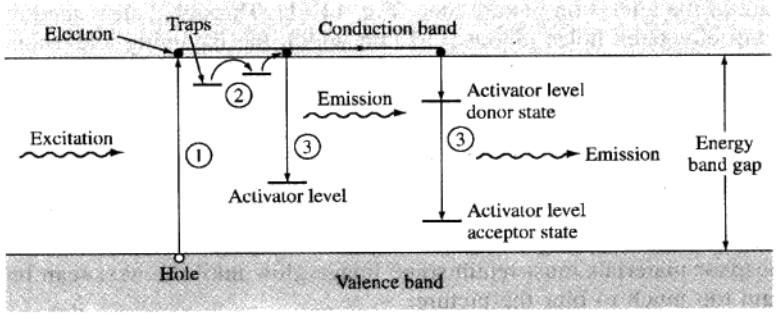

Figure 14.9
Energy changes during luminescence. (1) Electron-hole pairs are created by exciting electrons to the conduction band or to traps. (2) Electrons can be thermally excited from one trap to another or into the conduction band. (3) Electrons can drop to upper activator (donor) levels and then subsequently to lower acceptor levels, emitting visible light.

excited electrons are trapped in various ways at high energy levels and must get out of the traps before they can drop to lower energy levels and emit light of a characteristic spectral band. The trapping process is used to explain the delay in light emission by excited phosphors.

Luminescence processes are classified according to the energy source for electronic excitation. Two industrially important types are *photoluminescence* and *cathodoluminescence.*

14.5.1 Photoluminescence

In the common fluorescent lamp, photoluminescence converts ultraviolet radiation from a low-pressure mercury arc into visible light by using a halophosphate phosphor. Calcium halophosphate of the approximate composition $Ca_{10}F_2P_6O_{24}$ with about 20 percent of the F^- ions replaced with Cl^- ions is used as the host phosphor material for most lamps. Antimony (Sb^{3+}) ions provide a blue emission and manganese (Mn^{2+}) ions provide an orange-red emission band. By varying the Mn^{2+}, various shades of blue, orange, and white light may be obtained. The high-energy ultraviolet light from the excited mercury atoms causes the phosphor-coated inner wall of the fluorescent lamp tube to give off lower-energy, longer-wavelength visible light (Fig. 14.10).

14.5.2 Cathodoluminescence

This type of luminescence is produced by an energized cathode that generates a beam of high-energy bombarding electrons. Applications for this process include electron microscope, cathode-ray oscilloscope, and color television screen luminescences. The color television screen phosphorescence is especially interesting. The modern television set has very narrow (about 0.25 mm wide) vertical stripes of red-, green-, and blue-emitting phosphors deposited on the inner surface of the face plate of the television picture tube (Fig. 14.11). Through a steel shadow mask with small elongated holes (about 0.15 mm wide), the incoming television signal is scanned over the entire screen 30 times per second. The small size and large number of phosphor areas consecutively exposed in the rapid scan of 15,750 horizontal lines per second and the persistence of an image in the human visual system make possible a clear visible picture with good resolution. Commonly used phosphors for the colors are zinc sulfide (ZnS) with an Ag^+ acceptor and Cl^- donor for the blue color, (Zn,Cd)S with a Cu^+ acceptor and Al^{3+} donor for the green color, and yttrium oxysulfide (Y_2O_2S) with 3% europium (Eu) for the red color. The phosphor materials must retain some image glow until the next scan but must not retain too much to blur the picture.

The intensity of luminescence, I, is given by

$$\ln \frac{I}{I_0} = -\frac{t}{\tau} \tag{14.8}$$

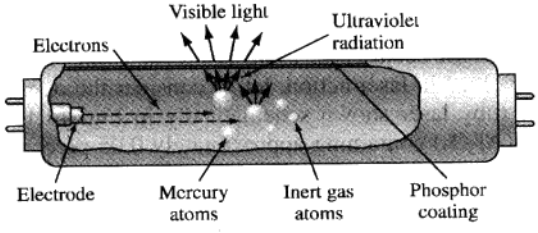

Figure 14.10
Cutaway diagram of a fluorescent lamp showing electron generation at an electrode and excitation of mercury atoms to provide the UV light to excite the phosphor coating on the inside of a lamp tube. The excited phosphor coating then provides visible light by luminescence.

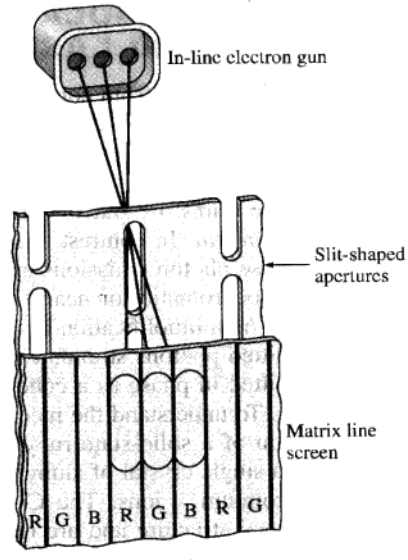

Figure 14.11
Diagram showing the arrangement of the R(red), G(green), and B(blue) vertical stripes of phosphors of a color television screen. Also shown are several of the elongated apertures of the steel shadow mask.
(*Courtesy of RCA.*)

where I_0 = initial intensity of luminescence and I = fraction of luminescence after time t. The quantity τ is the relaxation time constant for the material.

EXAMPLE PROBLEM 14.6

A color TV phosphor has a relaxation time of 3.9×10^{-3} s. How long will it take for the intensity of this phosphor material to decrease to 10 percent of its original intensity?

■ **Solution**
Using Eq. 14.8, $\ln(I/I_0) = -t/\tau$, or

$$\ln \frac{1}{10} = -\frac{t}{3.9 \times 10^{-3}\,\text{s}}$$

$$t = (-2.3)(-3.9 \times 10^{-3}\,\text{s}) = 9.0 \times 10^{-3}\,\text{s} \blacktriangleleft$$

14.6 STIMULATED EMISSION OF RADIATION AND LASERS

Light emitted from conventional light sources such as fluorescent lamps results from the transitions of excited electrons to lower energy levels. Atoms of the same elements in these light sources give off photons of similar wavelengths independently and randomly. Consequently, the radiation emitted is in random directions and the wave trains are out of phase with each other. This type of radiation is said to be *incoherent.* In contrast, a light source called a **laser** produces a **beam** of radiation whose photon emissions are in phase, or *coherent,* and are parallel, directional, and monochromatic (or nearly so). The word "laser" is an acronym whose letters stand for "*l*ight *a*mplification by *s*timulated *e*mission of *r*adiation." In lasers, some "active" emitted photons stimulate many others of the same frequency and wavelength to be emitted in phase as a coherent, intense light beam (Fig. 14.12).

To understand the mechanisms involved in laser action, let us consider the operation of a solid-state ruby laser. The ruby laser shown schematically in Fig. 14.13 is a single crystal of aluminum oxide (Al_2O_3) containing approximately 0.05 percent chromium^{3+} ions. The Cr^{3+} ions occupy substitutional lattice sites in the Al_2O_3 crystal structure and are responsible for the pink color of the laser rod. These ions act as fluorescent centers that, when excited, drop to lower energy levels, causing photon emissions at specific wavelengths. The ends of the ruby rod crystal are ground parallel for optical emission. A totally reflective mirror is placed parallel and near the back end of the crystal rod and another partially transmitting one at the front end of the laser, which allows the coherent laser beam to pass through.

High-intensity input from a xenon flash lamp can provide the necessary energy to excite the Cr^{3+} ion electrons from the ground state to high energy levels, as indicated by the E_3 band level of Fig. 14.14. This action in laser terminology is referred to as *pumping* the laser. The excited electrons of the Cr^{3+} ions may then drop back down to the ground state or to the metastable energy level E_2 of Fig. 14.14. However, before the stimulated emission of photons can occur in the laser, more electrons must be

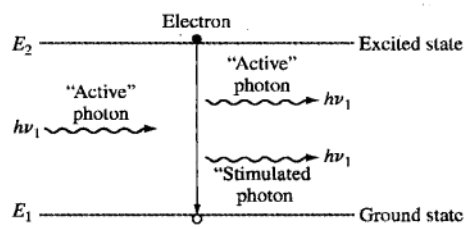

Figure 14.12
Schematic diagram illustrating the emission of a "stimulated" photon by an "active" photon of the same frequency and wavelength.

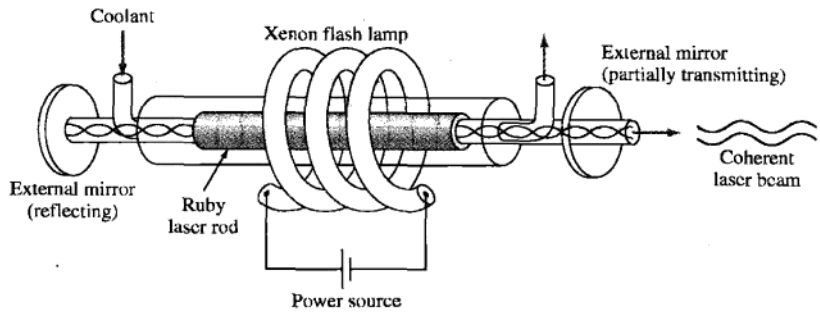

Figure 14.13
Schematic diagram of a pulsed ruby laser.

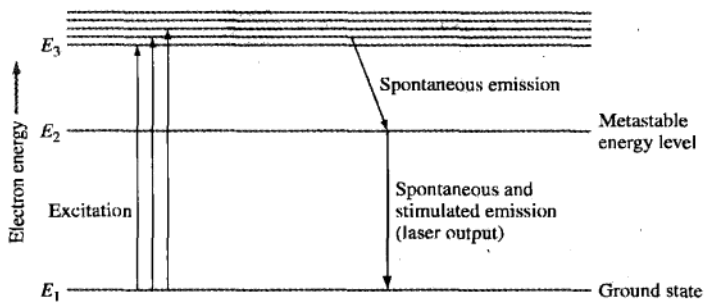

Figure 14.14
Simplified energy-level diagram for a three-level lasing system.

pumped into the high nonequilibrium metastable energy level E_2 than exist in the ground state (E_1). This condition of the laser is referred to as the **population inversion** of electron energy states as is schematically indicated in Fig. 14.15*b*; compare this condition to the equilibrium energy level condition of Fig. 14.15*a*.

The excited Cr^{3+} ions can remain in the metastable state for several milliseconds before spontaneous emission takes place by electrons dropping back to the ground state. The first few photons produced by electrons dropping from the metastable E_2 level of Fig. 14.14 to the ground level E_1 set off a stimulated-emission chain reaction, causing many of the electrons to make the same jump from E_2 to E_1. This action produces a large number of photons that are in phase and moving in a parallel direction (Fig. 14.15*c*). Some of the photons jumping from E_2 to E_1 are lost to the outside of the rod, but many are reflected back and forth along the ruby rod by the end mirrors. These stimulate more and more electrons to jump from E_2 and E_1, helping to build up a stronger coherent radiation beam (Fig. 14.15*d*). Finally, when a sufficiently intense coherent beam is built up inside the rod, the beam is transmitted as a high-intense-energy pulse ($\approx$ 0.6 ms) through the partially transmitting mirror at the front

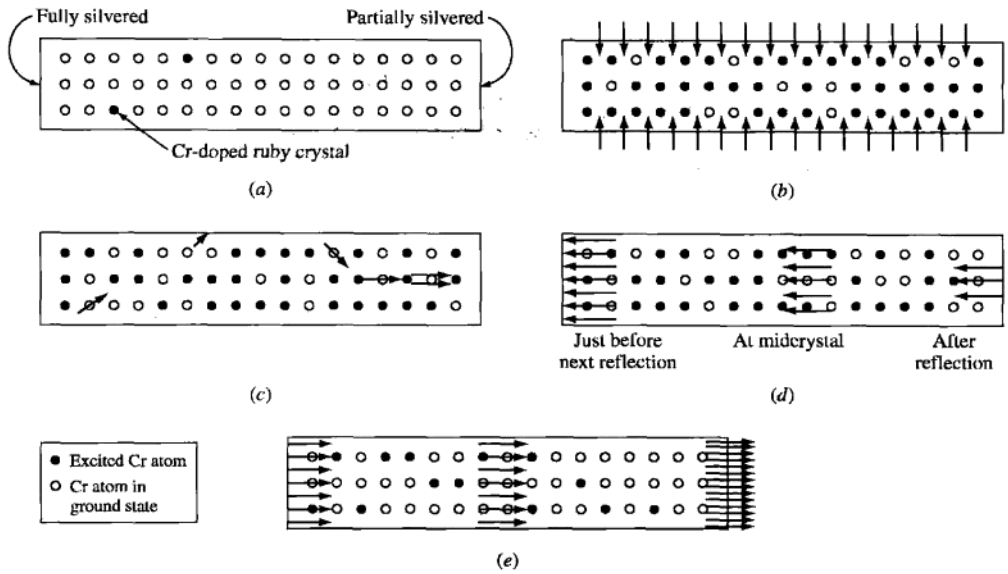

Figure 14.15
Schematic of the steps in the functioning of a pulsed ruby laser. (*a*) At equilibrium. (*b*) Excitation by xenon flash lamp. (*c*) A few spontaneously emitted photons start the stimulated emission of photons. (*d*) Reflected back, the photons continue to stimulate the emission of more photons. (*e*) The laser beam is finally emitted. (*From R.M. Rose, L.A. Shepard, and J. Wulff, "Structure and Properties of Materials," vol. IV, Wiley, 1965.*)

end of the laser (Figs. 14.15*e* and 14.13). The laser beam produced by the Cr^{3+} doped aluminum oxide (ruby) crystal rod has a wavelength of 694.3 nm, which is a visible red line. This type of laser, which can only be operated intermittently in bursts, is said to be a *pulsed* type. In contrast, most lasers are operated with a continuous beam and are called *continuous-wave* (CW) lasers.

14.6.1 Types of Lasers

There are many types of gas, liquid, and solid lasers used in modern technology. We shall briefly describe some important aspects of several of these.

Ruby Laser The structure and functioning of the ruby laser has already been described. This laser is not used much today because of the difficulties in growing the crystal rods compared to the ease of making neodymium lasers.

Neodymium-YAG Lasers The *neodymium-yttrium-aluminum-garnet* (Nd:YAG) laser is made by combining one part per hundred of Nd atoms in a host of a YAG crystal. This laser emits in the near-infrared at 1.06-μm wavelength with continuous

Table 14.2 Selected applications for lasers in materials processing

Applications	Type of laser	Comments
1. Welding	YAG*	High-average-power lasers for deep penetration and high-throughput welding
2. Drilling	YAG $CWCO_2$†	High peak-power densities for drilling precision holes with a minimum heat-affected zone, low taper, and maximum depths
3. Cutting	YAG $CWCO_2$	Precision cutting of complex two- and three-dimensional shapes at high rates in metals, plastics, and ceramics
4. Surface treatment	$CWCO_2$	Transformation hardening of steel surfaces by hardening them above austenitic temperatures with a scanning, defocused beam and allowing the metal to self-quench
5. Scribing	YAG $CWCO_2$	Scribing large areas of fully fired ceramics and silicon wafers to provide individual circuit substrates
6. Photolithography	Excimer	Line-narrowed and spectrally stabilized excimer photolithographic processing in the fabrication of semiconductors

*YAG = yttrium-aluminum-garnet is a crystalline host used in solid-state neodymium lasers.
†$CWCO_2$ = continuous-wave (as opposed to pulsed) carbon dioxide laser.

power up to about 250 W and with pulsed power as high as several megawatts. The YAG host material has the advantage of high thermal conductivity to remove excess heat. In materials processing, the Nd:YAG laser is used for welding, drilling, scribing, and cutting (Table 14.2).

Carbon Dioxide (CO_2) Lasers Carbon dioxide lasers are some of the most powerful lasers made. They operate mainly in the middle-infrared at 10.6 μm. They vary from a few milliwatts of continuous power to large pulses with as high as 10,000 J of energy. They operate by electron collisions exciting nitrogen molecules to metastable energy levels that subsequently transfer their energy to excite CO_2 molecules, which in turn give off laser radiation upon dropping to lower energy levels. Carbon dioxide lasers are used for metal-processing applications such as cutting, welding, and localized heat treatment of steels (Table 14.2).

Semiconductor Lasers Semiconductor, or diode, lasers, commonly about the size of a grain of salt, are the smallest lasers produced. They consist of a pn junction made with a semiconducting compound such as GaAs that has a large enough band gap for laser action (Fig. 14.16). Originally, the GaAs diode laser was made as a homojunction laser with a single pn junction (Fig. 14.16*a*). The resonant cavity of the laser is created by cleaving the crystal to make two end facets. The crystal-air interfaces cause the necessary reflections for laser action due to the difference in refractive indices of air and GaAs. The diode laser achieves population inversion by a strong forward bias of a heavily doped pn junction. A great number of electron-hole pairs are generated, and many of these in turn recombine to emit photons of light.

An improvement in efficiency was achieved with the *double heterojunction* (DH) laser (Fig. 14.16*b*). In a GaAs DH laser, a thin layer of p-GaAs is sandwiched between p- and n-$Al_xGa_{1-x}As$ layers that confine the electrons and holes within the

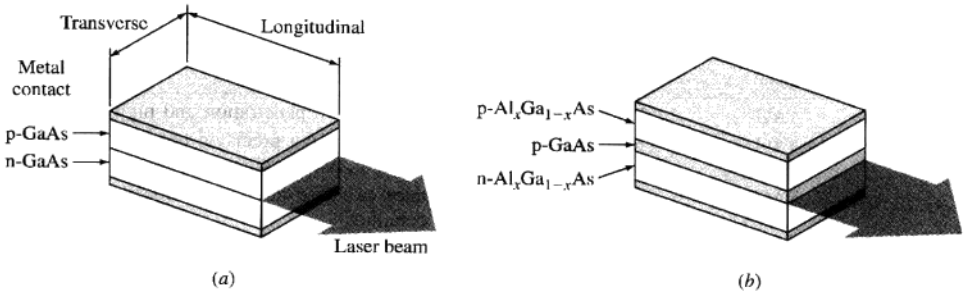

Figure 14.16
(*a*) Simple homojunction GaAs laser. (*b*) Double heterojunction GaAs laser. The p- and n-$Al_xGa_{1-x}As$ layers have wider band gaps and lower refractive indices and confine the electrons and holes within the active p-GaAs layer.

active p-GaAs layer. The AlGaAs layers have wider band gaps and lower refractive indices and so constrain the laser light to move in a miniature waveguide. The most widespread application of GaAs diode lasers currently is for compact disks.

14.7 OPTICAL FIBERS

Hair-thin ($\approx 1.25\ \mu$m diameter) optical fibers made primarily of silica (SiO_2) glass are used for modern **optical-fiber communication** systems. These systems consist essentially of a transmitter (i.e., a semiconductor laser) to encode electrical signals into light signals, optical fiber to transmit the light signals, and a photodiode to convert the light signals back into electrical signals (Fig. 14.17).

14.7.1 Light Loss in Optical Fibers

The optical fibers used for communications systems must have extremely low light loss (attenuation) so that an entering encoded light signal can be transmitted a long distance (that is, 40 km [25 mi]) and still be detected satisfactorily. For extremely low-light-loss glass for optical fibers, the impurities (particularly Fe^{2+} ions) in the SiO_2 glass must be very low. The light loss **(attenuation)** of an optical glass fiber is usually measured in *decibels per kilometer* (dB/km). The light loss in a light-transmitting material in dB/km for light transmission over a length l is related to the entering light intensity I_0 and the exiting light intensity I by

$$-\text{loss (dB/km)} = \frac{10}{l\,(\text{km})} \log \frac{I}{I_0} \qquad \textbf{(14.9)}$$

EXAMPLE PROBLEM 14.7

A low-loss silica glass fiber for optical transmission has a 0.20 dB/km light attenuation. (*a*) What is the fraction of light remaining after it has passed through 1 km of this glass fiber? (*b*) What is the fraction of light remaining after 40 km transmission?

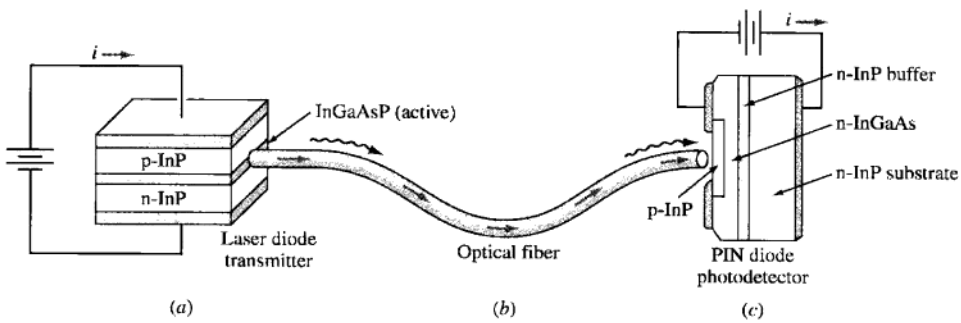

Figure 14.17
Basic elements of a fiber-optics communications system. (*a*) InGaAsP laser transmitter. (*b*) Optical fiber for transmitting light photons. (*c*) PIN diode photodetector.

■ **Solution**

$$\text{Attenuation (dB/km)} = \frac{10}{l\,(\text{km})} \log \frac{I}{I_0} \qquad (14.9)$$

where I_0 = light intensity at source
I = light intensity at detector

a. $-0.20 \text{ dB/km} = \dfrac{10}{1 \text{ km}} \log \dfrac{I}{I_0}$ or $\log \dfrac{I}{I_0} = -0.02$ or $\dfrac{I}{I_0} = 0.95$ ◀

b. $-0.20 \text{ dB/km} = \dfrac{10}{40 \text{ km}} \log \dfrac{I}{I_0}$ or $\log \dfrac{I}{I_0} = -0.80$ or $\dfrac{I}{I_0} = 0.16$ ◀

Note: Single-mode optical fibers today can transmit communication light data about 40 km without having to repeat the signal.

14.7.2 Single-Mode and Multimode Optical Fibers

Optical fibers for light transmission serve as **optical waveguides** for the light signals in optical communications. The retention of light within the optical fiber is made possible by having the light pass through the central core glass, which has a higher refractive index than the outer clad glass (Fig. 14.18). For the single-mode type, which has a core diameter of about 8 μm and an outer clad diameter of about 125 μm, there is only one acceptable guided light ray path (Fig. 14.18*a*). In the multimode-type optical glass fiber, which has a graded refractive index core, many wave modes pass through the fiber simultaneously, causing a more dispersed exiting

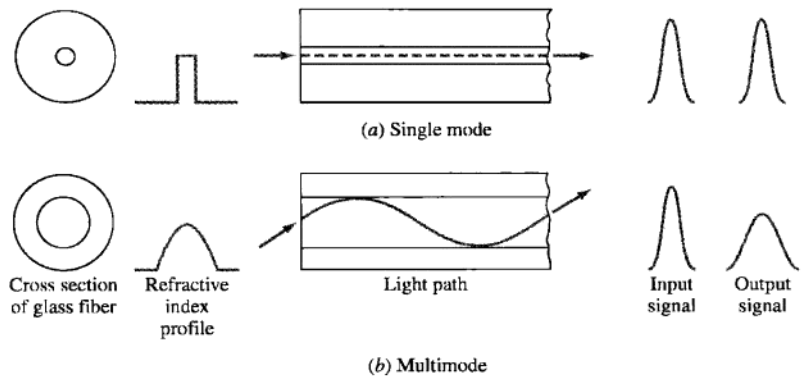

Figure 14.18
Comparison of (*a*) single-mode and (*b*) multimode optical fibers by cross section versus refractive index, light path, and signal input and output. The sharper output signal of the single-mode fiber is preferred for long-distance optical communications systems.

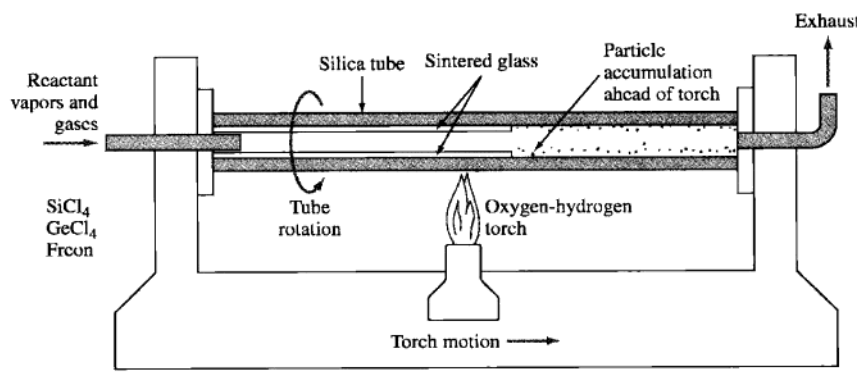

Figure 14.19
Schematic of the modified chemical vapor deposition process for the production of the glass preforms for making optical glass fibers.
(Property of AT&T Archives. Reprinted with permission of AT&T.)

signal than that produced by the single-mode fiber (Fig. 14.18*b*). Most new optical-fiber communication systems use single-mode fibers because they have lower light losses and are cheaper and easier to fabricate.

14.7.3 Fabrication of Optical Fibers

One of the most important methods for producing optical glass fibers for communication systems is the *modified chemical vapor deposition* (MCVD) process (Fig. 14.19). In this process, high-purity dry vapor of $SiCl_4$ with various amounts of $GeCl_4$ and fluorinated hydrocarbons vapor are passed through a rotating pure silica tube along with

pure oxygen. An external oxyhydrogen torch is moved along the outer diameter of the rotating tube, allowing the contents to react to form silica glass particles doped with the desired combinations of germanium and fluorine. GeO_2 increases the refractive index of SiO_2, and fluorine lowers it. Downstream from the reaction region, the glass particles migrate to the tube wall, where they are deposited. The moving torch that caused the reaction to form the glass particles then passes over and sinters them into a thin layer of doped glass. The thickness of the doped layer depends on the number of layers that are deposited by the repeated passes of the torch. At each pass, the composition of the vapors is adjusted to produce the desired composition profile so that the glass fiber subsequently produced will have the desired refractive index profile.

In the next step, the silica tube is heated to a high enough temperature that the glass approaches its softening point. The surface tension of the glass then causes the tube with the deposited glass layers to collapse uniformly into a solid rod called a *preform*. The glass preform from the MCVD process is then inserted into a high-temperature furnace, and glass fiber about 125 μm in diameter is drawn from it (Fig. 14.20). An in-line process applies a 60-μm-thick polymer coating to

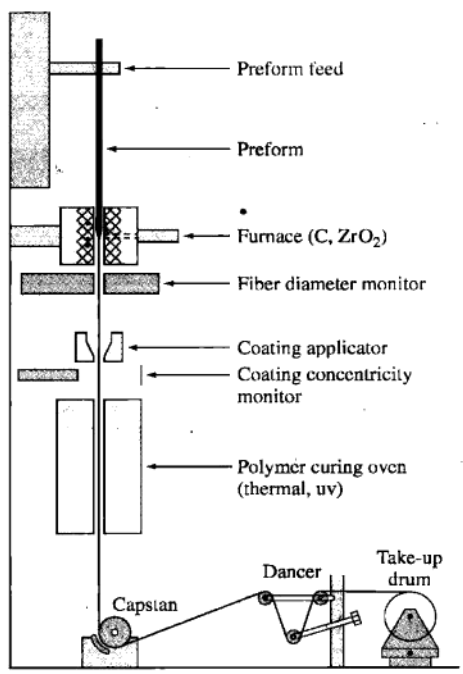

Figure 14.20
Schematic setup for drawing optical glass fiber from glass preform.
(From "Encyclopedia of Materials Science and Technology," MIT Press, 1986, p. 1992.)

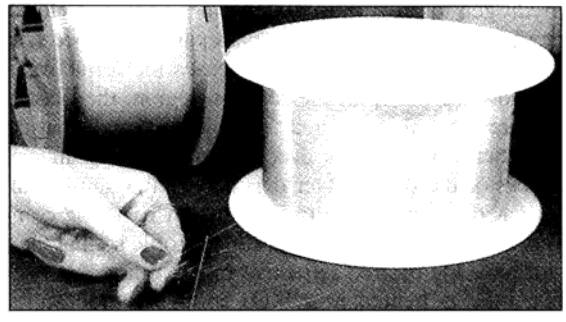

Figure 14.21
Spool of optical fiber.
(*Courtesy of AT&T.*)

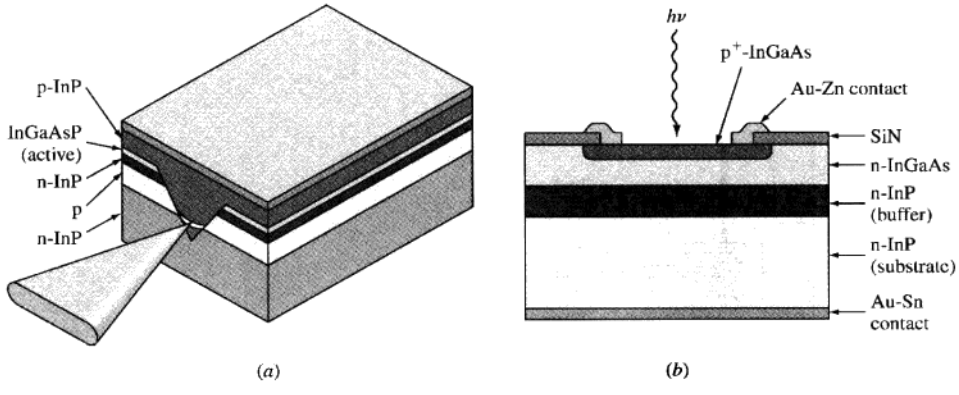

Figure 14.22
(*a*) Chemical substrate buried heterostructure InGaAsP laser diode used for long-distance fiber-optical communications systems. Note the focusing of the laser beam by the V channel. (*b*) PIN photodetector for optical communications systems.
(*Property of AT&T Archives. Reprinted with permission of AT&T.*)

protect the glass fiber surface from damage. Spools of finished glass fibers are shown in Fig. 14.21. Very close tolerances for the core and outer diameter of the fiber are essential so that the fiber can be spliced (joined) without high light losses.

14.7.4 Modern Optical-Fiber Communication Systems

Most modern optical-fiber communication systems use single-mode fiber with an InGaAsP double heterojunction laser diode transmitter (Fig. 14.22*a*) operated at the infrared wavelength of 1.3 μm, where light losses are at a minimum. An

InGaAs/InP PIN photodiode is usually used for the detector (Fig. 14.22*b*). With this system, optical signals can be sent about 40 km (25 mi) before the signal has to be repeated. In December 1988, the first transatlantic fiber-optic communications system began operation with a capacity of 40,000 simultaneous phone calls. By 1993, there were 289 undersea optical-fiber cable links.

Another advance in optical-fiber communication systems has been the introduction of *erbium-doped optical-fiber amplifiers* (EDFAs). An EDFA is a length (typically about 20 to 30 m [64 to 96 ft]) of optical silica fiber doped with the rare-earth element erbium to give fiber gain. When optically pumped with light from an outside semiconductor laser, the erbium-doped fiber boosts the power of all light signals passing through it with wavelengths centered on 1.55 μm. Thus, the erbium-doped optical fiber serves as both a lasing medium and a light guide. EDFAs can be used in optical transmission systems to boost the light signal power at the source (power amplifier), at the receiver (preamplifier), and along the fiber communication link (in-line repeater). The first EDFAs were used in 1993 in an AT&T network in a link between San Francisco and Point Arena, California.

14.8 SUPERCONDUCTING MATERIALS

14.8.1 The Superconducting State

The electrical resistivity of a normal metal such as copper decreases steadily as the temperature is decreased and reaches a low residual value near 0 K (Fig. 14.23). In contrast, the electrical resistivity of pure mercury as the temperature decreases drops suddenly at 4.2 K to an immeasurably small value. This phenomenon is called

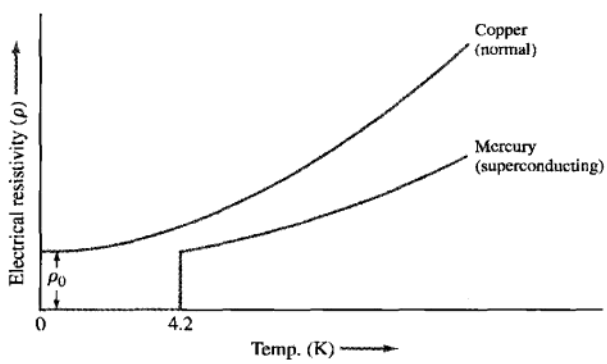

Figure 14.23
Electrical resistivity of a normal metal (Cu) compared to that of a superconductive metal (Hg) as a function of temperature near 0 K. The resistivity of the superconductive metal suddenly drops to an immeasurably small value.

Table 14.3 Critical superconducting temperatures T_c for selected metals, intermetallic, and ceramic compound superconductors

Metals	T_c (K)	H_0^* (T)	Intermetallic compounds	T_c (K)	Ceramic compounds	T_c (K)
Niobium, Nb	9.15	0.1960	Nb_3Ge	23.2	$Tl_2Ba_2Ca_2Cu_3O_x$	122
Vanadium, V	5.30	0.1020	Nb_3Sn	21	$YBa_2Cu_3O_{7-x}$	90
Tantalum, Ta	4.48	0.0830	Nb_3Al	17.5	$Ba_{1-x}K_xBiO_{3-y}$	30
Titanium, Ti	0.39	0.0100	NbTi	9.5		
Tin	3.72	0.0306				

*H_0 = critical field in teslas (T) at 0 K.

superconductivity, and the material that shows this behavior is called a *superconductive material.* About 26 metals are superconductive as are hundreds of alloys and compounds.

The temperature below which a material's electrical resistivity approaches zero is called the **critical temperature T_c.** Above this temperature, the material is called *normal,* and below T_c it is said to be *superconducting* or *superconductive.* Besides temperature, the superconducting state also depends on many other variables, the most important of which are the magnetic field B and current density J. Thus, for a material to be superconducting, the material's critical temperature, magnetic field, and current density must not be exceeded, and for each superconducting material there exists a critical surface in T, B, J space.

The critical superconducting temperatures of some selected metals, intermetallic compounds, and new ceramic compounds are listed in Table 14.3. The extremely high T_c values (90–122 K) of the newly discovered (1987) ceramic compounds are outstanding and were a surprise to the scientific community. Some aspects of their structure and properties will be discussed later in this section.

14.8.2 Magnetic Properties of Superconductors

If a sufficiently strong magnetic field is applied to a superconductor at any temperature below its critical temperature T_c, the superconductor will return to the normal state. The applied magnetic field necessary to restore normal electrical conductivity in the superconductor is called the **critical field H_c.** Figure 14.24*a* shows schematically the relationship between the critical magnetic field H_c and temperature (K) at zero current. It should be pointed out that a sufficiently high electrical **(critical) current density J_c** will also destroy superconductivity in materials. The curve of H_c versus T (K) can be approximated by

$$H_c = H_0\left[1 - \left(\frac{T}{T_c}\right)^2\right] \tag{14.10}$$

where H_0 is the critical field at $T = 0$ K. Equation 14.10 represents the boundary between the superconducting and normal states of the superconductor. Figure 15.24*b* shows the critical field versus temperature plots for several superconducting metals.

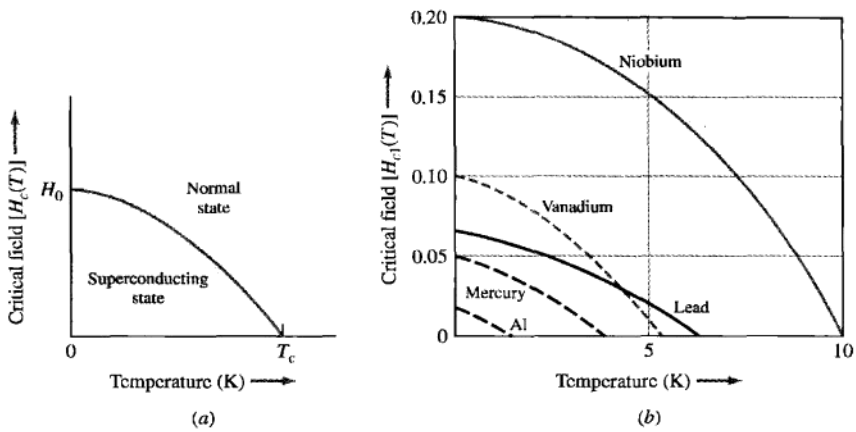

Figure 14.24
Critical field versus temperature. (*a*) General case. (*b*) Curves for several superconductors.

EXAMPLE PROBLEM 14.8

Calculate the approximate value of the critical field necessary to cause the superconductivity of pure niobium metal to disappear at 6 K.

■ Solution

From Table 14.3 at 0 K, the T_c for Nb is 9.15 K and its $H_0 = 0.1960$ T. From Eq. 14.10,

$$H_c = H_0\left[1 - \left(\frac{T}{T_c}\right)^2\right] = 0.1960\left[1 - \left(\frac{6}{9.15}\right)^2\right] = 0.112 \text{ T} \blacktriangleleft$$

According to their behavior in an applied magnetic field, metallic and intermetallic superconductors are classified into type I and type II superconductors. If a long cylinder of a **type I superconductor** such as Pb or Sn is placed in a magnetic field at room temperature, the magnetic field will penetrate normally throughout the metal (Fig. 14.25*a*). However, if the temperature of the type I superconductor is lowered below its T_c (7.19 K for Pb) and if the magnetic field is below H_c, the magnetic field will be expelled from the specimen except for a very thin penetration layer of about 10^{-5} cm at the surface (Fig. 14.25*b*). This property of a magnetic-field exclusion in the superconducting state is called the **Meissner effect.**

Type II superconductors behave differently in a magnetic field at temperatures below T_c. They are highly diamagnetic like type I superconductors up to a critical applied magnetic field, which is called the **lower critical field** H_{c1} (Fig. 14.26), and thus the magnetic flux is excluded from the material. Above H_{c1} the field starts to penetrate the type II superconductor and continues to do so until the **upper critical field** H_{c2} is reached. In between H_{c1} and H_{c2}, the superconductor is in the mixed state, and above H_{c2}, it returns to the normal state. In the region H_{c1} and H_{c2}, the

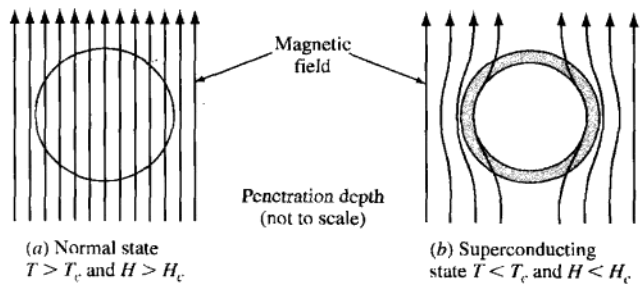

Figure 14.25
The Meissner effect. When the temperature of a type I superconductor is lowered below T_c and the magnetic field is below H_c, the magnetic field is completely expelled from a sample except for a thin surface layer.

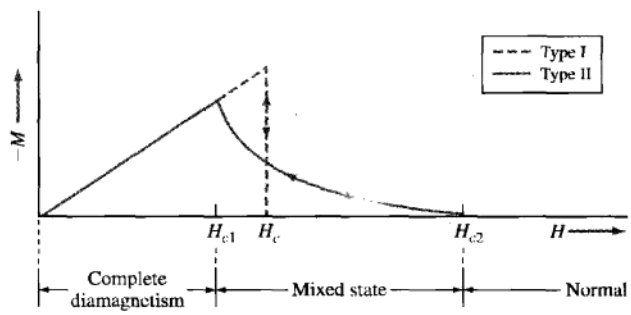

Figure 14.26
Magnetization curves for ideal type I and type II superconductors. Type II superconductors are penetrated by the magnetic field between H_{c1} and H_{c2}.

superconductor can conduct electrical current within bulk material, and thus this magnetic-field region can be used for high-current, high-field superconductors such as NiTi and Ni_3Sb, which are type II superconductors.

14.8.3 Current Flow and Magnetic Fields in Superconductors

Type I superconductors are poor carriers of electrical current since current can only flow in the outer surface layer of a conducting specimen (Fig. 14.27*a*). The reason for this behavior is that the magnetic field can only penetrate the surface layer, and current can only flow in this layer. In type II superconductors below H_{c1}, magnetic fields behave in the same way. However, if the magnetic field is between H_{c1} and H_{c2} (mixed state), the current can be carried inside the superconductor by filaments,

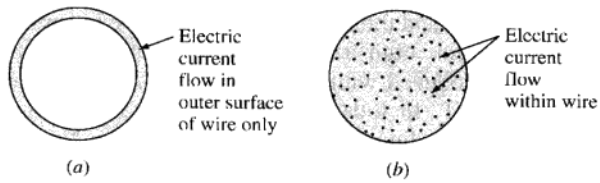

Figure 14.27
Cross section of a superconducting wire carrying an electrical current. (*a*) Type I superconductor or type II under low field ($H < H_{c1}$). (*b*) Type II superconductor under higher fields where current is carried by a filament network ($H_{c1} < H < H_{c2}$).

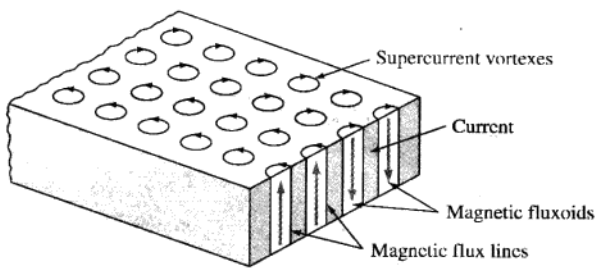

Figure 14.28
Schematic illustration showing magnetic fluxoids in a type II superconductor with the magnetic field between H_{c1} and H_{c2}.

as indicated in Fig. 14.27*b*. In type II superconductors when a magnetic field between H_{c1} and H_{c2} is applied, the field penetrates the bulk of the superconductor in the form of individual quantized flux bundles called **fluxoids** (Fig. 14.28). A cylindrical supercurrent vortex surrounds each fluxoid. With increasing magnetic-field strength, more and more fluxoids enter the superconductor and form a periodic array. At H_{c2}, the supercurrent vortex structure collapses, and the material returns to the normal conducting state.

14.8.4 High-Current, High-Field Superconductors

Although ideal type II superconductors can be penetrated by an applied magnetic field in the H_{c1} to H_{c2} range, they have a small current-carrying capacity below T_c since the fluxoids are weakly tied to the crystal lattice and are relatively mobile. The mobility of the fluxoids can be greatly impeded by dislocations, grain boundaries, and fine precipitates, and thus J_c can be raised by cold working and heat treatments. Heat treatment of the Nb–45 wt % Ti alloy is used to precipitate a hexagonal α phase in the BCC matrix of the alloy to help pin down the fluxoids.

The alloy Nb–45 wt % Ti and the compound Nb_3Sn have become the basic materials for modern high-current, high-field superconductor technology. Commercial Ni–45 wt % Ti has been produced with a $T_c \approx 9$ K and $H_{c2} \approx 6$ T and Nb_3Sn with a $T_c \approx 18$ K and $H_{c2} \approx 11$ T. In today's superconductor technology, these superconductors are used at liquid helium temperature (4.2 K). The Nb–45 wt % Ti alloy is more ductile and easier to fabricate than the Nb_3Sn compound and so is preferred for many applications even though it has lower T_c's and H_{c2}'s. Commercial wires are made of many NbTi filaments, typically about 25 μm in diameter, embedded in a copper matrix (Fig. 14.29). The purpose of the copper matrix is to stabilize the superconductor wire during operation so that hot spots will not develop that could cause the superconducting material to return to the normal state.

Applications for NbTi and Nb_3Sn superconductors include nuclear magnetic imaging systems for medical diagnosis and magnetic levitation of vehicles such as high-speed trains (Fig. 14.1). High-field superconducting magnets are used in particle accelerators in the high-energy physics field.

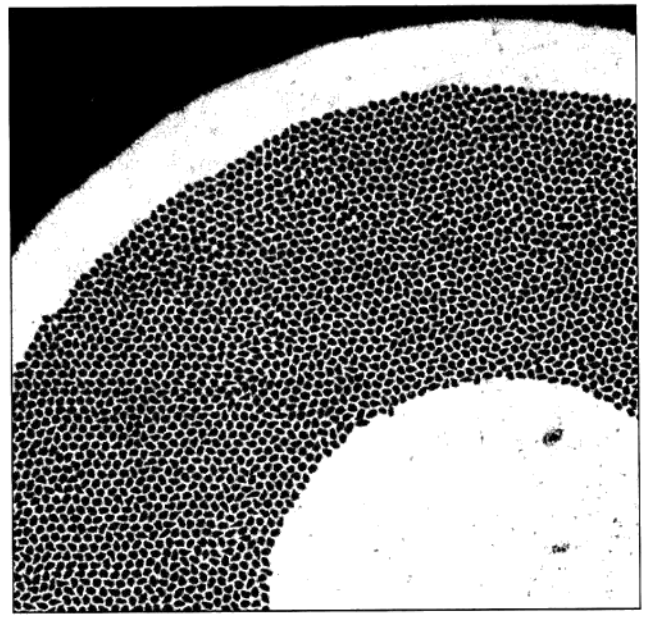

Figure 14.29
Cross section of Nb–46.5 wt % Ti–Cu composite wire made for the superconductor supercollider. The wire has a diameter of 0.0808 cm (0.0318 in), a Cu:NbTi volumetric ratio of 1.5, 7250 filaments of 6-μm diameters, and a $J_c = 2990$ A/mm^2 at 5 T and a $J_c = 1256$ A/mm^2 at 8 T (magnification 200×).
(Courtesy of Outokumpu Advanced Superconductors Inc.)

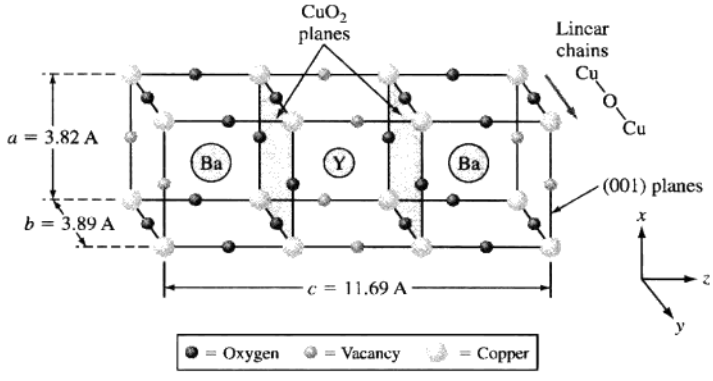

Figure 14.30
Idealized $YBa_2Cu_3O_7$ orthorhombic crystal structure. Note the location of the CuO_2 planes.

14.8.5 High Critical Temperature (T_c) Superconducting Oxides

In 1987, superconductors with critical temperatures of about 90 K were discovered, surprising the scientific community since up to that time the highest T_c for a superconductor was about 23 K. The most intensely studied high T_c material has been the $YBa_2Cu_3O_y$ compound, and so our attention will be focused on some aspects of its structure and properties. From a crystal structure standpoint, this compound can be considered to have a defective perovskite structure with three perovskite cubic unit cells stacked on top of each other (Fig. 14.30). (The perovskite structure for $CaTiO_3$ is shown in Fig. 11.12.) For an ideal stack of three perovskite cubic unit cells, the $YBa_2Cu_3O_y$ compound should have the composition $YBa_2Cu_3O_9$, in which y would equal 9. However, analyses show that y ranges from 6.65 to 6.90 for this material to be a superconductor. At $y = 6.90$, its T_c is highest (~90 K), and at $y = 6.65$, superconductivity disappears. Thus, oxygen vacancies play a role in the superconductivity behavior of $YBa_2Cu_3O_y$.

The $YBa_2Cu_3O_y$ compound, when slowly cooled from above 750°C in the presence of oxygen, undergoes a tetragonal to orthorhombic crystal structure change (Fig. 14.31*a*). If the oxygen content is close to $y = 7$, its T_c is about 90 K (Fig. 14.31*b*) and its unit cell has the constants $a = 3.82$ Å, $b = 3.88$ Å, and $c = 11.7$ Å (Fig. 14.30). To have high T_c values, oxygen atoms on the (001) planes must be ordered so that oxygen vacancies are in the a direction. Superconductivity is believed to be confined to the CuO_2 planes (Fig. 14.30), with the oxygen vacancies providing an electron coupling between the CuO_2 planes. A transmission electron micrograph (Fig. 14.32) shows the stacking of the Ba and Y atoms of the $YBa_2Cu_3O_y$ structure.

From an engineering viewpoint, the new high T_c superconductors hold much promise for technical advances. With T_c's at 90 K, liquid nitrogen can be used as a

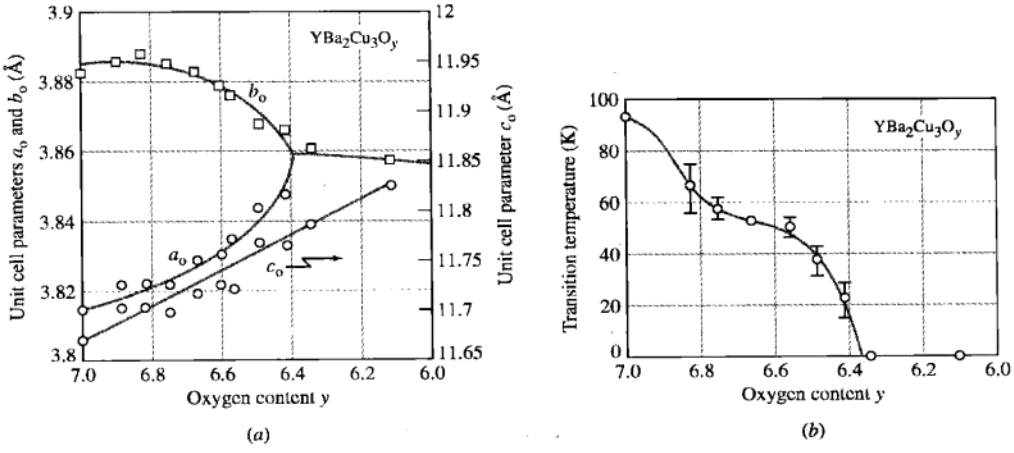

Figure 14.31
(a) Oxygen content versus unit cell constants for $YBa_2Cu_3O_y$. *(b)* Oxygen content versus T_c for $YBa_2Cu_3O_y$. Reproduced by permission of the MRS. Bulletin.
(From J.M. Tarascon and B.G. Bagley, "Oxygen Stoichiometry and the High T_C Superconducting Oxides," MRS Bulletin Vol. XIV, No. 1 (1989), p. 55.

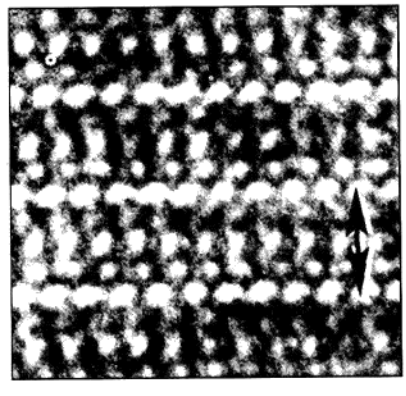

Figure 14.32
High-resolution TEM micrograph in the [100] direction down copper-oxygen chains and rows of Ba and Y atoms in the unit cell of $YBa_2Cu_3O_y$ as indicated by the arrow.
(After J. Narayan, JOM, January 1989, p. 18.)

refrigerant to replace the much more expensive liquid helium. Unfortunately, the high-temperature superconductors are essentially ceramics, which are brittle and in their bulk form have low current-density capability. The first applications for these materials will probably be in thin-film technology for electronic applications such as high-speed computers.

14.9 DEFINITIONS

Sec. 14.3

Index of refraction: the ratio of the velocity of light in vacuum to that through another medium of interest.

Sec. 14.4

Absorptivity: the fraction of the incident light that is absorbed by a material.

Sec. 14.5

Luminescence: absorption of light or other energy by a material and the subsequent emission of light of longer wavelength.

Fluorescence: absorption of light or other energy by a material and the subsequent emission of light within 10^{-8} s of excitation.

Phosphorescence: absorption of light by a phosphor and its subsequent emission at times longer than 10^{-8} s.

Sec. 14.6

Laser: acronym for *l*ight *a*mplification by *s*timulated *e*mission of *r*adiation.

Laser beam: a beam of monochromatic, coherent optical radiation generated by the stimulated emission of photons.

Population inversion: condition in which more atoms exist in a higher-energy state than in a lower one. This condition is necessary for laser action.

Sec. 14.7

Optical-fiber communication: a method of transmitting information by the use of light.

Light attenuation: decrease in intensity of the light.

Optical waveguide: a thin-clad fiber along which light can propagate by total internal reflection and refraction.

Sec. 14.8

Superconducting state: a solid in the superconducting state that shows no electrical resistance.

Critical temperature T_c: the temperature below which a solid shows no electrical resistance.

Critical current density J_c: the current density above which superconductivity disappears.

Critical field H_c: the magnetic field above which superconductivity disappears.

Meissner effect: the expulsion of the magnetic field by a superconductor.

Type I superconductor: one that exhibits complete magnetic-flux repulsion between the normal and superconducting states.

Type II superconductor: one in which the magnetic flux gradually penetrates between the normal and superconducting states.

Lower critical field H_{c1}: the field at which magnetic flux first penetrates a type II superconductor.

Upper critical field H_{c2}: the field at which superconductivity disappears for a type II superconductor.

Fluxoid: a microscopic region surrounded by circulating supercurrents in a type II superconductor at fields between H_{c2} and H_{c1}.

14.10 PROBLEMS

Answers to problems marked with an asterisk are given at the end of the book.

Knowledge and Comprehension Problems

14.1 Write the equation relating the energy of radiation to its wavelength and frequency, and give the SI units for each quantity.

14.2 What are the approximate wavelength and frequency ranges for (*a*) visible light, (*b*) ultraviolet light, and (*c*) infrared radiation?

14.3 If ordinary light is transmitted from air into a 1-cm-thick sheet of polymethacrylate, is the light sped up or slowed down upon entering the plastic? Explain.

14.4 Explain why cut diamonds sparkle. Why is PbO sometimes added to make decorative glasses?

14.5 What is Snell's law of light refraction? Use a diagram to explain.

14.6 Explain why metals absorb and/or reflect incident radiation up to the middle of the ultraviolet range.

14.7 Explain why gold is yellow in color and silver is "silvery."

14.8 Explain the process of luminescence.

14.9 Distinguish between fluorescence and phosphorescence.

14.10 Explain the luminescence effect operating in a fluorescent lamp.

14.11 Distinguish between incoherent and coherent radiation.

14.12 What do the letters in the acronymn *laser* stand for?

14.13 Explain the operation of the ruby laser.

14.14 What does the term *population inversion* refer to in laser terminology?

14.15 Describe the operation and application of the following types of lasers: (*a*) neodymium-YAG, (*b*) carbon dioxide, and (*c*) double heterojunction GaAs.

14.16 What are optical fibers?

14.17 What are the basic elements of an optical-fiber communications system?

14.18 What types of impurities are particularly detrimental to light loss in optical fibers?

14.19 Explain how optical fibers act as waveguides.

14.20 Distinguish between single-mode and multimode types of optical fibers. Which type is used for modern long-distance communication systems and why?

14.21 What types of lasers are used in modern long-distance optical-fiber systems and why?

14.22 What is the superconducting state for a material?

14.23 What is the significance of T_c, H_c, and J_c for a superconductor?

14.24 Describe the difference between type I and type II superconductors.

14.25 What is the Meissner effect?

14.26 Why are type I superconductors poor current-carrying conductors?

14.27 What are fluxoids? What role do they play in the superconductivity of type II superconductors in the mixed state?

14.28 How can fluxoids be pinned in type II superconductors? What is the consequence of pinning the fluxoids in a type II superconductor?

14.29 Describe the crystal structure of $YBa_2Cu_3O_7$. Use a drawing.

14.30 Why must the $YBa_2Cu_3O_y$ compound be cooled slowly from about 750°C in order for this compound to be highly superconductive?

14.31 What are some advantages and disadvantages of the new high-temperature oxide superconductors?

Application and Analysis Problems

*__14.32__ A photon in a ZnO semiconductor drops from an impurity level at 2.30 eV to its valence band. What is the wavelength of the radiation given off by the transition? If the radiation is visible, what is its color?

14.33 A semiconductor emits green visible radiation at a wavelength of 0.520 μm. What is the energy level from which photons drop to the valence band in order to give off this type of radiation?

14.34 What is the critical angle for light to be totally reflected when leaving a flat plate of polystyrene and entering the air?

*__14.35__ Calculate the reflectivity of ordinary light from a smooth, flat upper surface of (*a*) borosilicate glass ($n = 1.47$) and (*b*) polyethylene ($n = 1.53$).

14.36 Ordinary incident light strikes the flat surface of a transparent material with a linear absorption coefficient of 0.04 cm^{-1}. If the plate of the material is 0.80 cm thick, calculate the fraction of light absorbed by the plate.

14.37 Ordinary light strikes a flat surface of a plate of a transparent material. If the plate is 0.75 mm thick and absorbs 5.0 percent of the entering light, what is its linear absorption coefficient?

*__14.38__ Calculate the transmittance for a flat glass plate 6.0 mm thick with an index of refraction of 1.51 and a linear absorption coefficient of 0.03 cm^{-1}.

14.39 Why does a sheet of 2.0-mm-thick polyethylene have lower clarity than a sheet of the same thickness of polycarbonate plastic?

14.40 Calculate the minimum wavelength of the radiation that can be absorbed by the following materials: (*a*) GaP, (*b*) GaSb, and (*c*) InP.

14.41 Will visible light of a wavelength of 500 nm be absorbed or transmitted by the following materials: (*a*) CdSb, (*b*) ZnSe, and (*c*) diamond ($E_g = 5.40$ eV)?

14.42 Explain how the color picture is produced on a color television screen.

14.43 The intensity of an Al_2O_3 phosphor activated with chromium decreases to 15 percent of its original intensity in 5.6×10^{-3} s. Determine (*a*) its relaxation time and (*b*) its retained percent intensity after 5.0×10^{-2} s.

*__14.44__ A Zn_2SiO_4 phosphor activated with manganese has a relaxation time of 0.015 s. Calculate the time required for the intensity of this material to decrease to 8 percent of its original value.

14.45 If the original light intensity is reduced 6.5 percent after being transmitted 300 m through an optical fiber, what is the attenuation of the light in decibels per kilometer (dB/km) for this type of optical fiber?

14.46 Light is attenuated in an optical fiber operating at 1.55 μm wavelength at -0.25 dB/km. If 4.2 percent of the light is to be retained at a repeater station, what must the distance between the repeaters be?

14.47 The attenuation of a 1.3 μm optical-fiber undersea transatlantic cable is -0.31 dB/km, and the distance between repeaters in the system is 40.2 km (25 mi). What is the percent of the light retained at a repeater if we assume 100 percent at the start of a repeater?

14.48 How are optical fibers for communication systems fabricated? How do (*a*) GeO_2 and (*b*) F affect the refractive index of the silica glass?

***14.49** A single-mode optical fiber for a communications system has a core of SiO_2–GeO_2 glass with a refractive index of 1.4597 and a cladding of pure SiO_2 glass with a refractive index of 1.4580. What is the critical angle for light leaving the core to be totally reflected within the core?

14.50 Calculate the critical magnetic field H_c1 in teslas for niobium at 8 K. Use Eq. 14.10 and data from Table 14.3.

***14.51** If vanadium has an H_c value of 0.06 T and is superconductive, what must its temperature be?

Synthesis and Evaluation Problems

14.52 Design a semiconductor that would produce photons with wavelengths corresponding to those of green light. Perform a search to find out which semiconducting material would be suitable for this application.

14.53 Assume the impurity energy level in ZnS is 1.4 eV below its conduction band. What type of radiation would provide the charge carrier just enough energy to jump into the conduction band?

14.54 Select an optical plastic that has a critical angle of 45° for light to be totally reflected when leaving a flat plate and entering air. (Use Table 14.1.)

14.55 (*a*) Select a material from Table 14.1 that has a reflectivity of ordinary incident light of about 5%. (*b*) Select the material with the highest level of reflectivity. (*c*) Select the material with the lowest level of reflectivity. (Assume all the surfaces are polished.)

14.56 Design the thickness of a polished silicate glass that would result in (*a*) no more than 2% light lost due to absorption, and (*b*) no more than 4% light lost due to absorption. What is your conclusion? ($\alpha = 0.03\ cm^{-1}$)

CHAPTER 15

Magnetic Properties

(a)
(Courtesy of Zimmer, Inc.)

(b)

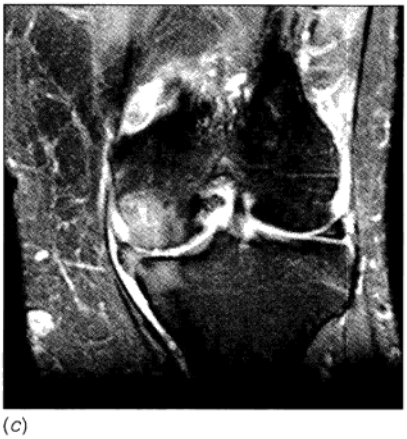

(c)

Magnetic resonance imaging (MRI) technique is used to extract high quality images from inside the human body. It gives physicians and researchers the ability to safely investigate diseases related to the heart, brain, spine, and other organs in the human body. The images produced by an MRI are primarily due to the existence of fat and water molecules that are mostly made up of hydrogen. In short, hydrogen produces a small magnetic signal which is detected by the instrument and used for mapping the tissue.

The MRI hardware is presented in the figure. It consists of a large magnet that produces the magnetic field; a gradient coil that produces a gradient in the field; and an RF coil that detects the signal from the molecules inside the human body. The magnet is the most expensive component of the system and is usually of the superconducting type (wire of several miles length). Overall the MRI is a complex system that requires expertise from mathematics, physics, chemistry, and materials scientists. It also requires expertise from bioengineers, imaging scientists, and architects to design and implement an efficient machine with safe application.

An example of the use of the MRI technology is in orthopedics, where damage to soft tissue can be imaged accurately. The images above show the MRI images of a healthy (left) and a torn anterior cruciate ligament (right). Depending on the extent of damage, the surgeon decides whether to pursue arthroscopic surgery to replace the injured ACL. ■

LEARNING OBJECTIVES

By the end of this chapter, students will be able to . . .

1. Briefly describe the two sources for magnetic moments in materials.
2. Describe magnetic hysteresis for a material.
3. Cite distinctive magnetic characteristics for hard magnetic and soft magnetic material.
4. Describe how increasing the temperature affects the alignment of magnetic dipoles in ferromagnetic material.
5. Describe the nature of paramagnetism.
6. Explain what alnico means.
7. Cite a few industrial applications of soft ferrites.
8. Briefly describe the source of antiferromagnetism.
9. Draw a hysteresis loop of a ferromagnetic material.
10. Describe relative magnetic permeability and magnetic permeability.

15.1 INTRODUCTION

Magnetic materials are necessary for many engineering designs, particularly in the area of electrical engineering. In general there are two main types: *soft* and *hard magnetic materials*. Soft magnetic materials are used for applications in which the material must be easily magnetized and demagnetized, such as cores for distribution power transformers (Fig. 15.1*a*), small electronic transformers, and stator and rotor materials for motors and generators. On the other hand, hard magnetic materials are used for applications requiring permanent magnets that do not demagnetize easily, such as the permanent magnets in loudspeakers, telephone receivers, synchronous and brushless motors, and automotive starting motors.

15.2 MAGNETIC FIELDS AND QUANTITIES

15.2.1 Magnetic Fields

Let us begin our study of magnetic materials by first reviewing some of the fundamental properties of magnetism and magnetic fields. The metals *iron, cobalt,* and *nickel* are the only three elemental metals that, when magnetized at room temperature, can produce a strong magnetic field around themselves. They are said to

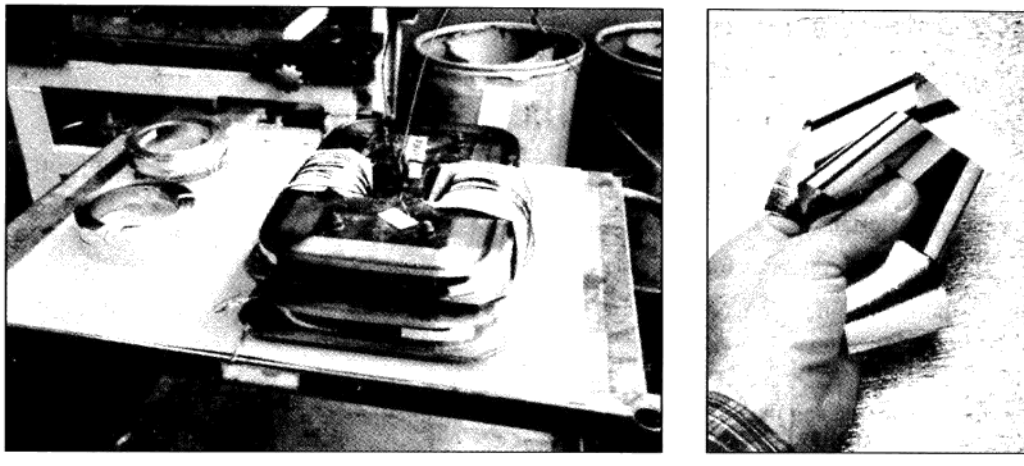

(*a*) (*b*)

Figure 15.1
(*a*) A new magnetic material for engineering designs: metallic glass material is used for the magnetic cores of distribution electric power transformers. The use of highly magnetically soft amorphous metallic glass alloys for transformer cores reduces core energy losses by about 70 percent compared with those made with conventional iron-silicon alloys.
(Courtesy of General Electric Co.)
(*b*) Strip of metallic glass ribbon.
(Courtesy of Metglas, Inc.)

be **ferromagnetic.** The presence of a **magnetic field** surrounding a magnetized iron bar can be revealed by scattering small iron particles on a sheet of paper placed just above the bar (Fig. 15.2). As shown in Fig. 15.2, the bar magnet has two magnetic poles, and magnetic field lines appear to leave one pole and enter the other.

In general, magnetism is dipolar in nature, and no magnetic monopole has ever been discovered. There are always two magnetic poles or centers of a magnetic field separated by a definite distance, and this dipole behavior extends to the small magnetic dipoles found in some atoms.

Magnetic fields are also produced by current-carrying conductors. Figure 15.3 illustrates the formation of a magnetic field around a long coil of copper wire, called a *solenoid,* whose length is long with respect to its radius. For a solenoid of n turns and length l, the magnetic field strength H is

$$H = \frac{0.4\pi ni}{l} \tag{15.1}$$

where i is the current. The magnetic field strength H has SI units of amperes per meter (A/m) and cgs units of oersteds (Oe). The conversion equality between SI and cgs units for H is $1\ \text{A/m} = 4\pi \times 10^{-3}$ Oe.

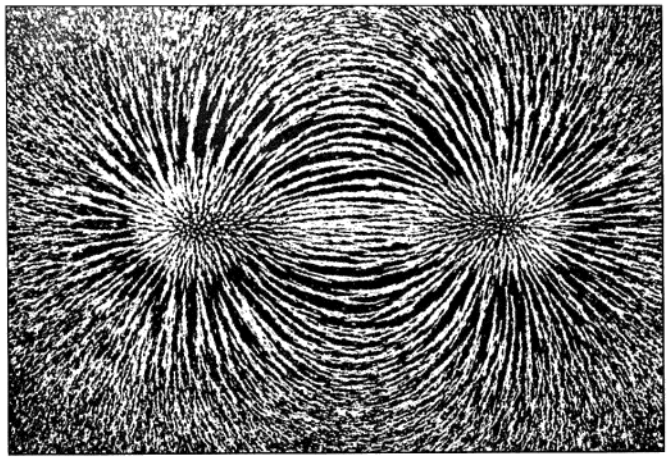

Figure 15.2
The magnetic field surrounding a bar magnet is revealed by the arrangement of iron filings lying on a sheet of paper above the magnet. Note that the bar magnet is dipolar and that magnetic lines of force appear to leave one end of the magnet and return to the other.
(Courtesy of the Physical Science Study Committee, as appearing in D. Halliday and R. Resnick, "Fundamentals of Physics," Wiley, 1974, p. 612.)

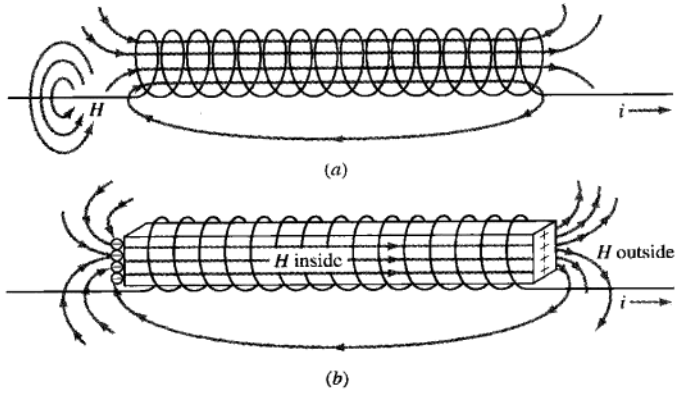

Figure 15.3
(*a*) Schematic illustration of a magnetic field created around a coil of copper wire, called a solenoid, by the passage of current through the wire. (*b*) Schematic illustration of the increase in magnetic field around the solenoid when an iron bar is placed inside the solenoid and current is passed through the wire.
(C.R. Barrett, A.S. Tetelman, and W.D. Nix, "The Principles of Engineering Materials," 1st ed., © 1973. Adapted by permission of Pearson Education, Inc., Upper Saddle River, NJ.)

15.2.2 Magnetic Induction

Now let us place a demagnetized iron bar inside the solenoid and apply a magnetizing current to the solenoid, as shown in Fig. 15.3*b*. The magnetic field outside the solenoid is now stronger with the magnetized bar inside the solenoid. The enhanced magnetic field outside the solenoid is due to the sum of the solenoid field itself and the external magnetic field of the magnetized bar. The new additive magnetic field is called the **magnetic induction,** or *flux density,* or simply *induction,* and is given the symbol B.

The magnetic induction B is the sum of the applied field H and the external field that arises from the magnetization of the bar inside the solenoid. The induced magnetic moment per unit volume due to the bar is called the *intensity of magnetization,* or simply **magnetization,** and is given the symbol M. In the SI system of units,

$$B = \mu_0 H + \mu_0 M = \mu_0(H + M) \tag{15.2}$$

where μ_0 = *permeability of free space* = $4\pi \times 10^{-7}$ tesla-meters per ampere (T · m/A).[1] μ_0 has no physical meaning and is only needed in Eq. 15.2 because SI units were chosen. The SI units for B are webers[2] per square meter (Wb/m^2), or teslas (T), and the SI units for H and M are amperes per meter (A/m). The cgs unit for B is the gauss (G) and for H, the oersted (Oe). Table 15.1 summarizes these magnetic units.

An important point to note is that for ferromagnetic materials, in many cases the magnetization $\mu_0 M$ is often much greater than the applied field $\mu_0 H$, and so we can often use the relation $B \approx \mu_0 M$. Thus, for ferromagnetic materials, sometimes the quantities B (magnetic induction) and M (magnetization) are used interchangeably.

15.2.3 Magnetic Permeability

As previously pointed out, when a ferromagnetic material is placed in an applied magnetic field, the intensity of the magnetic field increases. This increase in

[1]Nikola Tesla (1856–1943). American inventor of Yugoslavian birth who in part developed the polyphase induction motor and invented the Tesla coil (an air transformer). 1 T = 1 Wb/m^2 = 1 V · s/m^2.

[2]1 Wb = 1 V · s.

Table 15.1 Summary of the units for the magnetic quantities

Magnetic quantity	SI units	cgs units
B (magnetic induction)	weber/meter^2 (Wb/m^2) or tesla (T)	gauss (G)
H (applied field)	ampere/meter (A/m)	oersted (Oe)
M (magnetization)	ampere/meter (A/m)	
Numerical conversion factors:		
1 A/m = $4\pi \times 10^{-3}$ Oe		
1 Wb/m^2 = 1.0×10^4 G		
Permeability constant		
$\mu_0 = 4\pi \times 10^{-7}$ T · m/A		

magnetization is measured by a quantity called **magnetic permeability** μ, which is defined as the ratio of the magnetic induction B to the applied field H, or

$$\mu = \frac{B}{H} \tag{15.3}$$

If there is only a vacuum in the applied magnetic field, then

$$\mu_0 = \frac{B}{H} \tag{15.4}$$

where $\mu_0 = 4\pi \times 10^{-7}\ \mathrm{T \cdot m/A}$ = permeability of free space, as previously stated.

An alternative method used for defining magnetic permeability is the quantity **relative permeability** μ_r, which is the ratio of μ/μ_0. Thus

$$\mu_r = \frac{\mu}{\mu_0} \tag{15.5}$$

and

$$B = \mu_0 \mu_r H \tag{15.6}$$

The relative permeability μ_r is a dimensionless quantity.

The relative permeability is a measure of the intensity of the induced magnetic field. In some ways, the magnetic permeability of magnetic materials is analogous to the dielectric constant of dielectric materials. However, the magnetic permeability of a ferromagnetic material is not a constant but changes as the material is magnetized, as indicated in Fig. 15.4. The magnetic permeability of a magnetic material is usually

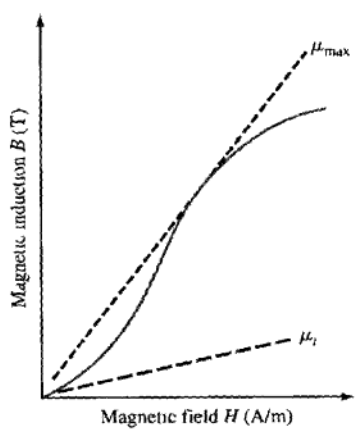

Figure 15.4
B-H initial magnetization curve for a ferromagnetic material. The slope μ_i is the initial magnetic permeability, and the slope μ_{max} is the maximum magnetic permeability

measured by either its initial permeability μ_i or its maximum permeability μ_{max}. Figure 15.4 indicates how μ_i and μ_{max} are measured from slopes of the B-H initial magnetizing curve for a magnetic material. Magnetic materials that are easily magnetized have high magnetic permeabilities.

15.2.4 Magnetic Susceptibility

Since the magnetization of a magnetic material is proportional to the applied field, a proportionality factor called the **magnetic susceptibility** χ_m is defined as

$$\chi_m = \frac{M}{H} \tag{15.7}$$

which is a dimensionless quantity. Weak magnetic responses of materials are often measured in terms of magnetic susceptibility.

15.3 TYPES OF MAGNETISM

Magnetic fields and forces originate from the movement of the basic electric charge, the electron. When electrons move in a conducting wire, a magnetic field is produced around the wire, as shown for the solenoid of Fig. 15.3. Magnetism in materials is also due to the motion of electrons, but in this case the magnetic fields and forces are caused by the intrinsic spin of electrons and their orbital motion about their nuclei (Fig. 15.5).

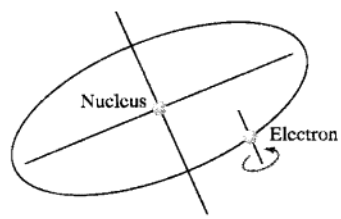

Figure 15.5
A schematic drawing of the Bohr atom indicating an electron spinning on its own axis and revolving about its nucleus. The spin of the electron on its axis and its orbital motion around its nucleus are the origins of magnetism in materials.

Table 15.2 Magnetic susceptibilities of some diamagnetic and paramagnetic elements

Diamagnetic element	Magnetic susceptibility $\chi_m \times 10^{-6}$	Paramagnetic element	Magnetic susceptibility $\chi_m \times 10^{-6}$
Cadmium	−0.18	Aluminum	+0.65
Copper	−0.086	Calcium	+1.10
Silver	−0.20	Oxygen	+106.2
Tin	−0.25	Platinum	+1.10
Zinc	−0.157	Titanium	+1.25

15.3.1 Diamagnetism

An external magnetic field acting on the atoms of a material slightly unbalances their orbiting electrons and creates small magnetic dipoles within the atoms that oppose the applied field. This action produces a negative magnetic effect known as **diamagnetism.** The diamagnetic effect produces a very small negative magnetic susceptibility of the order of $\chi_m \approx -10^{-6}$ (Table 15.2). Diamagnetism occurs in all materials, but in many its negative magnetic effect is canceled by positive magnetic effects. Diamagnetic behavior has no significant engineering importance.

15.3.2 Paramagnetism

Materials that exhibit a small positive magnetic susceptibility in the presence of a magnetic field are called *paramagnetic,* and the magnetic effect is termed **paramagnetism.** The paramagnetic effect in materials disappears when the applied magnetic field is removed. Paramagnetism produces magnetic susceptibilities in materials ranging from about 10^{-6} to 10^{-2} and is produced in many materials. Table 15.2 lists the magnetic susceptibilities of paramagnetic materials at 20°C. Paramagnetism is produced by the alignment of individual magnetic dipole moments of atoms or molecules in an applied magnetic field. Since thermal agitation randomizes the directions of the magnetic dipoles, an increase in temperature decreases the paramagnetic effect.

The atoms of some transition and rare earth elements possess incompletely filled inner shells with unpaired electrons. These unpaired inner electrons in atoms, since they are not counterbalanced by other bonding electrons in solids, cause strong paramagnetic effects and in some cases produce very much stronger ferromagnetic and ferrimagnetic effects, which will be discussed later.

15.3.3 Ferromagnetism

Diamagnetism and paramagnetism are induced by an applied magnetic field, and the magnetization remains only as long as the field is maintained. A third type of magnetism, called **ferromagnetism,** is of great engineering importance. Large

magnetic fields that can be retained or eliminated as desired can be produced in ferromagnetic materials. The most important ferromagnetic elements from an industrial standpoint are iron (Fe), cobalt (Co), and nickel (Ni). Gadolinium (Gd), a rare earth element, is also ferromagnetic below 16°C but has little industrial application.

The ferromagnetic properties of the transition elements Fe, Co, and Ni are due to the way the spins of the inner unpaired electrons are aligned in their crystal lattices. The inner shells of individual atoms are filled with pairs of electrons with opposed spins, and so they do not contribute to the resultant magnetic dipole moments. In solids, the outer valence electrons of atoms are combined with each other to form chemical bonds, and so there is no significant magnetic moment due to these electrons. In Fe, Co, and Ni, the unpaired inner 3*d* electrons are responsible for the ferromagnetism that these elements exhibit. The iron atom has four unpaired 3*d* electrons, the cobalt atom three, and the nickel atom two (Fig. 15.6).

In a solid sample of Fe, Co, or Ni at room temperature, the spins of the 3*d* electrons of adjacent atoms align in a parallel direction by a phenomenon called *spontaneous magnetization.* This parallel alignment of atomic magnetic dipoles occurs only in microscopic regions called *magnetic domains.* If the domains are randomly oriented, then there will be no net magnetization in a bulk sample. The parallel alignment of the magnetic dipoles of atoms of Fe, Co, and Ni is due to the creation of a positive exchange energy between them. For this parallel alignment to occur, the ratio of the atomic spacing to the diameter of the 3*d* orbit must be in the range from about 1.4 to 2.7 (Fig. 15.7). Thus Fe, Co, and Ni are ferromagnetic, but manganese (Mn) and chromium (Cr) are not.

Unpaired 3*d* electrons	Atom	Number of electrons	Electronic configuration 3*d* orbitals	4*s* electrons
3	V	23	↑↓ ↑ ↑ ↑ ↑	2
5	Cr	24	↑ ↑ ↑ ↑ ↑	1
5	Mn	25	↑ ↑ ↑ ↑ ↑	2
4	Fe	26	↑↓ ↑ ↑ ↑ ↑	2
3	Co	27	↑↓ ↑↓ ↑ ↑ ↑	2
2	Ni	28	↑↓ ↑↓ ↑↓ ↑ ↑	2
0	Cu	29	↑↓ ↑↓ ↑↓ ↑↓ ↑↓	1

Figure 15.6
Magnetic moments of neutral atoms of 3*d* transition elements.

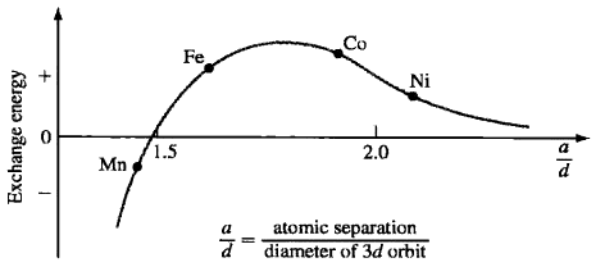

Figure 15.7
Magnetic exchange interaction energy as a function of the ratio of atomic spacing to the diameter of the 3*d* orbit for some 3*d* transition elements. Those elements that have positive exchange energies are ferromagnetic; those with negative exchange energies are antiferromagnetic.

15.3.4 Magnetic Moment of a Single Unpaired Atomic Electron

Each electron spinning on its own axis (Fig. 15.5) behaves as a magnetic dipole and has a dipole moment called the **Bohr magneton** μ_B. This dipole moment has a value of

$$\mu_B = \frac{eh}{4\pi m} \tag{15.8}$$

where e = electronic charge, h = Planck's constant, and m = electron mass. In SI units, $\mu_B = 9.27 \times 10^{-24}\ \text{A} \cdot \text{m}^2$. In most cases, electrons in atoms are paired, and so the positive and negative magnetic moments cancel. However, unpaired electrons in inner electron shells can have small positive dipole moments, as is the case for the 3*d* electrons of Fe, Co, and Ni.

EXAMPLE PROBLEM 15.1

Using the relationship $\mu_B = eh/4\pi m$, show that the numerical value for a Bohr magneton is $9.27 \times 10^{-24}\ \text{A} \cdot \text{m}^2$.

■ **Solution**

$$\mu_B = \frac{eh}{4\pi m} = \frac{(1.60 \times 10^{-19}\ \text{C})(6.63 \times 10^{-34}\ \text{J} \cdot \text{s})}{4\pi(9.11 \times 10^{-31}\ \text{kg})}$$
$$= 9.27 \times 10^{-24}\ \text{C} \cdot \text{J} \cdot \text{s/kg}$$
$$= 9.27 \times 10^{-24}\ \text{A} \cdot \text{m}^2 \blacktriangleleft$$

The units are consistent, as follows:

$$\frac{\text{C} \cdot \text{J} \cdot \text{s}}{\text{kg}} = \frac{(\text{A} \cdot \text{s})(\text{N} \cdot \text{m})(\text{s})}{\text{kg}} = \frac{\text{A} \cdot \cancel{\text{s}}}{\cancel{\text{kg}}}\left(\frac{\cancel{\text{kg}} \cdot \text{m} \cdot \text{m}}{\cancel{\text{s}}^2}\right)(\cancel{\text{s}}) = \text{A} \cdot \text{m}^2$$

EXAMPLE PROBLEM 15.2

Calculate a theoretical value for the saturation magnetization M_s in amperes per meter and saturation induction B_s in teslas for pure iron, assuming all magnetic moments due to the four unpaired 3*d* Fe electrons are aligned in a magnetic field. Use the equation $B_s \approx \mu_0 M_s$ and assume that $\mu_0 H$ can be neglected. Pure iron has a BCC unit cell with a lattice constant $a = 0.287$ nm.

■ Solution

The magnetic moment of an iron atom is assumed to be 4 Bohr magnetons. Thus,

$$M_s = \left[\frac{\dfrac{2 \text{ atoms}}{\text{unit cell}}}{\dfrac{(2.87 \times 10^{-10}\text{ m})^3}{\text{unit cell}}}\right]\left(\frac{4 \text{ Bohr magnetons}}{\text{atom}}\right)\left(\frac{9.27 \times 10^{-24}\text{ A} \cdot \text{m}^2}{\text{Bohr magneton}}\right)$$

$$= \left(\frac{0.085 \times 10^{30}}{\text{m}^3}\right)(4)(9.27 \times 10^{-24}\text{ A} \cdot \text{m}^2) = 3.15 \times 10^6 \text{ A/m} \blacktriangleleft$$

$$B_s \approx \mu_0 M_s \approx \left(\frac{4\pi \times 10^{-7}\text{ T} \cdot \text{m}}{\text{A}}\right)\left(\frac{3.15 \times 10^6\text{ A}}{\text{m}}\right) \approx 3.96 \text{ T} \blacktriangleleft$$

EXAMPLE PROBLEM 15.3

Iron has a saturation magnetization of 1.71×10^6 A/m. What is the average number of Bohr magnetons per atom that contribute to this magnetization? Iron has the BCC crystal structure with $a = 0.287$ nm.

■ Solution

The saturation magnetization M_s in amperes per meter can be calculated from Eq. 16.9 as

$$M_s = \left(\frac{\text{atoms}}{\text{m}^3}\right)\left(\frac{N\mu_B \text{ of Bohr magnetons}}{\text{atom}}\right)\left(\frac{9.27 \times 10^{-24}\text{ A} \cdot \text{m}^2}{\text{Bohr magneton}}\right)$$

$$= \text{ans. in A/m} \qquad (15.9)$$

$$\text{Atomic density (no. of atoms/m}^3) = \frac{2 \text{ atoms/BCC unit cell}}{(2.87 \times 10^{-10}\text{ m})^3/\text{unit cell}}$$

$$= 8.46 \times 10^{28} \text{ atoms/m}^3$$

We rearrange Eq. 15.9 and solve for $N\mu_B$. After substituting values for M_s, atomic density, and μ_B, we can calculate the value of $N\mu_B$.

$$N\mu_B = \frac{M_s}{(\text{atoms/m}^3)(\mu_B)}$$

$$= \frac{1.71 \times 10^6 \text{ A/m}}{(8.46 \times 10^{28}\text{ atoms/m}^3)(9.27 \times 10^{-24}\text{ A} \cdot \text{m}^2)} = 2.18\,\mu_B/\text{atom} \blacktriangleleft$$

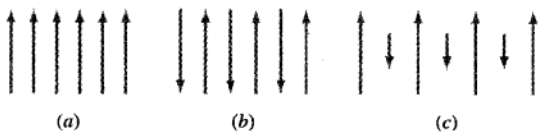

Figure 15.8
Alignment of magnetic dipoles for different types of magnetism: (*a*) ferromagnetism, (*b*) antiferromagnetism, and (*c*) ferrimagnetism.

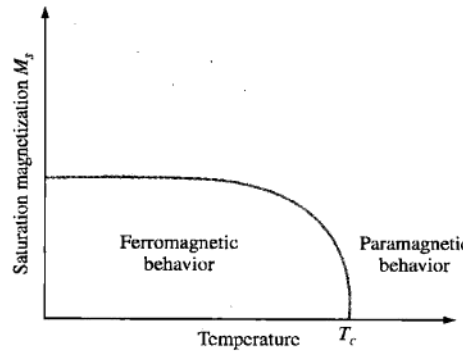

Figure 15.9
Effect of temperature on the saturation magnetization M_s of a ferromagnetic material below its Curie temperature T_c. Increasing the temperature randomizes the magnetic moments.

15.3.5 Antiferromagnetism

Another type of magnetism that occurs in some materials is **antiferromagnetism.** In the presence of a magnetic field, magnetic dipoles of atoms of antiferromagnetic materials align themselves in opposite directions (Fig. 15.8*b*). The elements manganese and chromium in the solid state at room temperature exhibit antiferromagnetism and have a negative exchange energy because the ratio of their atomic spacing to diameter of the 3*d* orbit is less than about 1.4 (Fig. 15.7).

15.3.6 Ferrimagnetism

In some ceramic materials, different ions have different magnitudes for their magnetic moments, and when these magnetic moments are aligned in an antiparallel manner, there is a net magnetic moment in one direction **(ferrimagnetism)** (Fig. 15.8*c*). As a group, ferrimagnetic materials are called *ferrites.* There are many types of ferrites. One group is based on magnetite, Fe_3O_4, which is the magnetic lodestone of the ancients. Ferrites have low conductivities that make them useful for many electronics applications.

15.4 EFFECT OF TEMPERATURE ON FERROMAGNETISM

At any finite temperature above 0 K, thermal energy causes the magnetic dipoles of a ferromagnetic material to deviate from perfect parallel alignment. Thus, the exchange energy that causes the parallel alignment of the magnetic dipoles in ferromagnetic materials is counterbalanced by the randomizing effects of thermal energy (Fig. 15.9). Finally, as the temperature increases, some temperature is reached

where the ferromagnetism in a ferromagnetic material completely disappears, and the material becomes paramagnetic. This temperature is called the **Curie temperature.** When a sample of a ferromagnetic material is cooled from a temperature above its Curie temperature, ferromagnetic domains reform and the material becomes ferromagnetic again. The Curie temperatures of Fe, Co, and Ni are 770°C, 1123°C, and 358°C, respectively.

15.5 FERROMAGNETIC DOMAINS

Below the Curie temperature, the magnetic dipole moments of atoms of ferromagnetic materials tend to align themselves in a parallel direction in small-volume regions called **magnetic domains.** When a ferromagnetic material such as iron or nickel is demagnetized by slowly cooling from above its Curie temperature, the magnetic domains are aligned at random so that there is no net magnetic moment for a bulk sample (Fig. 15.10).

When an external magnetic field is applied to a demagnetized ferromagnetic material, magnetic domains whose moments are initially parallel to the applied magnetic field grow at the expense of the less favorably oriented domains

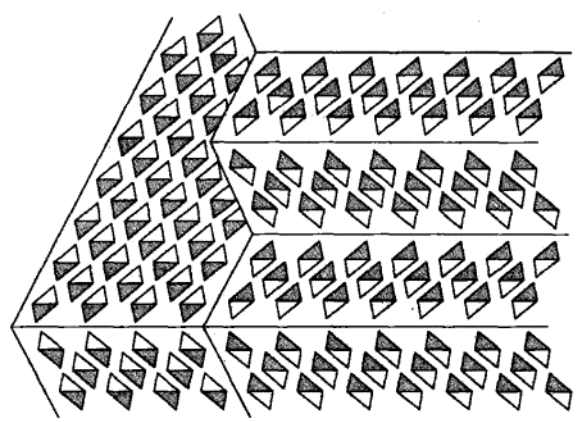

Figure 15.10
Schematic illustration of magnetic domains in a ferromagnetic metal. All the magnetic dipoles in each domain are aligned, but the domains themselves are aligned at random so that there is no net magnetization.
(From R.M. Rose, L.A. Shepard, and J. Wulff, "Structure and Properties of Materials," vol. IV: "Electronic Properties," Wiley, 1966, p. 193.)

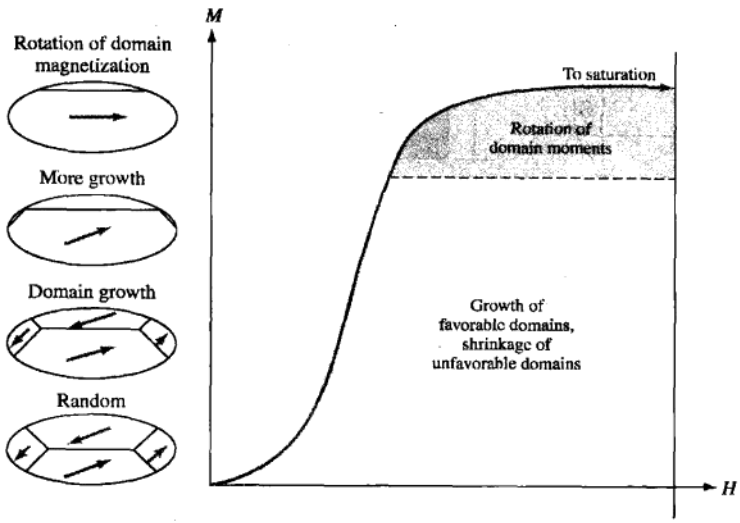

Figure 15.11
Magnetic domain growth and rotation as a demagnetized ferromagnetic material is magnetized to saturation by an applied magnetic field.
(From R.M. Rose, L.A. Shepard, and J. Wulff, "Structure and Properties of Materials," vol. IV: "Electronic Properties," Wiley, 1966, p. 193.)

(Fig. 15.11). The domain growth takes place by domain wall movement, as indicated in Fig. 15.11, and B or M increases rapidly as the H field increases. Domain growth by wall movement takes place first since this process requires less energy than domain rotation. When domain growth finishes, if the applied field is increased substantially, domain rotation occurs. Domain rotation requires considerably more energy than domain growth, and the slope of the B or M versus H curve decreases at the high fields required for domain rotation (Fig. 15.11). When the applied field is removed, the magnetized sample remains magnetized, even though some of the magnetization is lost because of the tendency of the domains to rotate back to their original alignment.

Figure 15.12 shows how the domain walls move under an applied field in iron single-crystal whiskers. The domain walls are revealed by the Bitter technique, in which a colloidal solution of iron oxide is deposited on the polished surface of the iron. The wall movement is followed by observation with an optical microscope. Using this technique, much information has been obtained about domain wall movement under applied magnetic fields.

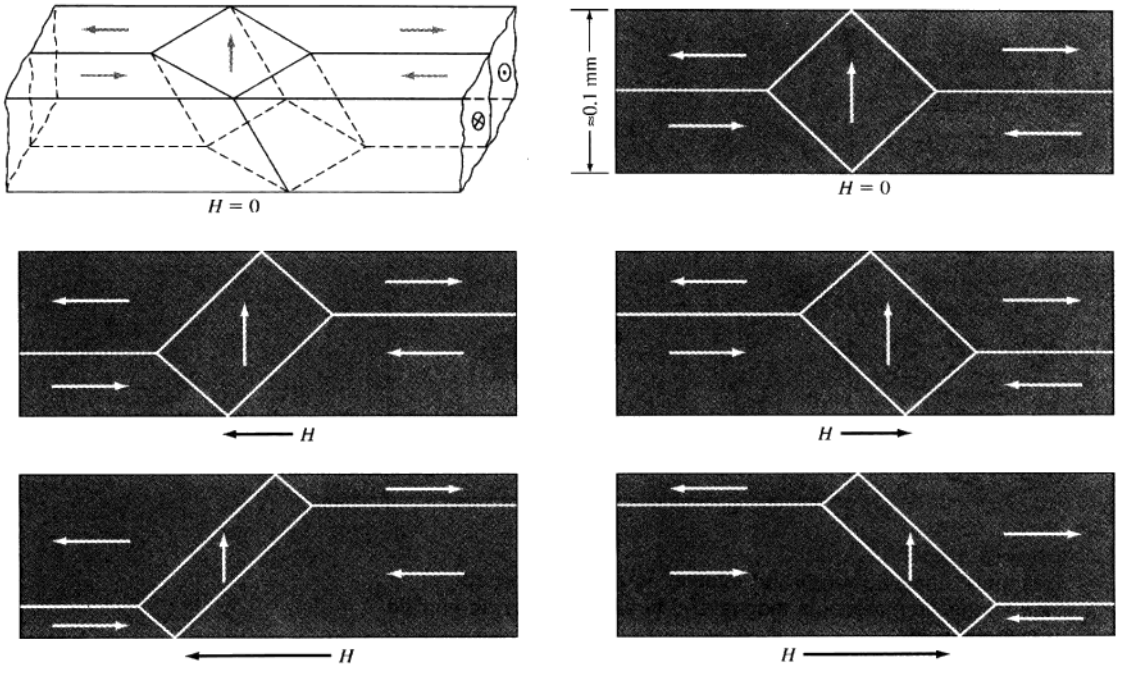

Figure 15.12
Movement of domain boundaries in an iron crystal produced by the application of a magnetic field. Note that as the applied field is increased, the domains with their dipoles aligned in the direction of the field enlarge and those with their dipoles opposed get smaller. (The applied fields on the left and right figures increase from top to bottom.)
(Courtesy of R.W. DeBlois, The General Electric Co., and C.D. Graham, the University of Pennsylvania.)

15.6 TYPES OF ENERGIES THAT DETERMINE THE STRUCTURE OF FERROMAGNETIC DOMAINS

The domain structure of a ferromagnetic material is determined by many types of energies, with the most stable structure being attained when the overall potential energy of the material is a minimum. The total magnetic energy of a ferromagnetic material is the sum of the contributions of the following energies: (1) exchange energy, (2) magnetostatic energy, (3) magnetocrystalline anisotropy energy, (4) domain wall energy, and (5) magnetostrictive energy. Let us now briefly discuss each of these energies.

15.6.1 Exchange Energy

The potential energy *within* a domain of a ferromagnetic solid is minimized when all its atomic dipoles are aligned in one direction **(exchange energy).** This alignment

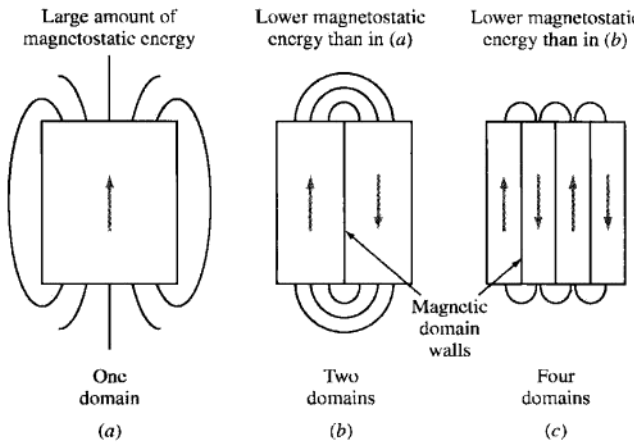

Figure 15.13
Schematic illustration showing how reducing the domain size in a magnetic material decreases the magnetostatic energy by reducing the external magnetic field. (*a*) One domain, (*b*) two domains, and (*c*) four domains.

is associated with a positive exchange energy. However, even though the potential energy within a domain is minimized, its external potential energy is increased by the formation of an external magnetic field (Fig. 15.13*a*).

15.6.2 Magnetostatic Energy

Magnetostatic energy is the potential magnetic energy of a ferromagnetic material produced by its external field (Fig. 15.13*a*). This potential energy can be minimized in a ferromagnetic material by domain formation, as illustrated in Fig. 15.13. For a unit volume of a ferromagnetic material, a single-domain structure has the highest potential energy, as indicated by Fig. 15.13*a*. By dividing the single domain of Fig. 15.13*a* into two domains (Fig. 15.13*b*), the intensity and extent of the external magnetic field is reduced. By further subdividing the single domain into four domains, the external magnetic field is reduced still more (Fig. 15.13*c*). Since the intensity of the external magnetic field of a ferromagnetic material is directly related to its magnetostatic energy, the formation of multiple domains reduces the magnetostatic energy of a unit volume of material.

15.6.3 Magnetocrystalline Anisotropy Energy

Before considering domain boundary (wall) energy, let us look at the effects of crystal orientation on the magnetization of ferromagnetic materials. Magnetization versus applied field curves for a single crystal of a ferromagnetic material can vary,

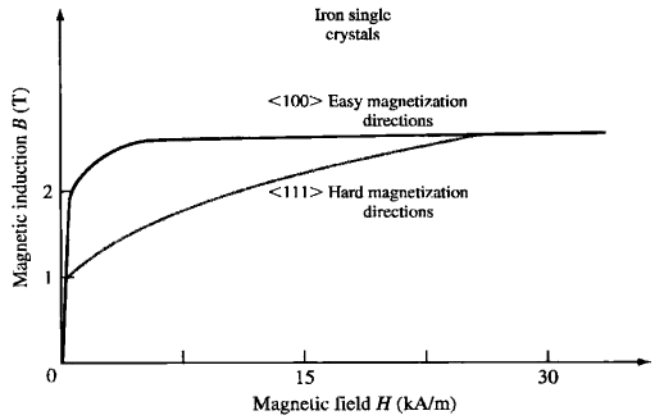

Figure 15.14
Magnetocrystalline anisotropy in BCC iron. Iron is magnetized easier in the ⟨100⟩ directions than in the ⟨111⟩ directions.

depending on the crystal orientation relative to the applied field. Figure 15.14 shows magnetic induction B versus applied field H curves for magnetizations in the ⟨100⟩ and ⟨111⟩ directions for single crystals of BCC iron. As indicated in Fig. 15.14, saturation magnetization occurs most easily (or with the lowest applied field) for the ⟨100⟩ directions and with the highest applied field in the ⟨111⟩ directions. The ⟨111⟩ directions are said to be the hard directions for magnetization in BCC iron. For FCC nickel, the easy directions of magnetization are the ⟨111⟩ directions and the ⟨100⟩ the hard directions; the hard directions for FCC nickel are just the opposite of those for BCC iron.

For polycrystalline ferromagnetic materials such as iron and nickel, grains at different orientations will reach saturation magnetization at different field strengths. Grains whose orientations are in the easy direction of magnetization will saturate at low applied fields, while grains oriented in the hard directions must rotate their resultant moment in the direction of the applied field and thus will reach saturation under much higher fields. The work done to rotate all the domains because of this anisotropy is called the **magnetocrystalline anisotropy energy.**

15.6.4 Domain Wall Energy

A *domain wall* is the boundary between two domains whose overall magnetic moments are at different orientations. It is analogous to a grain boundary where crystal orientation changes from one grain to another. In contrast to a grain boundary, at which grains change orientation abruptly and which is about three atoms wide, a domain changes orientation gradually with a domain boundary being about

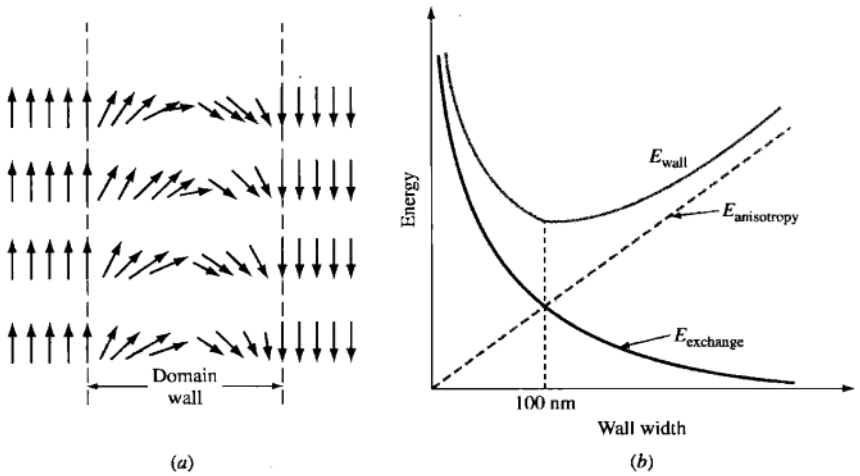

Figure 15.15
Schematic illustration of (*a*) magnetic dipole arrangements at domain (Bloch) wall and (*b*) relationship among magnetic exchange energy, magnetocrystalline anisotropy energy, and wall width. The equilibrium wall width is about 100 nm.
(C.R. Barrett, A.S. Tetelman, and W.D. Nix, "The Principles of Engineering Materials," 1st ed., © 1973. Adapted by permission of Pearson Education, Inc., Upper Saddle River, NJ.)

300 atoms wide. Figure 15.15*a* shows a schematic drawing of a domain boundary of 180 degrees change in magnetic moment direction that takes place gradually across the boundary.

The large width of a domain wall is due to a balance between two forces: exchange energy and magnetocrystalline anisotropy. When there is only a small difference in orientation between the dipoles (Fig. 15.15*a*), the exchange forces between the dipoles are minimized and the exchange energy is reduced (Fig. 15.15*b*). Thus, the exchange forces will tend to widen the domain wall. However, the wider the wall is, the greater will be the number of dipoles forced to lie in directions different from those of easy magnetization, and the magnetocrystalline anisotropy energy will be increased (Fig. 15.15*b*). Thus, the equilibrium wall width will be reached at the width where the sum of the exchange and magnetocrystalline anisotropy energies is a minimum (Fig. 15.15*b*).

15.6.5 Magnetostrictive Energy

When a ferromagnetic material is magnetized, its dimensions change slightly, and the sample being magnetized either expands or contracts in the direction of magnetization (Fig. 15.16). This magnetically induced reversible elastic strain ($\Delta l/l$) is called **magnetostriction** and is of the order of 10^{-6}. The energy due to the

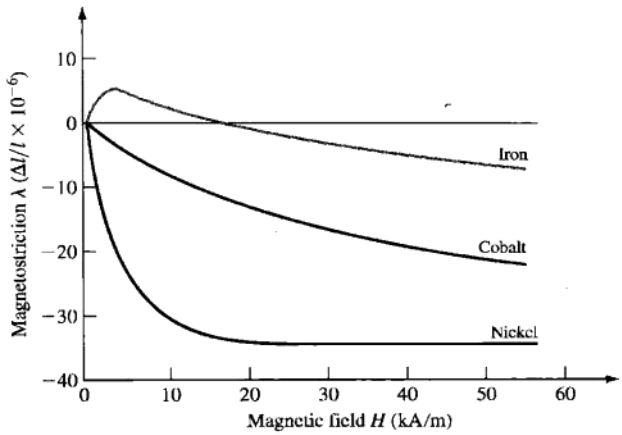

Figure 15.16
Magnetostrictive behavior of Fe, Co, and Ni ferromagnetic elements. Magnetostriction is a fractional elongation (or contraction), and in this illustration is in units of micrometers per meter.

mechanical stresses created by magnetostriction is called **magnetostrictive energy.** For iron, the magnetostriction is positive at low fields and negative at high fields (Fig. 15.16).

The cause of magnetostriction is attributed to the change in the bond length between the atoms in a ferromagnetic metal when their electron-spin dipole moments are rotated into alignment during magnetization. The fields of the dipoles may attract or repel each other, leading to the contraction or expansion of the metal during magnetization.

Let us now consider the effect of magnetostriction on the equilibrium configuration of the domain structure of cubic crystalline materials, such as those shown in Fig. 15.17*a* and *b*. Because of the cubic symmetry of the crystals, the formation of triangular-shaped domains, called *domains of closure,* at the ends of the crystal eliminates the magnetostatic energy associated with an external magnetic field and hence lowers the energy of the material. It might appear that very large domains such as those shown in Fig. 15.17*a* and *b* would be the lowest energy and most stable configuration since there is minimum wall energy. However, this is not the case since magnetostrictive stresses introduced during magnetization tend to be larger for larger domains. Smaller magnetic domains, such as those shown in Fig. 15.17*c*, reduce magnetostrictive stresses but increase domain wall area and energy. Thus, the equilibrium domain configuration is reached when the sum of the magnetostrictive and **domain wall energies** is a minimum.

In summary, the domain structure formed in ferromagnetic materials is determined by the various contributions of exchange, magnetostatic, magnetocrystalline

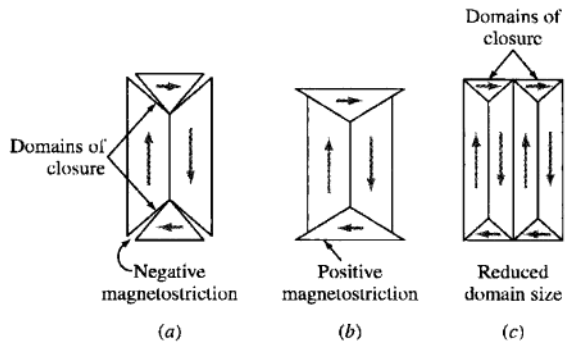

Figure 15.17
Magnetostriction in cubic magnetic materials. Schematic exaggeration of (*a*) negative and (*b*) positive magnetostriction pulling apart the domain boundaries of a magnetic material. (*c*) Lowering of magnetostrictive stresses by the creation of a smaller-domain-size structure.

anisotropic, domain wall, and magnetostrictive energies to its total magnetic energy. The equilibrium or most stable configuration occurs when the total magnetic energy is the lowest.

15.7 THE MAGNETIZATION AND DEMAGNETIZATION OF A FERROMAGNETIC METAL

Ferromagnetic metals such as Fe, Co, and Ni acquire large magnetizations when placed in a magnetizing field, and they remain in the magnetized condition to a lesser extent after the magnetizing field is removed. Let us consider the effect of an applied field H on the magnetic induction B of a ferromagnetic metal during magnetizing and demagnetizing, as shown in the B versus H graph of Fig. 15.18. First, let us demagnetize a ferromagnetic metal such as iron by slowly cooling it from above its Curie temperature. Then, let us apply a magnetizing field to the sample and follow the effect of the applied field on the magnetic induction of the sample.

As the applied field increases from zero, B increases from zero along curve OA of Fig. 15.18 until **saturation induction** is reached at point A. Upon decreasing the applied field to zero, the original magnetization curve is not retraced, and there remains a magnetic flux density called the **remanent induction** B_r (point C in Fig. 15.18). To decrease the magnetic induction to zero, a reverse (negative) applied field of the amount H_c, called the **coercive force,** must be applied (point D in Fig. 15.18). If the negative applied field is increased still more, eventually the material will reach saturation induction in the reverse field at point E of Fig. 15.18.

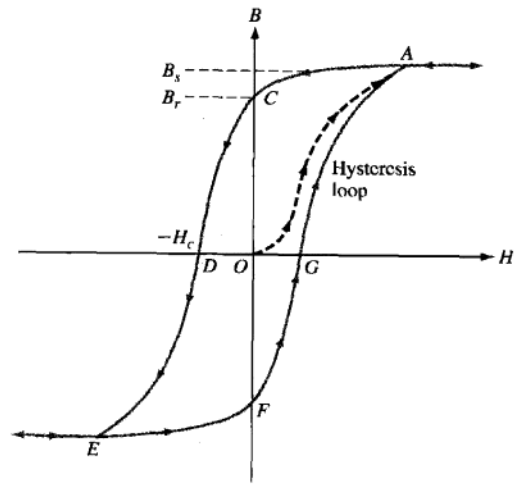

Figure 15.18
Magnetic induction *B* versus applied field *H* hysteresis loop for a ferromagnetic material. The curve *OA* traces out the initial *B* versus *H* relationship for the magnetization of a demagnetized sample. Cyclic magnetization and demagnetization to saturation induction traces out hysteresis loop *ACDEFGA*.

When the reverse field is removed, the magnetic induction will return to the remanent induction at point *F* in Fig. 15.18, and upon application of a positive applied field, the *B-H* curve will follow *FGA* to complete a loop. Further application of reverse and forward applied fields to saturation induction will produce the repetitive loop of *ACDEFGA*. This magnetization loop is referred to as a **hysteresis loop,** and its internal area is a measure of energy lost or the work done by the magnetizing and demagnetizing cycle.

15.8 SOFT MAGNETIC MATERIALS

A **soft magnetic material** is easily magnetized and demagnetized, whereas a *hard magnetic material* is difficult to magnetize and demagnetize. In the early days, soft and hard magnetic materials were physically soft and hard, respectively. Today, however, the physical hardness of a magnetic material does not necessarily indicate that it is magnetically soft or hard.

Soft materials such as the iron–3 to 4 percent silicon alloys used in cores for transformers, motors, and generators have narrow hysteresis loops with low coercive

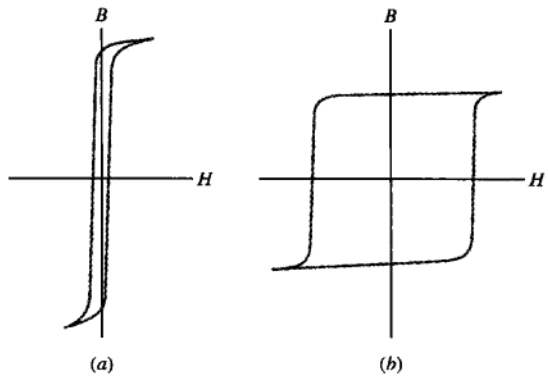

Figure 15.19
Hysteresis loops for (*a*) a soft magnetic material and (*b*) a hard magnetic material. The soft magnetic material has a narrow hysteresis loop that makes it easy to magnetize and demagnetize, whereas the hard magnetic material has a wide hysteresis loop that makes it difficult to magnetize and demagnetize.

forces (Fig. 15.19*a*). On the other hand, hard magnetic materials used for permanent magnets have wide hysteresis loops with high coercive forces (Fig. 15.19*b*).

15.8.1 Desirable Properties for Soft Magnetic Materials

For a ferromagnetic material to be soft, its hysteresis loop should have as low a coercive force as possible. That is, its hysteresis loop should be as thin as possible so that the material magnetizes easily and has a high magnetic permeability. For most applications, a high saturation induction is also an important property of soft magnetic materials. Thus, a very thin and high hysteresis loop is desirable for most soft magnetic materials (Fig. 15.19*a*).

15.8.2 Energy Losses for Soft Magnetic Materials

Hysteresis Energy Losses **Hysteresis energy losses** are due to dissipated energy required to push the domain walls back and forth during the magnetization and demagnetization of the magnetic material. The presence of impurities, crystalline imperfections, and precipitates in soft magnetic materials all act as barriers to impede domain wall movement during the magnetization cycle and so increase hysteresis energy losses. Plastic strain, by increasing the dislocation density of a magnetic material, also increases hysteresis losses. In general, the internal area of a hysteresis loop is a measure of the energy lost due to magnetic hysteresis.

In the magnetic core of an AC electrical power transformer using 60 cycles/s, electric current goes through the entire hysteresis loop 60 times per second, and in each cycle there is some energy lost due to movement of the domain walls of the magnetic material in the transformer core. Thus, increasing the AC electrical input frequency of electromagnetic devices increases the hysteresis energy losses.

Eddy-Current Energy Losses A fluctuating magnetic field caused by AC electrical input into a conducting magnetic core produces transient voltage gradients that create stray electric currents. These induced electric currents are called *eddy currents* and are a source of energy loss due to electrical resistance heating. **Eddy-current energy losses** in electrical transformers can be reduced by using a laminated or sheet structure in the magnetic core. An insulation layer between the conducting magnetic material prevents the eddy currents from going from one sheet to the next. Another approach to reducing eddy-current losses, particularly at higher frequencies, is to use a soft magnetic material that is an insulator. Ferrimagnetic oxides and other similar-type magnetic materials are used for some high-frequency electromagnetic applications and will be discussed in Sec. 15.9.

15.8.3 Iron-Silicon Alloys

The most extensively used soft magnetic materials are the iron–3 to 4 percent silicon alloys. Before about 1900, low-carbon plain-carbon steels were used for low-frequency (60 cycle) power application devices such as transformers, motors, and generators. However, with these magnetic materials, core losses were relatively high.

The addition of about 3 to 4 percent silicon to iron to make **iron-silicon alloys** has several beneficial effects for reducing core losses in magnetic materials:

1. Silicon increases the electrical resistivity of low-carbon steel and thus reduces the eddy-current losses.
2. Silicon decreases the magnetoanisotropy energy of iron and increases magnetic permeability and thus decreases hysteresis core losses.
3. Silicon additions (3 to 4 percent) also decrease magnetostriction and lower hysteresis energy losses and transformer noise ("hum").

However, on the detrimental side, silicon decreases the ductility of iron, so only up to about 4 percent silicon can be alloyed with iron. Silicon also decreases the saturation induction and Curie temperature of iron.

A further decrease in eddy-current energy losses in transformer cores was achieved by using a laminated (stacked-sheet) structure. For a modern power transformer core, a multitude of thin iron-silicon sheets about 0.010 to 0.014 in. (0.025 to 0.035 cm) thick are stacked on top of each other with a thin layer of insulation between them. The insulation material is coated on both sides of the iron-silicon sheets and prevents stray eddy currents from flowing perpendicular to the sheets.

Still another decrease in transformer-core energy loss was achieved in the 1940s by the production of grain-oriented iron-silicon sheet. By using a combination of

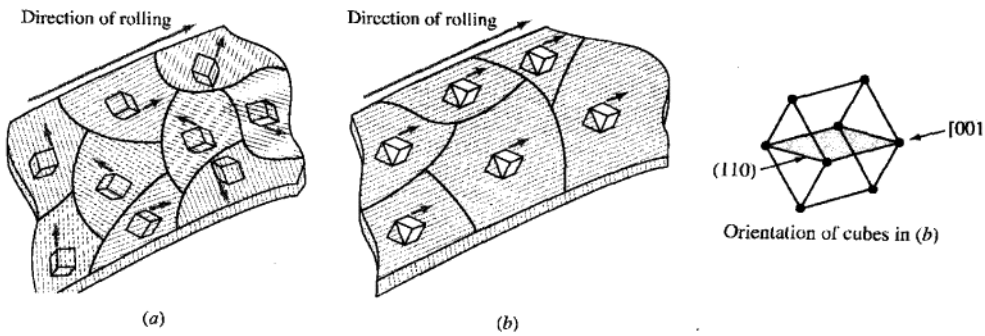

Figure 15.20
(*a*) Random and (*b*) preferred orientation (110) [001] texture in polycrystalline iron–3 to 4% silicon sheet. The small cubes indicate the orientation of each grain.
(*From R.M. Rose, L.A. Shepard, and J. Wulff, "Structure and Properties of Materials," vol. IV: "Electronic Properties," Wiley, 1966, p. 211.*)

Table 16.3 Selected magnetic properties of soft magnetic materials

Material and composition	Saturation induction B_s (T)	Coercive force H_c (A/cm)	Initial relative permeability μ_i
Magnetic iron, 0.2-cm sheet	2.15	0.88	250
M36 cold-rolled Si-Fe (random)	2.04	0.36	500
M6 (110) [001], 3.2% Si-Fe (oriented)	2.03	0.06	1,500
45 Ni-55 Fe (45 Permalloy)	1.6	0.024	2,700
75 Ni-5 Cu-2 Cr-18 Fe (Mumetal)	0.8	0.012	30,000
79 Ni-5 Mo-15 Fe-0.5 Mn (Supermalloy)	0.78	0.004	100,000
48% MnO-Fe_2O_3, 52% ZnO-Fe_2O_3 (soft ferrite)	0.36		1,000
36% NiO-Fe_2O_3, 64% ZnO-Fe_2O_3 (soft ferrite)	0.29		650

Source: G.Y. Chin and J.H. Wernick, "Magnetic Materials, Bulk," vol. 14: *Kirk-Othmer Encyclopedia of Chemical Technology*, 3rd ed., Wiley, 1981, p. 686.

cold work and recrystallization treatments, a *cube-on-edge* (COE) {110}⟨001⟩ grain-oriented material was produced on an industrial scale for Fe–3% Si sheet (Fig. 15.20). Since the [001] direction is an easy axis for magnetization for Fe–3% Si alloys, the magnetic domains in COE materials are oriented for easy magnetization upon the application of an applied field in the direction parallel to the rolling direction of the sheet. Thus, the COE material has a higher permeability and lower hysteresis losses than Fe-Si sheet with a random texture (Table 15.3).

15.8.4 Metallic Glasses

Metallic glasses are a relatively new class of metallic-type materials whose dominant characteristic is a noncrystalline structure, unlike normal metal alloys, which

Table 15.4 Metallic glasses: compositions, properties, and applications

Alloy (atomic %)	Saturation induction B_s (T)	Maximum permeability	Applications
$Fe_{78}B_{13}Si_9$	1.56	600,000	Power transformers, low core losses
$Fe_{81}B_{13.5}Si_{3.5}C_2$	1.61	300,000	Pulse transformers, magnetic switches
$Fe_{67}Co_{18}B_{14}Si_1$	1.80	4,000,000	Pulse transformers, magnetic switches
$Fe_{77}Cr_2B_{16}Si_5$	1.41	35,000	Current transformers, sensing cores
$Fe_{74}Ni_4Mo_3B_{17}Si_2$	1.28	100,000	Low core losses at high frequencies
$Co_{69}Fe_4Ni_1Mo_2B_{12}Si_{12}$	0.70	600,000	Magnetic sensors, recording heads
$Co_{66}Fe_4Ni_1B_{14}Si_{15}$	0.55	1,000,000	Magnetic sensors, recording heads
$Fe_{40}Ni_{38}Mo_4B_{18}$	0.88	800,000	Magnetic sensors, recording heads

Source: Metglas Magnetic Alloys, Allied Metglas Products.

have a crystalline structure. The atoms in normal metals and alloys when cooled from the liquid state arrange themselves into an orderly crystal lattice. Table 15.4 lists the atomic compositions of eight metallic glasses of engineering importance. These materials have important soft magnetic properties and consist essentially of various combinations of ferromagnetic Fe, Co, and Ni with the metalloids B and Si. Applications for these exceptionally soft magnetic materials include low-energy core-loss power transformers, magnetic sensors, and recording heads.

Metallic glasses are produced by a rapid solidification process in which molten metallic glass is cooled very rapidly (about 10^6°C/s) as a thin film on a rotating copper-surfaced mold (Fig. 15.21*a*). This process produces a continuous ribbon of metallic glass about 0.001 in. (0.0025 cm) thick and 6 in. (15 cm) wide.

Metallic glasses have some remarkable properties. They are very strong (up to 650 ksi [4500 MPa]), very hard with some flexibility, and very corrosion-resistant. The metallic glasses listed in Table 15.4 are magnetically very soft as indicated by their maximum permeabilities. Thus, they can be magnetized and demagnetized very easily. Domain walls in these materials can move with exceptional ease, mainly because there are no grain boundaries and no long-range crystal anisotropy. Figure 15.21*b* shows some magnetic domains in a metallic glass that were produced by bending the metallic glass ribbon. Magnetically soft metallic glasses have very narrow hysteresis loops, as is indicated in Fig. 15.21*c*, and thus they have very low hysteresis energy losses. This property has enabled the development of multilayered metallic glass power transformer cores that have 70 percent of the core losses of conventional iron-silicon cores (Fig. 15.1). Much research and development work in the application of metallic glasses for low-loss power transformers is in progress.

15.8.5 Nickel-Iron Alloys

The magnetic permeabilities of commercially pure iron and iron-silicon alloys are relatively low at low applied fields. Low initial permeability is not as important for power applications such as transformer cores since this equipment is operated at high magnetizations. However, for high-sensitivity communications equipment used to

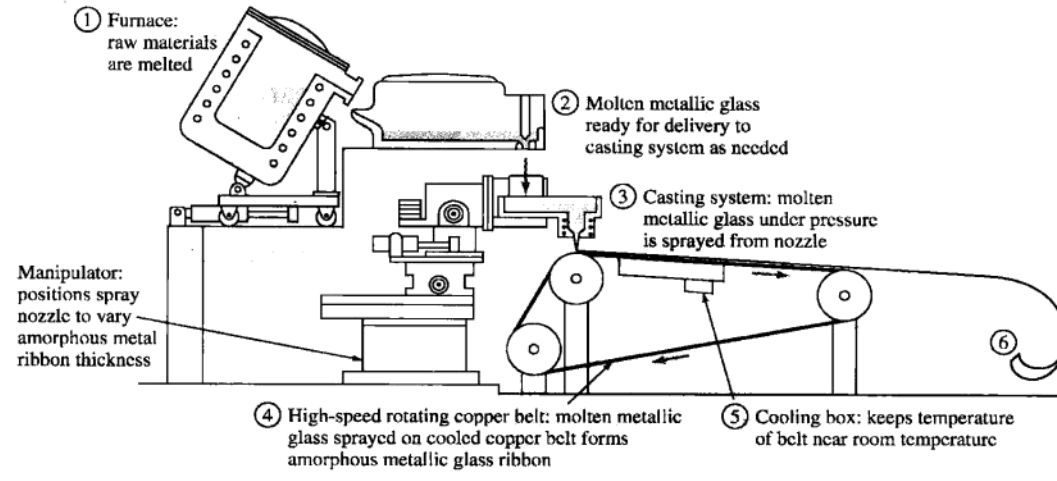

(*a*)

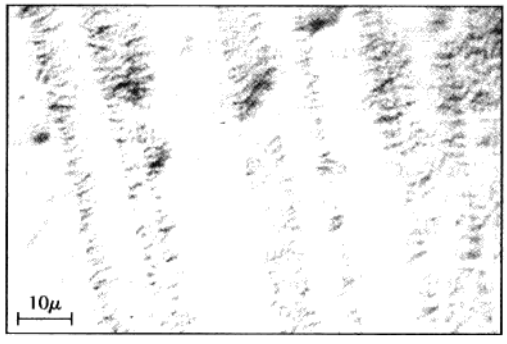

(*b*)

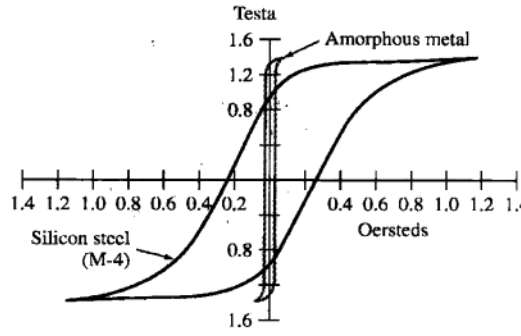

(*c*)

Figure 15.21

(*a*) Schematic drawing of the rapid solidification process for the production of metallic glass ribbon. (*After New York Times, Jan. 11, 1989, p. D7.*)

(*b*) Induced magnetic domains in a metallic glass. (*V. Lakshmanan and J.C.M. Li, Mater. Sci. Eng., 1988, p. 483.*)

(*c*) Comparison of the hysteresis loops of a ferromagnetic metallic glass and M-4 iron-silicon ferromagnetic sheet. (*From Electric World, September 1985.*)

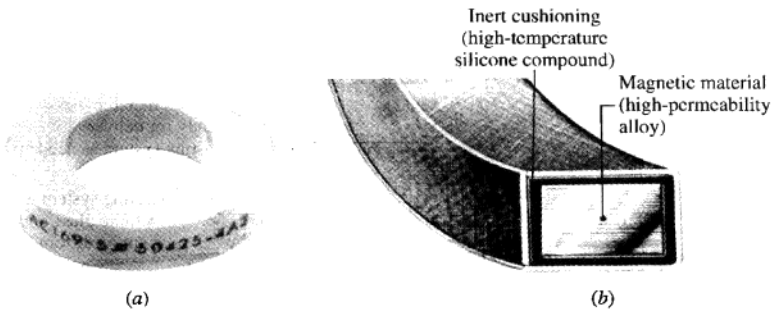

Figure 15.22
Tape-wound magnetic cores. (*a*) Encapsulated core. (*b*) Cross section of tape-wound core with phenolic encapsulation. Note that there is a silicone rubber cushion between the magnetic alloy tape and the phenolic encapsulation case. The magnetic properties of annealed high Ni-Fe tape-wound alloys are sensitive to strain damage.
(*Courtesy of Magnetics, a division of Spang & Company.*)

detect or transmit small signals, **nickel-iron alloys,** which have much higher permeabilities at low fields, are commonly used.

In general, two broad classes of Ni-Fe alloys are commercially produced, one with about 50 percent Ni and another with about 79 percent Ni. The magnetic properties of some of these alloys are listed in Table 15.3. The 50 percent Ni alloy is characterized by moderate permeability ($\mu_i = 2500$; $\mu_{max} = 25{,}000$) and high saturation induction [$B_s = 1.6$ T (16,000 G)]. The 79 percent Ni alloy has high permeability ($\mu_i = 100{,}000$; $\mu_{max} = 1{,}000{,}000$) but lower saturation induction [$B_s = 0.8$ T (8000 G)]. These alloys are used in audio and instrument transformers, instrument relays, and for rotor and stator laminations. Tape-wound cores, such as the cutaway section shown in Fig. 15.22, are commonly used for electronic transformers.

The Ni-Fe alloys have such high permeabilities because their magnetoanisotropy and magnetostrictive energies are low at the compositions used. The highest initial permeability in the Ni-Fe system occurs at 78.5% Ni–21.5% Fe, but rapid cooling below 600°C is necessary to suppress the formation of an ordered structure. The equilibrium ordered structure in the Ni-Fe system has an FCC unit cell with Ni atoms at the faces and Fe atoms at the face corners. The addition of about 5 percent Mo to the 78.5 percent Ni (balance Fe) alloy also suppresses the ordering reaction so that moderate cooling of the alloy from above 600°C is sufficient to prevent ordering.

The initial permeability of the Ni-Fe alloys containing about 56 to 58 percent Ni can be increased three to four times by annealing the alloy in the presence of a magnetic field after the usual high-temperature anneal. The magnetic anneal causes directional ordering of the atoms of the Ni-Fe lattice and thereby increases the initial permeability of these alloys. Figure 15.23 shows the effect of magnetic annealing on the hysteresis loop of a 65% Ni–35% Fe alloy.

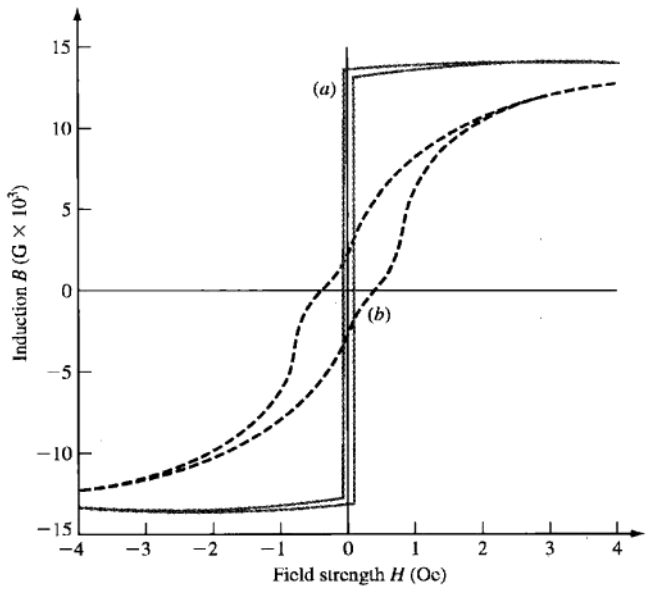

Figure 15.23
The effect of magnetic annealing on the hysteresis loop of a 65% Ni–35% Fe alloy. (*a*) 65 Permalloy annealed with field present; (*b*) 65 Permalloy annealed with field absent.
(*From K.M. Bozorth, "Ferromagnetism," Van Nostrand, 1951, p. 121.*)

15.9 HARD MAGNETIC MATERIALS

15.9.1 Properties of Hard Magnetic Materials

Permanent or **hard magnetic materials** are characterized by a high coercive force H_c and a high remanent magnetic induction B_r, as indicated schematically in Fig. 15.19*b*. Thus, the hysteresis loops of hard magnetic materials are wide and high. These materials are magnetized in a magnetic field strong enough to orient their magnetic domains in the direction of the applied field. Some of the applied energy of the field is converted into potential energy, which is stored in the permanent magnet produced. A permanent magnet in the fully magnetized condition is thus in a relatively high-energy state as compared to a demagnetized magnet.

Hard magnetic materials are difficult to demagnetize once magnetized. The demagnetizing curve for a hard magnetic material is chosen as the second quadrant of its hysteresis loop and can be used for comparing the strengths of permanent magnets. Figure 15.24 compares the demagnetizing curves of various hard magnetic materials.

The power or external energy of a permanent (hard) magnetic material is directly related to the size of its hysteresis loop. The magnetic potential energy of a hard

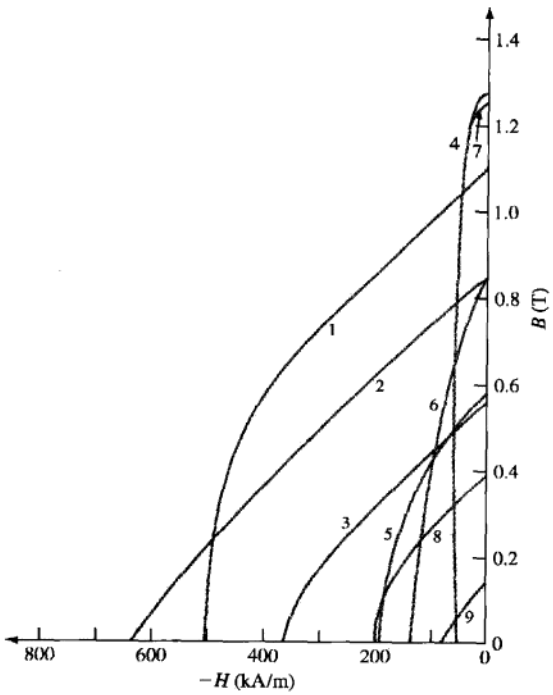

Figure 15.24
Demagnetization curves of various hard magnetic materials. 1: $Sm(Co,Cu)_{7.4}$; 2: $SmCo_5$; 3: bonded $SmCo_5$; 4: alnico 5; 5: Mn-Al-C; 6: alnico 8; 7: Cr-Co-Fe; 8: ferrite; and 9: bonded ferrite.
(From G.Y. Chin and J.H. Wernick, "Magnetic Materials, Bulk," vol. 14, Kirk-Othmer "Encyclopedia of Chemical Technology," 3d ed., Wiley, 1981, p. 673. Reprinted with permission of John Wiley & Sons, Inc.)

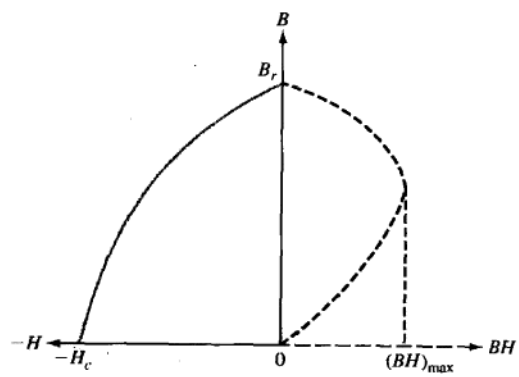

Figure 15.25
A schematic diagram of the energy product (B versus BH) curve of a hard magnetic material such as an alnico alloy is shown by the circular dashed line to the right of the B (induction) axis. The maximum energy product $(BH)_{max}$ is indicated at the intersection of the vertical dashed line and the BH axis.

magnetic material is measured by its **maximum energy product $(BH)_{max}$**, which is the maximum value of the product of B (magnetic induction) and H (the demagnetizing field) determined from the demagnetizing curve of the material. Figure 15.25 shows the external energy (BH) curve for a hypothetical hard magnetic material and its maximum energy product, $(BH)_{max}$. Basically, the maximum energy product of a hard magnetic material is the area occupied by the largest rectangle that can be inscribed in the second quadrant of the hysteresis loop of the material. The SI units for the energy product BH are kJ/m^3; the cgs system units are G · Oe. The SI units for the energy product $(BH)_{max}$ of joules per cubic meter are equivalent units to the product of the units of B in teslas and H in amperes per meter as follows:

$$\left[B\left(\frac{\cancel{\text{Wb}}}{\text{m}^2}\cdot\frac{1}{\cancel{\text{T}}}\cdot\frac{\cancel{\text{V}}\cdot\text{s}}{\cancel{\text{Wb}}}\right)\right]\left[H\left(\frac{\cancel{\text{A}}}{\text{m}}\cdot\frac{\text{J}}{\cancel{\text{V}}\cdot\cancel{\text{A}}\cdot\text{s}}\right)\right] = BH\left(\frac{\text{J}}{\text{m}^3}\right)$$

EXAMPLE PROBLEM 15.4

Estimate the maximum energy product $(BH)_{max}$ for the Sm $(Co,Cu)_{7.4}$ alloy of Fig. 15.24

■ Solution

We need to find the area of the largest rectangle that can be located within the second-quadrant demagnetization curve of the alloy shown in Fig 15.24. Four trial areas are listed:

Trial 1 ~ (0.8 T × 250 kA/m) = 200 kJ/m^3 (see Fig. EP15.4)
Trial 2 ~ (0 6 T × 380 kA/m) = 228 kJ/m^3
Trial 3 ~ (0.55 T × 420 kA/m) = 231 kJ/m^3
Trial 4 ~ (0.50 T × 440 kA/m) = 220 kJ/m^3

The highest value is about 231 kJ/m^3, which compares to 240 kJ/m^3 listed for the Sm (Cu,Co) alloy in Table 15.5.

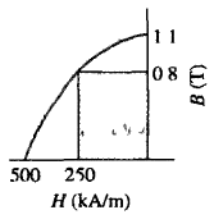

$(BH)_{max} \simeq (0\ 8\ T \times 250\ kA/m)$
$= 200\ kJ/m^3$

Figure EP15.4
Trial 1.

Table 15.5 Selected magnetic properties of hard magnetic materials

Material and composition	Remanent induction B_r (T)	Coercive force H_c (kA/m)	Maximum energy product $(BH)_{max}$ (kJ/m^3)
Alnico 1, 12 Al, 21 Ni, 5 Co, 2 Cu, bal Fe	0.72	37	11.0
Alnico 5, 8 Al, 14 Ni, 25 Co, 3 Cu, bal Fe	1.28	51	44.0
Alnico 8, 7 Al, 15 Ni, 24 Co, 3 Cu, bal Fe	0.72	150	40.0
Rare earth–Co, 35 Sm, 65 Co	0.90	675–1200	160
Rare earth–Co, 25.5 Sm, 8 Cu, 15 Fe, 1.5 Zr, 50 Co	1.10	510–520	240
Fe-Cr-Co, 30 Cr, 10 Co, 1 Si, 59 Fe	1.17	46	34.0
MO · Fe_2O_3 (M = Ba, Sr) (hard ferrite)	0.38	235–240	28.0

Source G Y Chin and J H Wernick, "Magnetic Materials, Bulk," vol 14 *Kirk-Othmer Encyclopedia of Chemical Technology,* 3rd ed., Wiley, 1981, p. 686

15.9.2 Alnico Alloys

Properties and Compositions The **alnico (*al*uminum-*ni*ckel-*co*balt) alloys** are the most important commercial hard magnetic materials in use today. They account for about 35 percent of the hard-magnet market in the United States. These alloys are

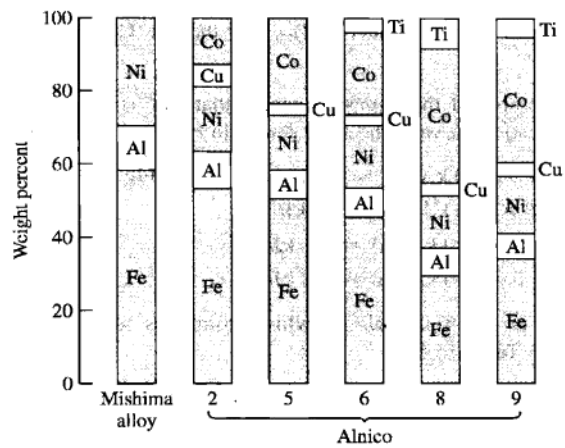

Figure 15.26
Chemical compositions of the alnico alloys. The original alloy was discovered by Mishima in Japan in 1931.
(From B.D. Cullity, "Introduction to Magnetic Materials," Addison-Wesley, 1972, p. 566. Reprinted by permission of Elizabeth M. Cullity.)

characterized by a high energy product [$(BH)_{max}$ = 40 to 70 kJ/m^3 (5 to 9 MG · Oe)], a high remanent induction [B_r = 0.7 to 1.35 T (7 to 13.5 kG)], and a moderate coercivity [H_c = 40 to 160 kA/m (500 to 2010 Oe)]. Table 15.5 lists some magnetic properties of several alnico and other permanent magnetic alloys.

The alnico family of alloys are iron-based alloys with additions of Al, Ni, and Co plus about 3 percent Cu. A few percent Ti is added to the high-coercivity alloys, alnicos 6 to 9. Figure 15.26 shows bar graphs of the compositions of some of the alnico alloys. Alnicos 1 to 4 are isotropic, whereas alnicos 5 to 9 are anisotropic due to being heat-treated in a magnetic field while the precipitates form. The alnico alloys are brittle and so are produced by casting or by powder metallurgy processes. Alnico powders are used primarily to produce large amounts of small articles with complex shapes.

Structure Above their solution heat-treatment temperature of about 1250°C, the alnico alloys are single-phase with a BCC crystal structure. During cooling to about 750°C to 850°C, these alloys decompose into two other BCC phases, α and α'. The matrix α phase is rich in Ni and Al and is weakly magnetic. The α' precipitate is rich in Fe and Co and thus has a higher magnetization than the Ni-Al–rich α phase. The α' phase tends to be rodlike, aligned in the ⟨100⟩ directions, and about 10 nm in diameter and about 100 nm long.

If the 800°C heat treatment is carried out in a magnetic field, the α' precipitate forms fine elongated particles in the direction of the magnetic field (Fig. 15.27) in a matrix of the α phase **(magnetic anneal).** The high coercivity of the alnicos is attributed to the difficulty of rotating single-domain particles of the α' phase based on shape anisotropy. The larger the aspect (length-to-width) ratio of the rods and the

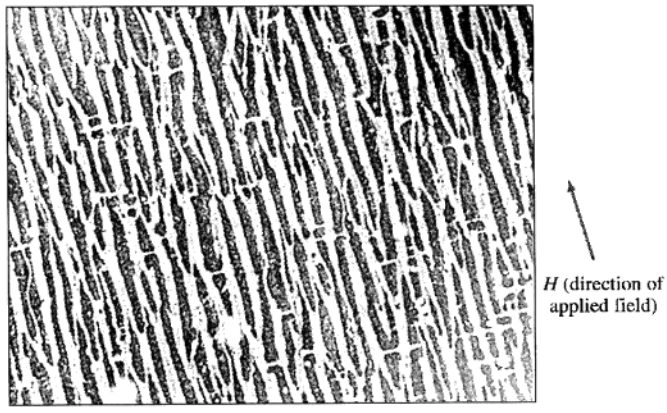

Figure 15.27
Replica electron micrograph showing the structure of alnico 8 (Al–Ni-Co-Fe-Ti) alloy after an 800°C heat treatment for 9 min in an applied magnetic field. The α phase (Ni-Al–rich) is light, and the α' phase (Fe-Co–rich) is dark. The α' phase is highly ferromagnetic, which is elongated in the direction of the applied field, creating anisotropy of the coercive force.
(Courtesy of K.J. deVos, 1966.)

smoother their surface, the greater the coercivity of the alloy. Thus, the forming of the precipitate in a magnetic field makes the precipitate longer and thinner and so increases the coercivity of the alnico magnetic material. It is believed that the addition of titanium to some of the highest-strength alnicos increases their coercivities by increasing the aspect ratio of the α' rods.

15.9.3 Rare Earth Alloys

Rare earth alloy magnets are produced on a large scale in the United States and have magnetic strengths superior to those of any commercial magnetic material. They have maximum energy products $(BH)_{max}$ to 240 kJ/m^3 (30 MG · Oe) and coercivities to 3200 kA/m (40 kOe). The origin of magnetism in the rare earth transition elements is due almost entirely to their unpaired $4f$ electrons in the same way that magnetism in Fe, Co, and Ni is due to their unpaired $3d$ electrons. There are two main groups of commercial rare earth magnetic materials: one based on single-phase $SmCo_5$ and the other on precipitation-hardened alloys of the approximate composition $Sm(Co,Cu)_{7.5}$.

$SmCo_5$ single-phase magnets are the most widely used type. The mechanism of coercivity in these materials is based on nucleation and/or pinning of domain walls at surfaces and grain boundaries. These materials are fabricated by powder metallurgy techniques using fine particles (1 to 10 μm). During pressing, the particles are aligned in a magnetic field. The pressed particles are then carefully sintered to prevent particle growth. The magnetic strengths of these materials are high, with $(BH)_{max}$ values in the range of 130 to 160 kJ/m^3 (16 to 20 MG · Oe).

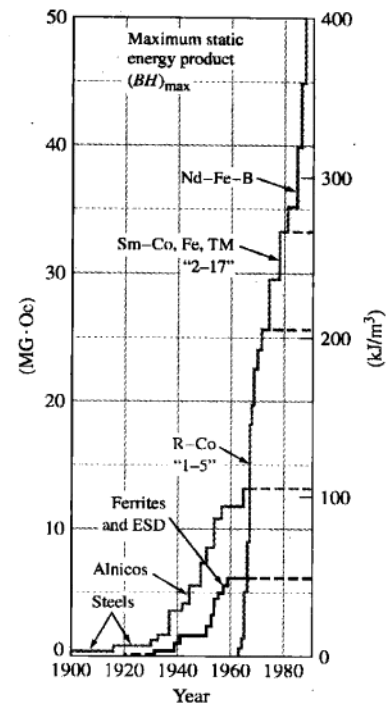

Figure 15.28
Progress in permanent-magnet quality in the twentieth century as measured by the maximum energy product $(BH)_{max}$.
(From K.J. Strnat, "Soft and Hard Magnetic Materials with Applications," ASM Inter. 1986, p. 64. Used by permission of ASM International.)

In the precipitation-hardened $Sm(Co,Cu)_{7.5}$ alloy, part of the Co is substituted by Cu in $SmCo_5$ so that a fine precipitate (about 10 nm) is produced at a low aging temperature (400°C to 500°C). The precipitate formed is coherent with the $SmCo_5$ structure. The coherency mechanism here is mainly based on the homogeneous pinning of domain walls at the precipitated particles. These materials are also made commercially by powder metallurgy processes using magnetic alignment of the pa ticles. The addition of small amounts of iron and zirconium promotes the development of higher coercivities. Typical values for an $Sm(Co_{0.68}Cu_{0.10}Fe_{0.21}Zr_{0.01})_{7.4}$ commercial alloy are $(BH)_{max} = 240\ kJ/m^3$ (30 MG · Oe) and $B_r = 1.1$ T (11,000 G). Figures 15.24 and 15.28 show the outstanding improvement in magnetic strengths achieved with rare earth magnetic alloys.

Sm-Co magnets are used in medical devices such as thin motors in implantable pumps and valves and in aiding eyelid motion. Rare earth magnets are also used for electronic wristwatches and traveling-wave tubes. Direct-current and synchronous motors and generators are produced by using rare earth magnets, resulting in a size reduction.

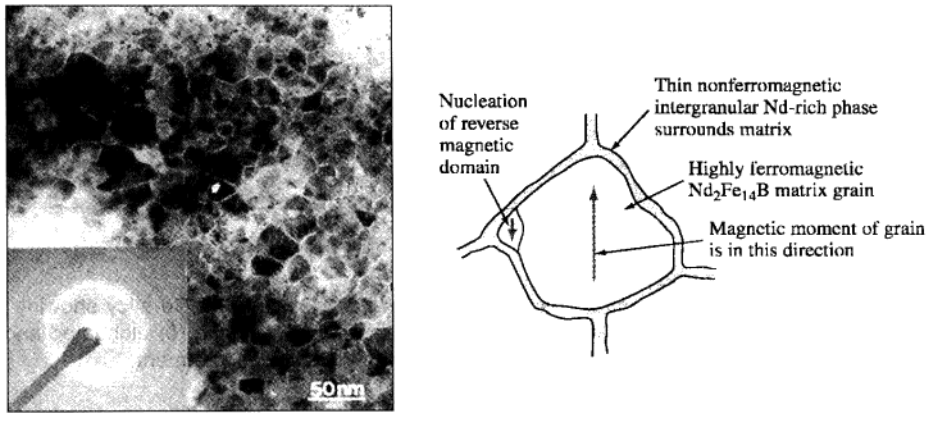

Figure 15.29
(*a*) Bright-field electron transmission micrograph of an optimally quenched Nd-Fe-B ribbon showing randomly oriented grains surrounded by a thin intergranular phase marked by the arrow.
(After J.J. Croat and J.F. Herbst, MRS Bull., June 1988, p. 37.)
(*b*) Single $Nd_2Fe_{14}B$ grain showing nucleation of reverse magnetic domain.

15.9.4 Neodymium-Iron-Boron Magnetic Alloys

Hard Nd-Fe-B magnetic materials with $(BH)_{max}$ products as high as 300 kJ/m^3 (45 MG · Oe) were discovered in about 1984, and today these materials are produced by both powder metallurgy and rapid-solidification melt-spun ribbon processes. Figure 15.29*a* shows the microstructure of a $Nd_2Fe_{14}B$-type rapidly solidified ribbon. In this structure, highly ferromagnetic $Nd_2Fe_{14}B$ matrix grains are surrounded by a nonferromagnetic Nd-rich thin intergranular phase. The high coercivity and associated $(BH)_{max}$ energy product of this material result from the difficulty of nucleating reverse magnetic domains that usually nucleate at the grain boundaries of the matrix grains (Fig. 15.29*b*). The intergranular nonferromagnetic Nd-rich phase forces the $Nd_2Fe_{14}B$ matrix grains to nucleate their reverse domains in order to reverse the magnetization of the material. This process maximizes H_c and $(BH)_{max}$ for the whole bulk aggregate of the material. Applications for Nd-Fe-B permanent magnets include all types of electric motors, especially those like automotive starting motors where reduction in weight and compactness are desirable.

15.9.5 Iron-Chromium-Cobalt Magnetic Alloys

A family of magnetic **iron-chromium-cobalt alloys** were developed in 1971 and are analogous to the alnico alloys in metallurgical structure and permanent magnetic properties, but the former are cold-formable at room temperature. A typical composition for an alloy of this type is 61% Fe–28% Cr–11% Co. Typical magnetic properties of Fe-Cr-Co alloys are B_r = 1.0 to 1.3 T (10 to 13 kG), H_c = 150 to 600 A/cm

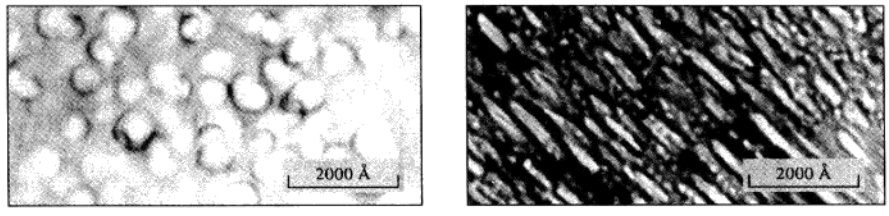

Figure 15.30
Transmission electron micrographs of an Fe–34% Cr–12% Co alloy showing (*a*) spherical precipitates produced before deformation and (*b*) elongated and aligned particles after deformation and alignment by final heat treatment.
[*After S. Jin et al., J. Appl. Phys.*, **53**:*4300(1982).*]

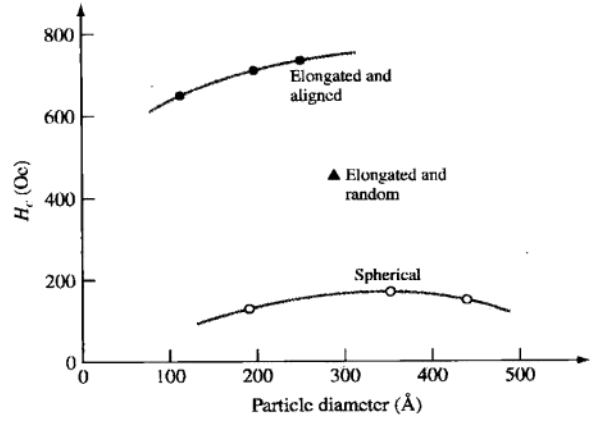

Figure 15.31
Coercivity versus particle diameter for differently shaped particles in an Fe–34% Cr–12% Co alloy. Note the great increase in coercivity by changing from a spherical shape to an elongated shape.
[*From S. Jin et al., J. Appl. Phys.*, **53**:*4300(1982).*]

(190 to 753 Oe), and $(BH)_{max}$ = 10 to 45 kJ/m^3 (1.3 to 1.5 MG · Oe). Table 16.5 lists some typical properties of an Fe-Cr-Co magnetic alloy.

The Fe-Cr-Co alloys have a BCC structure at elevated temperatures above about 1200°C. Upon slow cooling (about 15°C/h) from above 650°C, precipitates of a Cr-rich α_2 phase (Fig. 15.30*a*) with particles of about 30 nm (300Å) form in a matrix of an Fe-rich α_1 phase. The mechanism for coercivity in the Fe-Cr-Co alloys is the pinning of domain walls by the precipitated particles since the magnetic domains extend through both phases. Particle shape (Fig. 15.30*b*) is important since elongation of the particles by deformation before a final aging treatment greatly increases the coercivity of these alloys, as clearly indicated in Fig. 15.31.

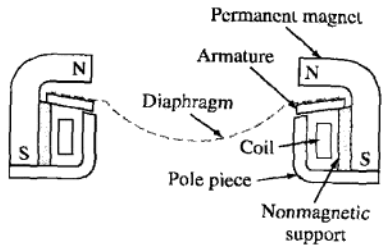

Figure 15.32
Use of ductile permanent Fe-Cr-Co alloy in a telephone receiver. Cross-sectional view of the U-type telephone receiver indicating position of permanent magnet.
[*After S. Jin et al., IEEE Trans. Magn.*, 17:2935(1981).]

Fe-Cr-Co alloys are especially important for engineering applications where their cold ductility allows high-speed room-temperature forming. The permanent magnet for many modern telephone receivers is an example of this cold-deformable permanent magnetic alloy (Fig. 15.32).

15.10 FERRITES

Ferrites are magnetic ceramic materials made by mixing iron oxide (Fe_2O_3) with other oxides and carbonates in the powdered form. The powders are then pressed together and sintered at a high temperature. Sometimes finishing machining is necessary to produce the desired part shape. The magnetizations produced in the ferrites are large enough to be of commercial value, but their magnetic saturations are not as high as those of ferromagnetic materials. Ferrites have domain structures and hysteresis loops similar to those of ferromagnetic materials. As in the case of the ferromagnetic materials, there are *soft* and *hard ferrites.*

15.10.1 Magnetically Soft Ferrites

Soft ferrite materials exhibit ferrimagnetic behavior. In soft ferrites, there is a net magnetic moment due to two sets of unpaired inner-electron spin moments in opposite directions that do not cancel each other (Fig. 15.8*c*).

Composition and Structure of Cubic Soft Ferrites Most cubic soft ferrites have the composition $MO \cdot Fe_2O_3$, where M is a divalent metal ion such as Fe^{2+}, Mn^{2+}, Ni^{2+}, or Zn^{2+}. The structure of the soft ferrites is based on the inverse spinel structure, which is a modification of the spinel structure of the mineral spinel ($MgO \cdot Al_2O_3$). Both the spinel and inverse spinel structures have cubic unit cells consisting of eight subcells, as shown in Fig. 15.33*a*. Each of the subcells consists of one molecule of $MO \cdot Fe_2O_3$. Since each subunit contains one $MO \cdot Fe_2O_3$ molecule and

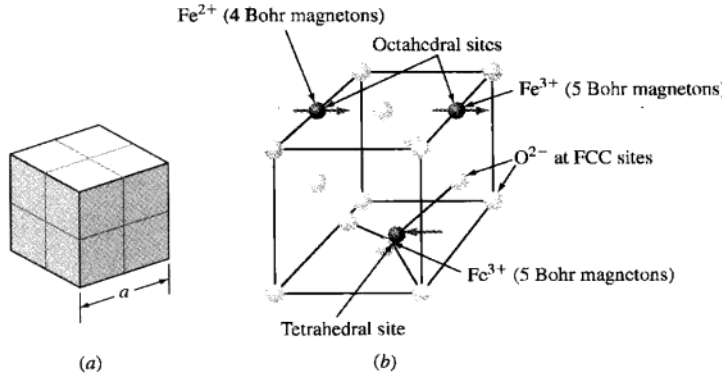

Figure 15.33
(*a*) Unit cell of soft ferrite of the type $MO \cdot Fe_2O_3$. This unit cell consists of eight subcells. (*b*) The subcell for the $FeO \cdot Fe_2O_3$ ferrite. The magnetic moments of the ions in the octahedral sites are aligned in one direction by the applied magnetic field, and those in the tetrahedral sites are aligned in the opposite direction. As a result, there is a net magnetic moment for the subcell and hence the material.

Table 15.6 Metal ion arrangements in a unit cell of a spinel ferrite of composition $MO \cdot Fe_2O_3$

Type of interstitial site	Number available	Number occupied	Normal spinel	Inverse spinel
Tetrahedral	64	8	8 M^{2+}	8 Fe^{3+} $\leftarrow$
Octahedral	32	16	16 Fe^{3+}	8 Fe^{3+} $\rightarrow$, 8 M^{2+} $\rightarrow$

since there are seven ions in this molecule, each unit cell contains a total of 7 ions $\times$ 8 subcells = 56 ions per unit cell. Each subunit cell has an FCC crystal structure made up of the four ions of the $MO \cdot Fe_2O_3$ molecule (Fig. 15.33*b*). The much smaller metal ions (M^{2+} and Fe^{3+}), which have ionic radii of about 0.07 to 0.08 nm, occupy interstitial spaces between the larger oxygen ions (ionic radius $\approx$ 0.14 nm).

As previously discussed, in an FCC unit cell there are the equivalent of four octahedral and eight tetrahedral interstitial sites. In the normal spinel structure, only half the octahedral sites are occupied, and so only $\frac{1}{2}$(8 subcells $\times$ 4 sites/subcell) = *16 octahedral sites are occupied* (Table 15.6). In the normal spinel structure, there are 8 $\times$ 8 (tetrahedral sites per subcell) = 64 sites/unit cell. However, in the normal spinel structure, only one-eighth of the 64 sites are occupied so that only *eight of the tetrahedral sites are occupied* (Table 15.6).

In the **normal spinel-structure** unit cell there are eight $MO \cdot Fe_2O_3$ molecules. In this structure the 8 M^{2+} ions occupy 8 tetrahedral sites and the 16 Fe^{3+} ions occupy 16 octahedral sites. However, in the **inverse spinel structure** there is a different arrangement of the ions: the 8 M^{2+} ions occupy 8 octahedral sites, and the 16 Fe^{3+} ions are divided so that 8 occupy octahedral sites and 8 tetrahedral sites (Table 15.6).

Ion	Number of electrons	Electron configuration 3*d* orbitals	Ionic magnetic moment (Bohr magnetons)
Fe^{3+}	23	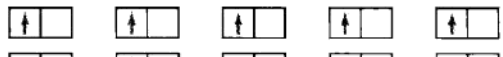	5
Mn^{2+}	23	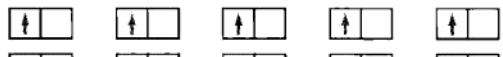	5
Fe^{2+}	24	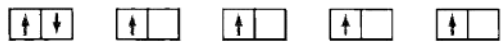	4
Co^{2+}	25	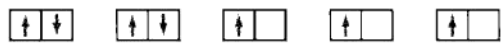	3
Ni^{2+}	26	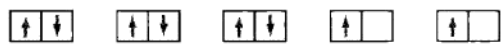	2
Cu^{2+}	27	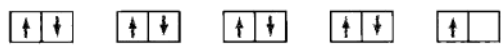	1
Zn^{2+}	28	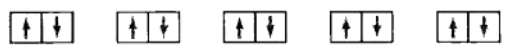	0

Figure 15.34
Electronic configurations and ionic magnetic moments for some 3*d* transition-element ions.

Table 15.7 Ion arrangements and net magnetic moments per molecule in normal and inverse spinel ferrites

Ferrite	Structure	Tetrahedral sites occupied	Octahedral sites occupied		Net magnetic moment (μ_s/molecule)
$FeO \cdot Fe_2O_3$	Inverse spinel	Fe^{3+} 5 ←	Fe^{2+} 4 →	Fe^{3+} 5 →	4
$ZnO \cdot Fe_2O_3$	Normal spinel	Zn^{2+} 0	Fe^{3+} 5 ←	Fe^{3+} 5 →	0

Net Magnetic Moments in Inverse Spinel Ferrites To determine the net magnetic moment for each $MO \cdot Fe_2O_3$ ferrite molecule, we must know the 3*d* inner-electron configuration of the ferrite ions. Figure 15.34 gives this information. When the Fe atom is ionized to form the Fe^{2+} ion, there are *four* unpaired 3*d* electrons left after the loss of two 4*s* electrons. When the Fe atom is ionized to form the Fe^{3+} ion, there are *five* unpaired electrons left after the loss of two 4*s* and one 3*d* electrons.

Since each unpaired 3*d* electron has a magnetic moment of one Bohr magneton, the Fe^{2+} ion has a moment of four Bohr magnetons and the Fe^{3+} ion a moment of five Bohr magnetons. In an applied magnetic field, the magnetic moments of the octahedral and tetrahedral ions oppose each other (Fig. 15.33*b*). Thus, in the case of the ferrite $FeO \cdot Fe_2O_3$, the magnetic moments of the eight Fe^{3+} ions in octahedral sites will cancel the magnetic moments of the eight Fe^{3+} ions in the tetrahedral sites. Thus, the resultant magnetic moment of this ferrite will be due to the eight Fe^{2+} ions at eight octahedral sites, which have moments of four Bohr magnetons each (Table 15.7). A theoretical value for the magnetic saturation of the $FeO \cdot Fe_2O_3$ ferrite is calculated in Example Problem 15.5 on the basis of the Bohr magneton strength of the Fe^{2+} ions.

EXAMPLE PROBLEM 15.5

Calculate the theoretical saturation magnetization M in amperes per meter and the saturation induction B_s in teslas for the ferrite $FeO \cdot Fe_2O_3$. Neglect the $\mu_0 H$ term for the B_s calculation. The lattice constant of the $FeO \cdot Fe_2O_3$ unit cell is 0.839 nm.

■ Solution

The magnetic moment for a molecule of $FeO \cdot Fe_2O_3$ is due entirely to the four Bohr magnetons of the Fe^{2+} ion since the unpaired electrons of the Fe^{3+} ions cancel each other. Since there are eight molecules of $FeO \cdot Fe_2O_3$ in the unit cell, the total magnetic moment per unit cell is

$$(4 \text{ Bohr magnetons/subcell})(8 \text{ subcells/unit cell}) = 32 \text{ Bohr magnetons/unit cell}$$

Thus,

$$M = \left[\frac{32 \text{ Bohr magnetons/unit cell}}{(8.39 \times 10^{-10} \text{ m})^3/\text{unit cell}}\right]\left(\frac{9.27 \times 10^{-24} \text{ A} \cdot \text{m}^2}{\text{Bohr magneton}}\right)$$
$$= 5.0 \times 10^5 \text{ A/m} \blacktriangleleft$$

B_s at saturation, assuming all magnetic moments are aligned and neglecting the H term, is given by the equation $B_s \approx \mu_0 M$. Thus,

$$B_s \approx \mu_0 M \approx \left(\frac{4\pi \times 10^{-7} \text{ T} \cdot \text{m}}{\text{A}}\right)\left(\frac{5.0 \times 10^5 \text{ A}}{\text{m}}\right)$$
$$= 0.63 \text{ T} \blacktriangleleft$$

Iron, cobalt, and nickel ferrites all have the inverse spinel structure, and all are ferrimagnetic due to a net magnetic moment of their ionic structures. Industrial soft ferrites usually consist of a mixture of ferrites since increased saturation magnetizations can be obtained from a mixture of ferrites. The two most common industrial ferrites are the nickel-zinc-ferrite ($Ni_{1-x}Zn_xFe_{2-y}O_4$) and the manganese-zinc-ferrite ($Mn_{1-x}Zn_xFe_{2+y}O_4$).

Properties and Applications of Soft Ferrites

Eddy-Current Losses in Magnetic Materials Soft ferrites are important magnetic materials because, in addition to having useful magnetic properties, they are insulators and have high electrical resistivities. A high electrical resistivity is important in magnetic applications that require high frequencies since if the magnetic material is conductive, eddy-current energy losses would be great at the high frequencies. Eddy currents are caused by induced voltage gradients, and thus the higher the frequency, the greater the increase in eddy currents. Since soft ferrites are insulators, they can be used for magnetic applications such as transformer cores that operate at high frequencies.

Applications for Soft Ferrites Some of the most important uses for soft ferrites are for low-signal, memory-core, audiovisual, and recording-head applications. At low signal levels, soft ferrite cores are used for transformers and low-energy inductors. A large tonnage usage of soft ferrites is for deflection-yoke cores, flyback transformers, and convergence coils for television receivers.